EVALUATION OF DEFLECTION DUCTILITY INDEX OF RECTANGULAR CONCRETE BEAMS REINFORCED WITH REBARS MILLED FROM SCRAP METALS

BY

APEH ABAH JOSEPH

DEPARTMENT OF BUILDING,

AHMADU BELLO UNIVERSITY,

ZARIA, NIGERIA

AUGUST, 2016

EVALUATION OF DEFLECTION DUCTILITY INDEX OF RECTANGULAR CONCRETE BEAMS REINFORCED WITH REBARS MILLED FROM SCRAP METALS

BY

APEH ABAH JOSEPH

Ph.D/Env-Design/40696/2012-2013

A THESIS SUBMITTED TO THE SCHOOL OF POSTGRADUATE STUDIES,

AHMADU BELLO UNIVERSITY, ZARIA IN PARTIAL FULFILLMEMENT OF THE REQUIREMENTS FOR THE AWARD OF

DOCTORATE DEGREE IN CONSTRUCTION TECHNOLOGY

DEPARTMENT OF BUILDING,

FACULTY OF ENVIRONMENTAL DESIGN,

AHMADU BELLO UNIVERSITY,

ZARIA, NIGERIA

AUGUST, 2016

DECLARATION

I declare that the work in this thesis entitled 'Evaluation of deflection ductility index of rectangular concrete beams reinforced with rebars milled from scrap metal' was performed by the author, Apeh Abah Joseph in the Department of Building under the supervision of Professor O.G. Okoli, Professor M.M. Garba and Professor I.K. Zubairu.

The information obtained from the literature has been duly acknowledged in the text and a list of references provided. No part of this thesis was previously presented for award of any type of certificate at any University or tertiary institution.

_____ _____

Apeh Abah Joseph Date

(Ph,D/Env-Design/40696/2012-2013)

CERTIFICATION

This Project thesis entitled **Evaluation of deflection ductility index of rectangular concrete beams reinforced with rebars milled from scrap metals** meets the regulations governing the award of the degree of Doctor of Philosophy in Construction Technology of the Ahmadu Bello University, Zaria and is approved for its contribution to body of Knowledge and Literary presentation.

…… Date……

Professor O.G. Okoli

Chairman, Supervisory committee

…… Date……

Professor M.M. Garba

Member, Supervisory Committee

…… Date ……

Professor I.K. Zubairu

Member, Supervisory Committee

…… Date ……

Dr. Dikko Kado

Head of Department

…… Date ……

Professor Kabir Bala

DEAN, Post graduate School

DEDICATION

To my children, Mike and Mary, my lovely Pearls.

ACKNOWLEDGEMENTS

To the Omnipotent and Omniscience Lord Jesus Christ whose love and mercy made the completion of this work possible, be thou glorified.

With a sincere gratitude that I acknowledge the contribution of my supervisory team in the persons of Professor Godwin O. Okoli, Professor Magaji M. Garba and Professor Ibrahim K. Zubairu. The direction of this work was fine- tuned by your contributions. From the bosom of my heart I salute my elder brother, Mike Ikeh Apeh for his continuous supplications to God for the success of the study.

The contributions of the former Head of Department, Professor Kabir Bala who facilitated the research work in the first place and that of Dr. Dikko Kado, the current Head of the Department are well acknowledged. I appreciate the contributions of Dr. H.T. Kimeng of Architecture Department, Professor O.S. Abejide and Professor S.P. Ejeh of Civil Engineering Department for their valuable inputs, taking time out of their tight schedules to go through my seminar papers and making very useful contributions which gave well defined direction to the study.

I want to express my profound gratitude to the Head of Department of Civil Engineering, Kaduna Polytechnic whose kind permission enabled the use of their Laboratory for the experimental study. My gratitude also goes to Engineer Ben Adejo, Head of Structures laboratory and Mr Sadiq for their contributions during the casting and testing of specimens.

My profound gratitude also goes to my junior brother, George A. Apeh of Yaba College of Technology, Lagos who helped in the search for suitable testing equipment for the

study. My appreciation goes to the Department of Building laboratory staff in the persons of Messrs Saidu, M.S, Audi S.R and Abdulaziz, A.S. Finally, I wish to thank all and sundry who in one way or the other contributed to the successful completion of this study.

ABSTRACT

Ductility index is essential both in structures and structural elements in service. Its inadequacy may lead to brittle failure and jeopardy of lives. In reinforced concrete beams that experience large inelastic deformation in service, its ductility index cannot be over-emphasized. In Nigeria, the steel sector is now sustained through the recycling of scrap metals obtained mainly from municipal solid wastes which find application in the construction Industry. The study evaluated the deflection ductility index of rectangular concrete beams reinforced with rebars milled from scrap metals. This was achieved by designing a typical beam, produced samples and assessed the deflection ductility index experimentally and analytically. Eighteen (100 mm x 200 mm x 1000 mm) concrete beams reinforced with rebars milled from scrap metals were produced; six each with concrete strength of 20.33N/mm^2, 26.71N/mm^2, 30N/mm^2 and steel ratio (ρ) of 0.0058 to 0.012 respectively. The samples were tested under a four-point loading and analyzed with the aid of a Computer MATLAB programme using the Hognestad models for concrete and steel, theoretical equations of strain compatibility and equilibrium of forces at the beam section. Based on the test data obtained in the Laboratory and analytical approach, the failure mode of most beams was classified as ductile flexural failure accompanied by yielding of the tension steel preceding the crushing of concrete. The crack width of the beams ranged from 0.198 to 0.320 mm and within ACI 224 specification. The flexural capacity of the test samples ranged from 43.25 to 88.25kN with a deflection ductility index of 1.72 to 2.75 which depends on concrete strength and steel ratio. Reduction in stiffness of the beams is dependent on steel ratio. The analytical Load-deflection relationship compared with experimental values showed good agreement. This confirms

the applicability of the theoretical approach which provides a useful tool for evaluating the deflection ductility index and load-deflection response of rectangular concrete beams reinforced with rebars milled from scrap metals. An empirical model for predicting the deflection ductility index of a concrete rectangular beam reinforced with rebars milled from scrap metals was developed. Rebars milled from scrap metals can be used for reinforced concrete beams but such beams lack adequate ductility, neither redistribute moment(s) (when used as continuous beams) nor can they be considered as structural members capable of sustaining large displacements. However, such rebars should be produced at an approved standard. The production of such rebars requires as little as 26% amount of energy that would be required to produce steel from raw materials extracted from natural sources and the emission of co_2 is reduced by 56%.

TABLE OF CONTENTS

CHAPTER 2

LITERATURE REVIEW

CHAPTER 5 SUMMARY, CONCLUSION AND RECOMMENDATIONS

LIST OF FIGURES

LIST OF TABLES

LIST OF PLATES

LIST OF APPENDICES

NOTATIONS

A_s = Area of steel reinforcing bars

α = parameter of equivalent stress block defining the depth of stress block

b = width of beam section of fiber

β = parameter of equivalent stress block defining the average stress

c = depth of neutral axis

d = effective depth of beam

δ = deflection

Δ_μ = deflection at ultimate state of beam

Δ_y = deflection at yielding of steel

E_s = Modulus of elasticity of steel

E_d = dynamic modulus of elasticity of beam

ε_c = strain on any fiber in the compressive section of beam

ε_{cm} = strain on extreme fiber in the compressive section of beam

ε_{cu} = maximum strain at failure = 0.003

ε_{st} = strain in steel at yield point of steel

ε_o = strain at maximum stress = 0.002

F_c = compressive force due to concrete section of beam

F_s = tensile force due to steel section of the beam

f_{cu} = compressive strength of concrete

f_c, ρ_c = concrete stress in beam section

F_y = Yield strength of steel

Ig = Gross moment of inertia at beam section

I_{cr} = Moment of inertia of cracked section of beam

Ie = effective moment of inertia of beam section

L = effective span of beam

M_{cc}=Moment due to compressive section of concrete beam

M_s = Moment due to tensile steel section of beam

M = Overall moment due to the beam section

M_a = applied moment

M_{cr} = Cracking moment of beam section

Φ = curvature of fiber

P = Load

ρ = tensile steel ratio, $\rho = A_s/bd$

ρ_b= balanced steel ratio , $\rho_b = \frac{0.85fc\ \beta}{fy}\ (\frac{600}{600+fy})$

U.P.V = Ultrasonic pulse velocity

μ_Δ = deflection ductility index

Δ_μ = deflection at ultimate state of beam

Δ_y = deflection at yield point of steel

Z = lever arm

CHAPTER 1
INTRODUCTION

1.1 BACKGROUND

In reinforced concrete design, members are designed to have adequate strength and ductility to satisfy ultimate limit states. Ductility is a structural design requirement used in most design codes (ACI 318). In steel, reinforced concrete structures or structural elements, ductility is defined as the extent of plastic deformation of the member which in most cases is due to the steel. It is also the ability of the member to undergo large-deformations in the inelastic range without a substantial reduction in strength (Ashour, 2000). Being a qualitative value representing inelastic deformation shown in materials, structural section and structural member, it is imperative that the members have certain level of ductility to prevent abrupt brittle failure and secure strain energy absorption capacity of the member. Also, it is an important safety coefficient which delays local failure by redistributing the excessive stress in a critical section to other sections in statically indeterminate structures (Park and Paulay, 1975).

Ductility index can be used to measure ductility. It is defined as the ratio of deflection at ultimate state to the deflection at yield point of steel in a member as in Equation (1):

$$\mu_{\Delta} = \frac{\Delta u}{\Delta y} \qquad (1)$$

where $\Delta_{u,}$ is deflection at ultimate limit state, Δ_y is deflection at yield point of steel respectively and μ_{Δ} is deflection ductility index.

The displacement ductility index required of typical reinforced concrete beams may vary between 1 for elastically responding beam to 6 for ductile beams depending on the level of deformation used to determine the required strength of the beam (Kumar *et al*, 2008).

Ashour (2000) mentioned that the displacement ductility, μ_{Δ}, in the range of 3 to 5 is considered imperative for adequate ductility, especially for seismic design and redistribution of moments. Generally, high ductility ratios indicate that a structural member is capable of undergoing large deformations prior to failure.

Kumar *et al*, (2006) worked on six high performance concrete beams with varying concrete strength and tensile reinforcement ratio (ρ) and obtained displacement ductility indices of 1.17 - 2.26. Zaki *et al*, (2011) used steel slag coarse aggregate and obtained values ranging from 2.22 – 9.66. The effect of tensile reinforcement ratio and size on ductility of beams have been reported in other investigations (Shin *et al* 2010; Appa and Vijanand 2008; Kumar, *et al, (*2006). Other factors influencing ductility of beams are concrete strength, axial rigidity of the member (Yang *et al*, 2000), and steel properties (Grimaldi and Remaldi, 2000). However, the study focused on other aspects more beneficial to occupants such as the evaluation of deflection ductility index of concrete beams reinforced with rebars produced from 100% scrap metals in Nigeria which has direct bearing on the safety of occupants.

1.2 STATEMENT OF THE PROBLEM

Reinforced concrete members in service experience large inelastic deformation therefore adequate ductility is essential to avoid brittle failure and enhance energy dissipation potential. The adequacy of ductility in reinforced concrete (RC) beams is largely controlled by steel reinforcing bars (Rai *et al*, 2012). It places certain special requirements on their properties such as yield strength (f_y), the ratio of ultimate tensile strength to yield strength which are sensitive to the method of rebar manufacturing

(Towl and Brunell, 2005; Brooke *et al*,2005). These properties can be obtained by tensile strength test on bar samples in the laboratory. Furthermore, the strength and ductility characteristics of RC members are related to the cracking phenomenon and the materials behaviour (Grimaldi and Renaldi, 2000). In service, the member undergoes deformation which is essentially resisted by the concrete (un-cracked zone) until the beam cracks when the steel bar takes over résistance of the load and the deformation in steel continues up to yield point. Beyond the yield point, deformation is no longer elastic up to failure point of the beam. Deflection ductility index of the beam is evaluated from the load – deformation response of the beam.

Evaluation of ductility index of concrete beams with rebars produced from scrap metal is imperative in order to ascertain the adequacy or otherwise of ductility of the beams. Establishment of such status helps in understanding functionality and behaviour in service of such structural members. Research studies on strength and ductility characteristics of reinforcing steel bars milled from scrap metal by Kankam and Adom-Asamoah, (2002); Alabi and Onyeji, (2010); Ejeh and Jibrin, (2012), Jibrin and Ejeh, (2013) showed the reinforcing bars do not meet the BS 4449, (2005) maximum limit of 0.25% for carbon requirements for mild steel. The Phosphorous and Sulphur impurities in the steel bar from three companies exceeded the preferred limit of 0.05% for Phosphorous and 0.01% for Sulphur. These excess carbon, Sulphur and Phosphorous contents increase the strength and hardness of the steel and same time decreases their ductility making them brittle. Actual behavior of such reinforcing steel bars has not been ascertained as indicated by Kankam and Asamoah, (2002); yet they are being used in construction of buildings and other infrastructure as mild steel bars to the detriment of

occupants and the society at large. The implication of its continuous use in building cannot be over – emphasized. Not much work has been done on ductility index of concrete beams reinforced with such rebars produced from scrap metals as in Nigeria. Consequently, this was addressed herein as follows:

(a) Production of concrete beams reinforced with rebars produced from 100% scrap metals.

(b) Assessment of the deflection ductility indices of beams analytically using Hognestad Model and theoretical equations of beam sections are compared with experimental values.

(c) Investigation of the effect of reinforcement ratio (ρ) on the deflection ductility indices of RC beams.

(d) Determination of the effect of concrete strength on the deflection ductility indices of RC beams.

(e) Development of an empirical model that predicts the deflection ductility indices of the beams

1.3 JUSTIFICATION OF RESEARCH

In the design of reinforced concrete flexural members, it is important to ensure that the members do not exhibit brittle failure and are capable of sustaining large deformations near maximum load whose capacities give ample warning before failure; this guarantees adequate ductility which is imperative and of primary concern to safety of the structure. Since a structure well designed should usually provide a certain amount of ductility

(Carrillo *et al*, 2014), it is imperative that this amount of ductility be assessed so as to determine its adequacy.

The deflection ductility index of rectangular concrete beam with rebars produced from 100% scrap metals is yet to be established. The establishment of this index will serve as a base for classification of such beams into elastically responding or ductile structural elements. It will also serve as a veritable evaluation parameter for unraveling the problem surrounding the incessant collapse of buildings.

This has been addressed by the study which established that beams reinforced with rebars milled from scrap metal are elastically responding structural element (Kumar *et. al*, 2008), neither redistribute moment(s) (when used as continuous beams) nor capable of sustaining large inelastic displacements (Ashour, 2000). The study further established that the incessant collapse of buildings may not be unconnected with the ductility index of rebars milled from scrap metals as the bars with ductility index (1.72 to 2.75) are being used in construction work in most construction sites. Ashour (2000) has mentioned that reinforced concrete structural elements such as beams with ductility index of 3.0 to 5.0 has adequate ductility to sustain large displacements and capable of redistributing moment(s) (when used as a continuous beam).

An empirical model for the prediction of deflection ductility index of the beam was developed. The model shows that the ductility index of the rebars is dependent on concrete strength and the steel ratio. This is useful to structural engineers in the design of structures and structural elements that may be subjected to large displacements. With the use of the model and knowledge of concrete strength and steel ratio, the rigorous use of Load-deflection analysis in order to evaluate the ductility index of beams can be

circumvented. The result(s) obtained from the study also gives insight on the behaviour of the beams which should be valuable for future applications and development of design guidelines for such rebars since it is still used in construction works. It would potentially afford regulating Institutions new knowledge that will enhance compliance to specifications in design codes.

By using scrap metals as reinforcing bars in structures and structural elements rather than virgin materials (metal ores dugged from earth) in the production of rebars, carbon dioxide emissions which leads to global warming are reduced by 56 percent (ISRI,2015). Furthermore, the production of such rebars requires as little as 26% of amount of energy that would be required to produce steel from raw materials extracted from natural source (MCA, 2004).

1.4 **SIGNIFICANCE OF THE STUDY**

The study is an evaluation of the deflection ductility index of rectangular concrete beams reinforced with rebars milled from scrap metals. With the collapse of the Nigeria steel sector (Ohimain, 2013), now being sustained through recycling of scrap metals to produce rebars which find application on construction sites; The frequent collapse of buildings on our construction sites is worrisome, besides, researchers have expressed concerns about the uncertainty of ductility of concrete beams reinforced with rebars milled from scrap metals. The issue has been investigated through tests performed on eighteen concrete beams reinforced with such rebars.

The study is significant in a number of ways both from the theoretical and practical perspectives. From the theoretical perspective, a theoretical approach which evaluates the

deflection ductility index and load-deflection response of rectangular concrete beams reinforced with rebars milled from scrap metals was developed. This was based on the use of three fundamental principles of mechanics and the Hognestad Models for concrete and steel to determine the ductility index and load– deflection relationship of rectangular concrete beams reinforced with rebars milled from scrap metals. This enhanced the development of the theoretical approach and agreed well with experimental values. In other words, evaluation of deflection ductility index and load-deflection response of rectangular concrete beams reinforced with rebars milled from scrap metals can be achieved analytically with the aid of values of constituent variables obtained experimentally. Furthermore, the algorithms of the theoretical approach was used to write a computer programme for the evaluation of ductility index and load-deflection response of rectangular concrete beams reinforced with rebars milled from scrap metals. This approach has not yet been explored. This is beneficial to researchers as a new veritable tool for the development of new frontiers in the analysis of rectangular concrete beams reinforced with such rebars. The theoretical model has been developed to different scales. The response of a structure under load depends, to a large extent, on the stress-strain relation of the constituent materials. It has thus been necessary to define the constitutive relationships of all the materials. The material scale model has been used on the cross-section of the element to obtain a cross-section scale model. This model is in form of Load-deflection relations for the cross section. Utilizing the cross section model the element model has been developed to predict the load-deflection relation of the beam. The element model can be used in determining the overall behavior of the structure that consists of several elements.

From the practical perspective, the study can be a learning paradigm for students of building at the post graduate level to enhance their knowledge and practice in the field. The theoretical knowledge acquired from the study is further strengthened with the practical aspect as they are better informed on how to tackle the incessant collapse of buildings in Nigeria as rebars milled from scrap metals are continuously utilized for construction works.

1.5 Aim and Objectives

1.5.1 Aim

The aim of this research is to evaluate the deflection ductility index of a rectangular concrete beam reinforced with rebars produced from scrap metals with a view to developing an empirical model that predicts the deflection ductility indices of the beam.

1.5.2 Objectives

The objectives of the research are:

(a) To produce concrete beams reinforced with rebars produced from 100% scrap metals.

(b) To assess the deflection ductility indices of the beams experimentally and analytically using Hognestad Model (as modified by Magregor (1997) and theoretical equations based on beam sections which are compared with experimental values.

(c) To investigate the effect of tensile reinforcement ratios on the ductility indices of the beams.

(d) To determine the effect of concrete strengths on the ductility indices of the beams.

(e) To develop an empirical model that predicts the deflection ductility indices of concrete beams.

1.6 SCOPE AND LIMITATIONS OF STUDY

1.6.1 Scope

This research is an experimental and theoretical evaluation of the deflection ductility index of concrete beams reinforced with rebars produced from 100% scrap metals. It establishes an empirical model that predicts the deflection ductility indices of rectangular concrete reinforced beams, evaluate the flexural behavior of the beams in terms of first crack load, crack width, ultimate flexural capacity, stiffness, failure mode and shows the effects of tensile reinforcement ratio and concrete strength on the deflection ductility indices.

1.6.2 Limitations

The reinforcement bars used for the study were produced from mills whose raw material is 100% scrap metals with supposedly high carbon content and other impurities due to the absence of a metal refining stage in the production process as noted by Ndiaye *et al*, (2009). The study did not consider the possible slippage of the beams at the support during loading. Furthermore, owing to the loading limitations a maximum beam span of 1000 mm of the test specimen was used. Also, the yield strength of the reinforcement bars determined, are at the elastic limit only.

CHAPTER 2

LITERATURE REVIEW

2.1 Ductility in Reinforced Concrete Beams

The ductility of a beam can best be represented with reference to a tri-linear (Load-deflection) curve in Figure 2.1 which captures the basic load-deformation characteristics of bending action; where the extent of the curve between yielding of steel and ultimate failure of beam represents the ability of the beam to deform without any loss of strength. Defined as ductility, it is an important design requirement. The ductility of a beam is usually measured in terms of an index called deflection ductility, μ_{Δ}, which is the ratio of the deflection at the ultimate state of beam, $\Delta_{u,}$ to the deflection at yield point of steel, Δ_{y}, that is, (Park *et al*., 2009):

$$\mu_{\Delta} = \frac{\Delta u}{\Delta y} \qquad (2.1)$$

Ductility index provide an opportunity for forces to redistribute in an indeterminate structure resulting in a better index of structural safety against failure. With a sufficient ductility index, excessive deformations will be observed before failure, allowing occupants to evacuate the structure. A closer view of Equation (2.1) shows that the computation of deflections in RC beams plays a critical role in the evaluation of deflection ductility indices of beams. The work of Preetha *et.al*, (2013) on ductility behaviour of reinforced concrete beams with a ductility index of 4.17 was based on deflection computations.

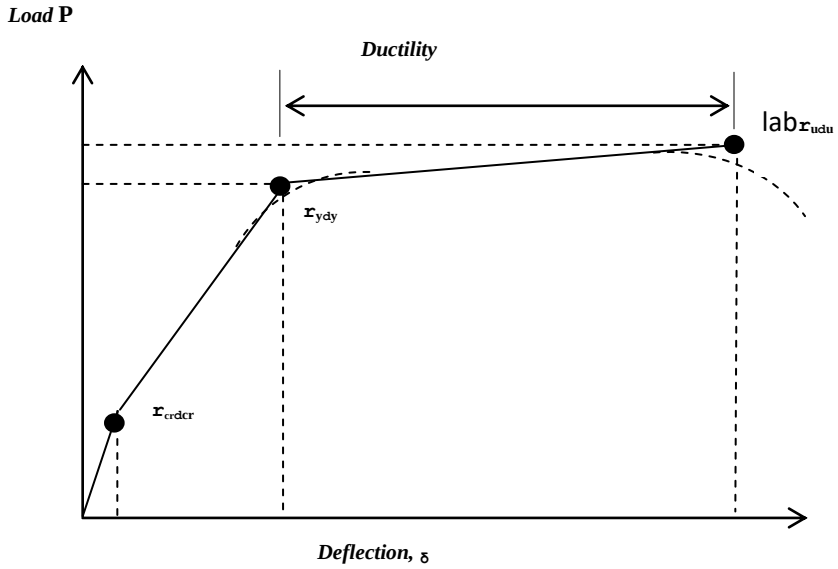

Figure 2.1: Load-deflection relatic

2.2 Deflection

At service load of beams, deflections are of main concern because its excessiveness is visually unpleasant, create service problems and cause damage to non-structural element. Hence, control of deflections under service load constitutes one of the major design requirements. However, for ductility of beams, deflection measurement is from inception of the beam's loading to ultimate failure point with emphasis on yield point of steel (used as reinforcement) and the ultimate failure of the beam. The deflection of a beam is in general calculated from the basic moment-curvature (M – Φ) or load-deflection (P-δ) relationships of the sections along the length of the member. For small deflections, the elastic bending theory is as expressed in (CEB, 1993):

$$\Phi_x = \frac{M_x}{EI} = \frac{d^2 \Delta}{dx^2} \tag{2.2}$$

In which M_x= Moment at a distance x from the support; Φ_x= curvature at x, Δ = deflection at x; EI = flexural rigidity of the cross section. Thus, for a prismatic beam (EI = constant), deflection can be calculated by double integration and moment area

method. The maximum deflection for a prismatic member loaded as in figure 2.2 is expressed as in (ACI 318M, 2005):

$$\Delta_{max} = \frac{23\ PL^3}{1296EI} \tag{2.3}$$

Where P = Load, L= span, EI = flexural rigidity. For a prismatic member, EI= constant. But in the case of reinforced concrete, both the modulus of elasticity of concrete, E_c and the moment of inertia of the section, I may change. The value of E_c is generally affected by creep and shrinkage of the concrete. Even if E_c isassumed constant, there is aneed to evaluate an equivalent moment of inertia to be able to use equation 2.3. The value of gross moment of inertia, I_g, for beam that has not cracked is calculated and expressed as:

$$I_g = \frac{bh^3}{12} \tag{2.4}$$

For a cracked section, the moment of inertia, I_{cr}, is given by the relation as expressed in (ACI 318M 2005):

$$I_{cr} = 0.18(n\rho)^{0.25}\, bd^3/_{12} \tag{2.5}$$

The effective moment of inertia, I_e, for a beam section is given as in (ACI 318M 2005):

$$I_e = \left[\frac{Mcr}{Ma}\right]^3 I_g + \left[1 - \left(\frac{Mcr}{Ma}\right)^3\right] I_{cr} \leq I_g \tag{2.6}$$

In which M_a = moment in the section at the stage of loading for the deflection sought, I_g = gross moment of inertia, I_{cr} = moment of inertia of the cracked transformed section and M_{cr} = moment due to cracking based on gross section and a modulus of rupture value as specified in ACI 318 (2005) and given as:

$$M_{cr} = \frac{f_r I_g}{y_t} \tag{2.7}$$

Where $f_r = 0.62\sqrt{f_c}$, modulus of rupture (2.8)

Y_t, the depth of the neutral axis from the tensile section of the beam and f_c is the concrete strength.

The value of I_e is calculated by using equation (2.6) at the desired loading stage within the anticipated range of service and this I_e value is used in equation (2.3), to find the maximum deflection of a reinforced concrete beam.

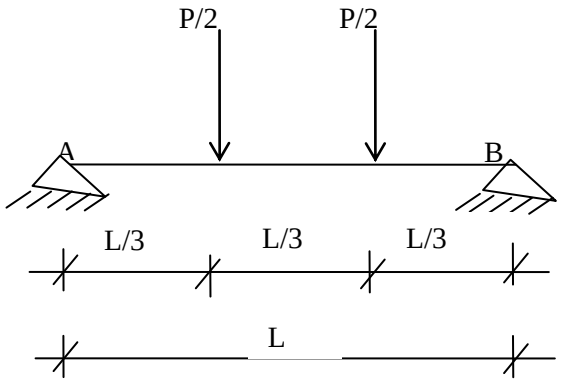

Figure 2.2: Prismatic Member

2.3 LOAD-DEFLECTION RESPONSE OF A BEAM

The load-deformation response in the perspective of the general flexural theory for reinforced concrete can be discussed by considering the beam section

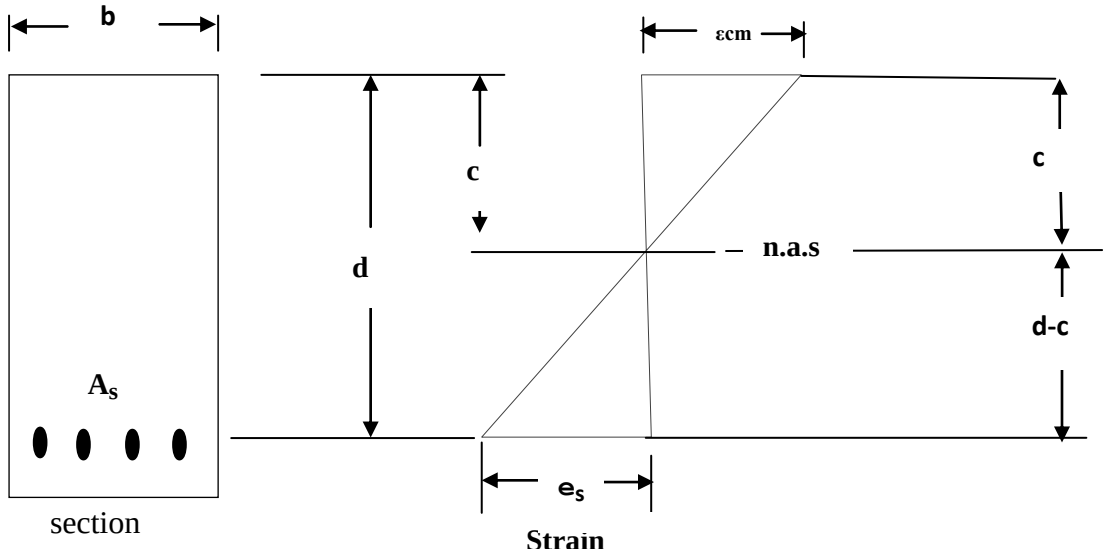

Figure 2.3: stress – strain diagram of beam section

When a bending moment, M is applied, the stresses, strains and the resulting deformation due to the applied moment must satisfy the three fundamental principles of mechanics of deformable bodies which are (Ng and Lee, 2002) :

(i) Equilibrium of forces, (ii) Compatibility of strains, (iii) Satisfaction of material laws to obtain a rational solution. Equilibrium relates applied loads to the stresses generated, compatibility connects deformation with the resulting strains and constitutive laws provide a bridge between stresses and strains. Thus, it is possible to analytically describe the complete load-deformation response of a section throughout the entire loading history of the member. The bending moment, M, will cause rotation of the section. The manner in which this rotation takes place provides the necessary compatibility condition. Plane section before bending remain plane after bending; a hypothesis originally proposed by Bernoulli about a century ago, has been universally accepted as a reasonable proposition for a bending problem. By virtue of this hypothesis, strain in the concrete is taken proportional to the distance from the neutral axis or, in other words, the strains along the depth of the cross section is distributed linearly (Park and Paulay, 1975) as shown in Figure 2.3. The maximum compressive strain in concrete, ε_{cm} occurs at top surface of section.The tensile strain in steel, ε_{st}, occurs at the bottom. The compatibility equations for this singly reinforced concrete beam section can be expressed as in (Wright and Macgregor, 2012):

$$\frac{\varepsilon_{cm}}{c} = \frac{\varepsilon_{st}}{d-c} \tag{2.9}$$

$$\varepsilon_{st} = \varepsilon_{cm} \frac{(d - c)}{c} \tag{2.10}$$

The distribution of stresses along the depth of the cross section depends on the strain value, the two being connected by appropriate material laws. For steel in compression,

the stress-strain relationship is identical to that in tension provided premature buckling is prevented. In the case of concrete in compression, the stress-strain relationship will be somewhat different from that obtained by testing standard concrete cylinder under uniform compression because a strain gradient exists in a flexural member (Chen and Ho, 2014). Usually, a reduction factor for the concrete strength is used to take into account of the effect of strain gradient. Denoting this strength as f_c, the complete material laws for concrete and steel reinforcement for a flexural member may be represented by the curves in Figures 2.4(a) and (b) respectively. Mathematically, stress may be expressed as a function of strain as (Chen and Ho, 2014):

$$f_c = f_1\ (\varepsilon_c) \tag{2.11}$$

$$f_s = f_2\ (\varepsilon_s) \tag{2.12}$$

With the strain diagrams across the section and the stress-strain relationships of concrete and reinforcing bars when known, the stress resultants, C_c and T_s for the compression and tension stress blocks in concrete may be written as (Chen and Ho, 2014):

$$C_c = \alpha_c f_c b_c \tag{2.13}$$

$$T_s = \alpha_t f_t b\ (d - c) \tag{2.14}$$

Where α_c and α_t denote the mean stress factors for the compression and tension stress blocks, respectively.

Denoting the distance of the line of action of the compressive and tensile stress resultants, C_c and T_s, from the top face as γ_cc and γ_tc, respectively the force and moment equilibrium equations for the flexural problem under consideration can be written as:

$$C_c = A_s f_s \tag{2.15}$$

Where, C_c is the compression force acting at the concrete section which is also equal to the tensile force acting at the tensile section. Similarly,

$$M = C_c \gamma_c = A_s f_s \gamma_t c \qquad (2.16)$$

Where, M is the bending moment acting either at the concrete or steel section.

The values of the stress block (γ_c and γ_t) can be obtained by integration of the section once the respective stress block and the stage of loading concerned is defined

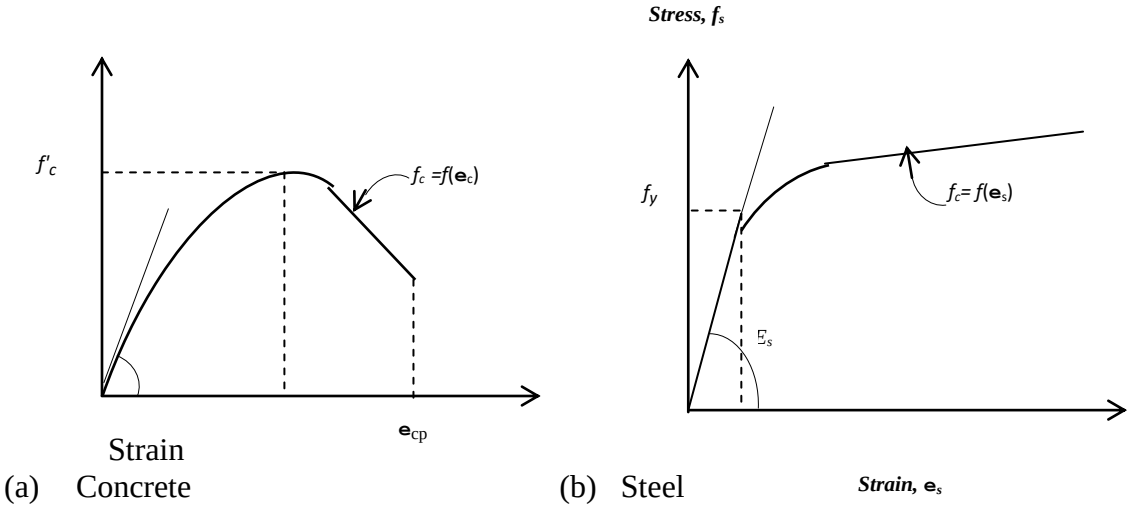

Figure 2.4: Typical material laws for concrete and steel in compression

In an analysis problem, the cross sectional parameters, b, d, A_s are given. Therefore, we have five unknowns which can be theoretically solved by using five equations ($\Sigma P_v = 0$; $\Sigma P_h = 0$; $\Sigma v_x = 0$; $\Sigma m_x = 0$ and compatibility equations). However, due to non-linearity of some of the equations, no closed-form solution is possible. One convenient way of solving this problem is to assume a value for the concrete strain, ε_{cm}, which increases as the applied moment (or load) is used, thus providing the additional condition needed to obtain the solution. For an assumed value, ε_{cm}, stress, f_s and strain, ε_s in the reinforcing bars, the neutral axis depth, c and the corresponding applied moment, M can be obtained.

The curvature of the section can then be calculated from the linear strain distribution shown in Figure 2.5 as (Wright and Macgregor, 2012):

$$\Phi=\frac{\varepsilon_{cm}}{c} \qquad (2.17)$$

By selecting a series of incremental values for ε_{cm} and calculating the corresponding moments M and curvatures Φ from Equations (2.16) and (2.17), the complete response of the section in terms of moment – curvature relationship can be obtained, the terminating point being represented byε_{cm}, reaching a value,ε_{cm}, the crushing strain of the concrete. The values of ε_{cm} is usually specified in the code of practice. According to the ACI 318-2005, it is taken as 0.003 and for BS 8110; 1997, it is taken as 0.0035 for concrete.

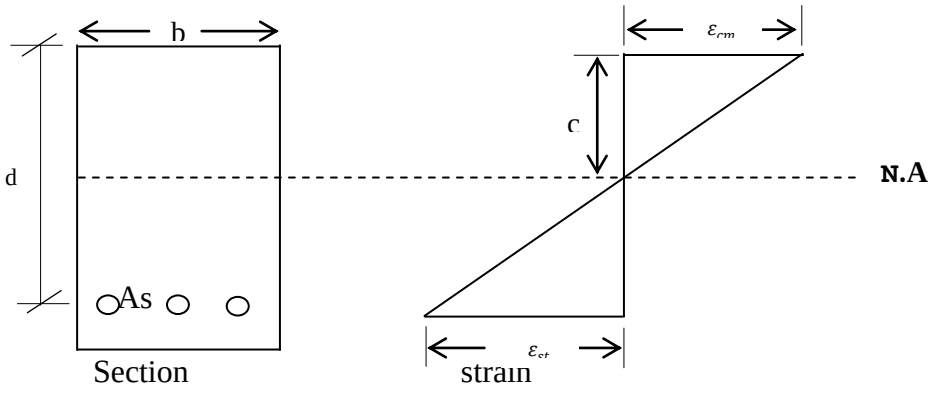

Figure 2.5: Linear strain distribution in RC beam section

A typical moment – curvature (M- Φ) curve that can be constructed using the general bending theory as shown in Figure 2.6 (Wright and Macgregor, 2012).This curve represents the fundamental characteristics of a flexural member, from which the deformations, such as deflections curvature and rotations of the member are calculated.

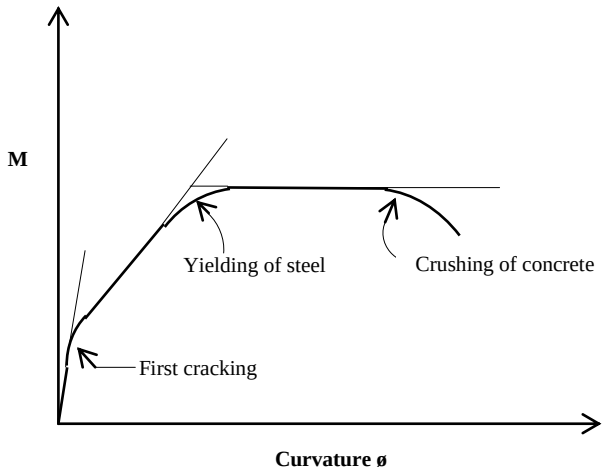

Figure 2.6: Typical Moment-curvature relation for a beam section

2.3.2 Crack in structural elements

Formation of flexural cracks in beams is detrimental to structural safety as it affects the serviceability of the structure. Excessive crack width can impair corrosion resistance. Therefore, control of cracking helps improve serviceability. The role of cracks in the corrosion of reinforcing steel is controversial (ACI 224). One view point is that cracks reduce the service life of structures by permitting more rapid penetration of carbonation and allow chloride ions, moisture and oxygen to reach the reinforcing steel. Another point of view is that while cracks accelerate the on-set of corrosion, the corrosion is localized. With time, chlorides and water penetrate un- cracked concrete and initiate more widespread corrosion. Consequently, after a few years of service, there is little difference between the amount of corrosion in cracked and un-cracked concrete. Whichever is the case, it is obvious that crack width need to be controlled to enhance serviceability.

Sofi and PhaniKumar (2015) opined that in the investigation of flexural crack width, the following factors are imperative:

1. Stress or strain in steel is the most important parameter.

2. The thickness of concrete cover and the cross-sectional area of concrete surrounding each bar are also important geometric variables;

3. The crack width on the tension face is affected by the strain gradient from the level of the steel to the extreme tension face.

Research studies on cracking behavior of beams have been conducted by researchers. The CEB-FIP model code for concrete structures (1990) gives the European approach to crack width evaluation and permissible crack widths. It further, proposed an equation for predicting crack width for reinforced concrete beams. Crack control is provided by calculating the probable crack width and proportioning structural elements so that the computed width is less than some predefined value. Most equations predict the probable maximum crack width, which usually means that about 90% of the crack widths in the member are below the measured value (experimental value). Research, however, has shown that isolated cracks in beams in excess of twice the computed maximum can occur (Holmberg and Lindgren, 1970) although generally, the coefficient of variation of crack width is about 40% (Leonhardt, 1977). There is evidence that this range in crack width variability can increase with size of the member (ACI Committee 224, 1972).

ACI 318-95 proposed equation (2.18) for predicting the probable maximum crack width

$$W_{cr} = 0.0763\, f_s (d_c\, A)^{1/3} \times 10^{-3} \qquad 2.18$$

However, ACI 224-01R crack width prediction equation which has an edge over others was adopted for the study and is as stated in equation (2.19).

$$W_{cr} = [(11 \times 10^{-6})\, (d_c\, A_c / n\beta)^{1/3}] f_{st} \qquad 2.19$$

The code has also provided a guide for reasonable crack width for reinforced concrete beam exposed to varying conditions (Table 2.1).

Table 2.1: ACI 224 Guide for reasonable crack width for reinforced concrete beam

Exposure Condition	Crack width (mm)
Dry air of protective membrane	0.41
Humidity, moist air, soil	0.30
Deicing chemicals	0.18
Sea water, sea water spray, wetting and drying	0.15
Water retaining structures	0.10

Source: ACI 224

2.4 Design for Minimum Ductility

2.4.1 Code provisions

To avoid going through time consuming nonlinear moment-curvature or Load-deflection analysis, some simplified design guidelines have been established in numerous design codes for providing minimum flexural ductility of RC beams. These guidelines restrict either the amount of tension steel ratio within a certain fraction of the balanced steel ratio, or the neutral axis depth at ultimate state within a certain fraction of the effective depth or the neutral axis depth respective to the balanced section. The provisions for minimum flexural ductility in RC beams by various renowned design codes are summarized as follows:

(i) ACI 318-2002: Limits the tensile strain in the extreme tension steel to 0.004, which is more or less equal to the tension steel ratio of 0.75 of the balanced steel ratio.

(ii) NZS 3101-1995: Restricts the neutral axis depth to $0.75x_b$, where x_b is the neutral axis depth of the balanced section.

(iii) BS 8110-1997: and DGHSC (Concrete Society 1998) specifies the neutral axis depth to be less than or equal to 0.5d for all concrete grades with $f_{cu} \leq 60\text{N/mm}^2$, which is further extended to 100N/mm^2 in DGHSC; where d is the effective depth of the beam section and f_{cu} is the concrete cube strength.

(iv) EC 2 (1992): Limits the neutral axis depth to 0.45d for f_{cu} < 50N/mm^2 or 0.35d for $f_{cu} \geq$ 50N/mm^2.

(v) GB 50011 (2007): Requires the neutral axis depth to be smaller than 0.35d for all concrete grades. It should be noted that most of the provisions in the above codes were derived using test results of normal strength reinforced concrete beams and are independent of the material strengths (for example concrete strength and steel yield strength).

As a result, the minimum flexural ductility that is ensured in Normal strength reinforced concrete beam (NSRC) could be fairly guaranteed. Therefore the above limiting factors should be dependent on the material strengths in addition to just the tension steel ratio, ρ or neutral axis depth), and they should be derived using nonlinear moment-curvature or load-deflection analysis.

2.5 STRESS-STRAIN RELATIONSHIP OF CONSTITUTIVE MATERIALS

In nonlinear moment-curvature or load- deflection analysis, it is necessary to know the stress-strain relationship of each constitutive material in order to trace the stress-strain paths from which the axial force and the moment equilibriums of the section could be determined. Ho and Pam (2000) states that the complete load-deflection behavior of NSRC beams could be determined accurately only if the stress-strain Curve for normal strength concrete and steel is employed.

2.5.1 Steel reinforcement

Typical bilinear stress-strain curve of steel reinforcement consists of a linearly elastic and a perfectly plastic portion. BS 8110 (1997) and ACI 318 (2002) assume that the stress-strain curve of steel reinforcement is symmetrical in compression and tension and the

strain hardening portion is neglected. Mathematically, the bilinear stress-strain relationship of steel is expressed as:

(a)linearly-elastic portion ($0 \leq \varepsilon_s \leq \varepsilon_y$). In the linearly elastic portion, the stress is proportional to the strain, related by the proportionality constant, E_s, which could be determined from the actual tensile test of reinforcement. For analytical purpose, E_s may be taken fairly accurate as 200000N/mm^2. As such, the stress in steel is taken as:

$$f_s = E_s \varepsilon_s \tag{2.18}$$

(b) Perfectly-Plastic Portion ($\varepsilon_s > \varepsilon_y$)

In the yield plateau, the stress remains constant at yield stress, f_y until it reaches the fracture strain:

$$\varepsilon_y = {f_y}/{E_s} \tag{2.19}$$

and $f_s = f_y$ (2.20)

2.5.2 Concrete

The stress- strain curve of un-confined concrete in BS 8110 (1997) for design of RC beams extends only from zero to the ultimate concrete strain which is equal to 0.0035. Such stress-strain curve is only sufficient for nonlinear moment-curvature analysis up to the point of peak moment. For evaluation of the complete moment-curvature that extends well into the post-peak range of RC beams, a better concrete stress-strain curve extending well beyond the point of peak stress is needed. The Hognestad stress-strain model (modified by Macgregor (1997) for concrete and steel was used for this study.

2.6 Failure Modes of Beam Section

RC beams containing various combinations of structural parameters such as concrete compressive strength, tension steel ratio and compression steel ratio will have more or less a similar flexural performance at elastic stage. Nevertheless, they will exhibit different flexural behavior within the inelastic range with different modes of failure. The post-peak behavior and failure modes of typical Reinforced Concrete beam, could be categorized into three groups, namely tension failure, concrete compression failure and combined failure. Depending on the amount of tension and/or compression reinforcement, the beam will fail in different fashions. The work of Pam et al, (2001) on simply – supported beams made of Normal strength concrete (NSC) and High strength concrete (HSC) showed that initially fine vertical cracks appeared at the elastic stage when the bending moment reached 50% to 60% of the flexural strength. Upon further loading, the flexural cracks formed previously developed in length and width, as well as increased in number. At the same time, there are some minor inclined cracks between the simple support and the point of load application, that is, within the region of bending moment and shear interaction. Theses crack patterns can be used to determine the failure mode of the beam.

2.6.1 Under-reinforced sections

Under-reinforced concrete beams contain tension reinforcement ratio, ρ less than the balanced steel ratio, ρ_b, which is the amount of tension steel ratio that leads to the "balanced failure" of a beam section. In this type of beam, the flexural cracks formed during the elastic stage keep on extending and increasing in number until the beam reaches the post peak region. Meanwhile, it is observed that the tension reinforcement

yields before the concrete crushes in compression, which leads to a large inelastic deflection at the section subject to the largest bending moment. The large deformation provides sufficient ample warning before the beam reaches failure and thus indicates an excellent flexural ductility performance. This type of beam is suitable in the typical construction of RC moment-resisting frames obeying the design philosophy of "strong column – weak beam" (Park and Paulay 1975) such that large rotational demand in the potential plastic hinge could be accommodated.

2.6.2 Over – reinforced Sections

Over-reinforced concrete beams contain tension reinforcement ratio, ρ more than the balance steel ratio, ρ_b. In this type of section, the extreme compressive concrete fiber will reach the ultimate concrete strain, ε_{cu}, prior to yielding of tension reinforcement in the post-peak stage. As a result, crushing of concrete occur while the tension steel remains elastic. After reaching the peak moment capacity, the beam experiences only small deflection at critical section. Depending on the amount of tension reinforcement, the failure mode could vary from brittle to explosive manner (Pam *et al.*, 2001). Obviously, over-reinforced concrete beams are not suitable for RC moment resisting frames adopting "strong column – weak beam" design philosophy, as large ductility capacity could never be met in the potential plastic hinge region within the beam.

2.6.3 Balanced Section

Theoretically speaking, in between the failure modes of under- and over- reinforced concrete sections, there exists failure mode such that the compression crushing of concrete occurs simultaneously with the yielding of tension reinforcement after the beam has reached the peak moment capacity but prior to the failure moment. Such a section is

defined as the balanced section and its tension steel ratio is exactly the same as the balanced steel ratio. In this type of section, even though the tension steel yields when reaching ultimate, however, it is accompanied by the compression failure of concrete. Hence, the failure mode of the balanced section is also considered sudden and brittle, (Pam *et. al*., 2001) which is regarded unsuitable in the design of RC moment-resisting frame in earthquake resistant structures.

2.7 Recycling building materials

As global population increase, so too will the need for accommodation. However, current mainstream building methods are unsustainable producing large amounts of carbon dioxide (Co_2) both during construction and throughout a building's life. However, sustainability is becoming a priority for developers, and with many exciting innovations taking place in the construction industry. This can be achieved through the recycling of building materials.

2.7.1 Recycling scrap metal

A building material at the end of its useful life becomes a scrap and is usually dumped. This dumping of scrap promotes leaching of toxic substances into the environment as well as causing visual pollution, safety issues and degradation of wildlife habitats. Hence the dire need for scrap and scrap metal in particular to be recycled rather than dumped, the waste problem would be solved and significant energy savings realized.

Steel is the World's, as well as North America's most recycled material (ISRI, 2015). In the United States alone, nearly 70 million tons of steel were recycled in 2002. Every ton of steel that is recycled saves 1,134 Kg of iron ore, 635.04 Kg of Coal, and 54.43 Kg of

Limestone (MCA, 2004). New steel made with recycled material uses as little as 26% of the amount of energy that would be required to make steel from raw materials extracted from natural source (MCA, 2004). This shows that there is a dire need for steel recycling for sustainability.

Two different processes, the basic oxygen furnace (BOF) and the electric arc furnace (EAF) are used to produce steel. Both processes consume recycled scrap steel to produce new steel. According to the steel recycling institute (www.recycle-steel.org) the total recycled content from BOF production of 50.1143 million tons of steel in north America during 2002 was 16.0548 million tons or 32.0% total recycled content. The post-consumer recycled content was 22.6% and the post = industrial minus recycled content was 8.4%. The total recycled content from EAF production of 49.1598 million tons of steel in North America during 2002 was 47.1598 million tons or 95% total recycled content. The post-consumer recycled content is 59.0% and the post-industrial recycled content is 31.9%. From the comparison of both method of production, EAF process uses almost all scrap metal.

2.7.2 Recycling non-ferrous metal

2.7.2.1 Aluminum recycling

Aluminum is also recycled extensively from both post-consumer and post-industrial sources and provides the most valuable component for most municipal recycling efforts. A survey in late 2003 indicated that the recycled content of domestically produced, flat-rolled Aluminum products for the building and construction market was approximately 80-85%. In addition, at the end of their long useful life, Aluminum roofing and siding panels can be repeatedly recycled back into similar products with no loss of quality.

Producing Aluminum from recycled materials requires only 5% of the energy required to produce Aluminum from bauxite ore, and every ton of recycled aluminum saves four tons of bauxite ore (MCA, 2004). Additionally, using recycled Aluminum instead of raw materials reduces air pollution generation such as Co2, S0x, Nox by 95% and water pollution by 97% (MCA, 2004).

2.7.2.2 Copper recycling

Copper is also a routinely recycled non- ferrous metal with the highest scrap value of any building metal. Copper being a non-ferrous metal with high cost makes it a favoured product for collection and sale to non-ferrous-scrap recycling Companies. The scrap is melted down and reformed into a new, appropriate product. This re-melting takes only about **15%** of the total energy consumed in mining, milling, smelting and refining Copper from ore. The average recycled content of all copper products is 44%. Copper wire is the biggest consumer of Copper and that Copper must be pure. As a result, Copper wire production uses little Copper scrap. The remaining Copper market including Copper roofing, contains 75% scrap. Almost 50% of this is post consumer scrap.

2.7.2.3 Zinc recycling

Over 30% of Zinc used in all applications comes from recycling. In building applications especially in Europe, more than 90% of old rolled Zinc products are recovered and generally recycled into other types of Zinc products. At the end of its life, rolled Zinc products used in building applications have an attractive residual value of up to 75% of the price of new Zinc. The average recycled content of Zinc in building products is estimated to be less than 9% (MCA, 2004).

The amount of energy used to produce Zinc from its ore is the lowest of all non-ferrous metals on the market. Energy consumption is even lower when Zinc is produced from recycled material; between 0.49% and 19.70% of the amount of energy used to produce Zinc from ore (MCA, 2004).

2.7.2.4 Recycling building components

Metal roofing and siding panels are made with the highest recycled content from the most recyclable materials on Earth, making them a great choice not only for present use, but, also future generations' use (MCA, 2004). Because recycling saves much of the energy required to produce metal products, recycled content is also being recognized and done for economic and environmental reasons.

Among numerous design considerations such as landscaping that saves water or highly reflective metal roofs that reduce air conditioning load to save energy, Leadership in energy and environmental design (LEED) rating system considers the 'post- consumer' and 'post-industrial recycled content of building materials. Although recyclability is not a part of the LEED rating system, it is still good to know that metal panels may be recycled when their useful life ends many years from now and contribute again to future products recycled content and recyclability of Steel, Aluminum, Copper, Zinc and other metals, allow for metal construction products to be reused over and over again with little or no loss in value.

The use of recycled metal products and recycling scrap metal can contribute greatly to the sustainability of building materials. The benefits can be summarized as follows:

(a) Conserve valuable natural resources and raw materials.

(b) Avoid air and water pollution; using recycled materials generally creates less pollution.

(c) Save land fill space by ‘closing the loop’. Recycling also ensures materials don’t become littered.

(d) Reducing the need to dig for virgin materials conserves soil integrity and wildlife habitats.

(e) Saves energy, recycled products require less energy to manufacture thus conserving oil and reducing greenhouse gas emissions.

(f) Reduce cost of sourcing raw materials; these savings should be passed on to the consumers in reduced prices.

2.8 Reinforcing Steel Bar from Metal Scrap

The production of reinforcing steel bar from metal scrap consists of collecting scrap metals, sorting them, melting in a furnace, mixing with ingredients (additives), casting the molten metal into moulds for making the ingots. After the solidification of the ingots, the moulds are stripped. The ingot is then placed in a soaking pit for heating to ensure that entire uniformity of cross-section is achieved. This is then followed by rolling of the stock and cooled in air. The rolled bar is subjected to cold working by twisting to increase the strength of the bar. Finally, the bar is inspected and stored.

Reinforcing steel bars production from scrap metals has attracted the attention of researchers like Torok *et al,* (2000) who tried to classify the scrap metal commonly used into three groups: namely home scrap, process scrap and obsolete scrap according to the place of generation, chemical composition or physical properties. The most difficult to

handle among the group for steel maker is the obsolete scrap, because its recovery is difficult; This type of scrap is often mixed or coated with other materials such as copper, glass, plastic, zinc etc. The chemical composition of obsolete scrap fluctuates widely depending on its origin and can affect the mechanical properties of the reinforcing bars.

For the proper behavior of engineered structures, a complete understanding and knowledge of the real behavior of materials is of prime importance. The physical properties of structural materials are expected to meet the demand of fundamental assumptions underlying structural codes of practice on which designs are based. Locally manufactured reinforcing steel bars from scrap metal are typical examples.

In developing countries such as Nigeria, Kenya, Ghana and Senegal where imported steel is very expensive, milling companies have taken up the challenge to recycle obsolete vehicle and machine metal parts for the production of structural and reinforcing steel bars. Research studies on strength and ductility characteristics of reinforcing steel bars milled from scrap metal by Kankam and Adom-Asamoah (2002); Alabi and Onyeji (2010); Ejeh and Jibrin (2012) showed that reinforcing bars do not meet the BS 4449 (2005) maximum limit of 0.25% for carbon requirements for mild steel. The phosphorus and Sulfur impurities in the steel bar from three Companies exceeded the preferred limit of 0.05% for phosphorus and 0.01% for Sulfur. These excess carbon, sulfur and phosphorus contents increase the strength and hardness of the steels and at the same time decreases their ductility, making them brittle.

The British standard BS 4449 (2005) defines the characteristic strength of steel reinforcement as that value of the yield stress below which not more than 5% of the test material should fail. The presence of variation in the strength of bars is as a result of such

factors as variation in the chemical composition and heat treatment. With regard to quality control of chemical properties, steel manufacturers must give the results of chemical composition analysis for carbon (c), manganese (Mn), Silicon (Si), Sulfur (S) and Phosphorus (P) for all steels. The BS 4449(2005) and KS 573 give maximum chemical percentage composition of mild steel as S 0.06%, P 0.06%, C 0.25%, M_n 0.65% and Si 0.25%. The different elements have varying effects on the behavior of mild steel. The carbon level affects the strength and hardening properties of steel. Higher carbon contents increase strength but reduce ductility. Excessive levels of Phosphorus and Sulfur, which are non-metallic impurities reduce fracture toughness. For modern steel-making practice, Sulphur and phosphorus are preferably maintained at less than 0.01%. Steel grade with a high level of dissolved gasses, particularly oxygen and Nitrogen, can behave in a brittle manner, if not controlled by addition of small elements with a particular affinity for them to float out in the liquid steel at high temperature. Manganese, Chromium, Molybdenum, Nickel and copper also affect the strength to a lesser extent than carbon, although their sole effect is on the Microstructure of the steel. Research by Shunichi and Morifumi (2006) showed that addition of alloying elements such as Niobium and Vanadium was effective to increase strength of reinforcing steel bars.

2.8.1 Reinforcing bar produced from scrap metals in Nigeria

Typically, scrap ferrous metal are generated at household, mechanic garages and other commercial ventures (Figure 2.7). Scavengers, that is, waste pickers recover scrap iron from waste dumps and sell them to scrap dealers who in turn supply the scrap to steel mills using thirty tons truck (Plate 2.1). The steel mills recycle the scraps to produce reinforcing bar as shown in the flow chart in Figure 2.8.

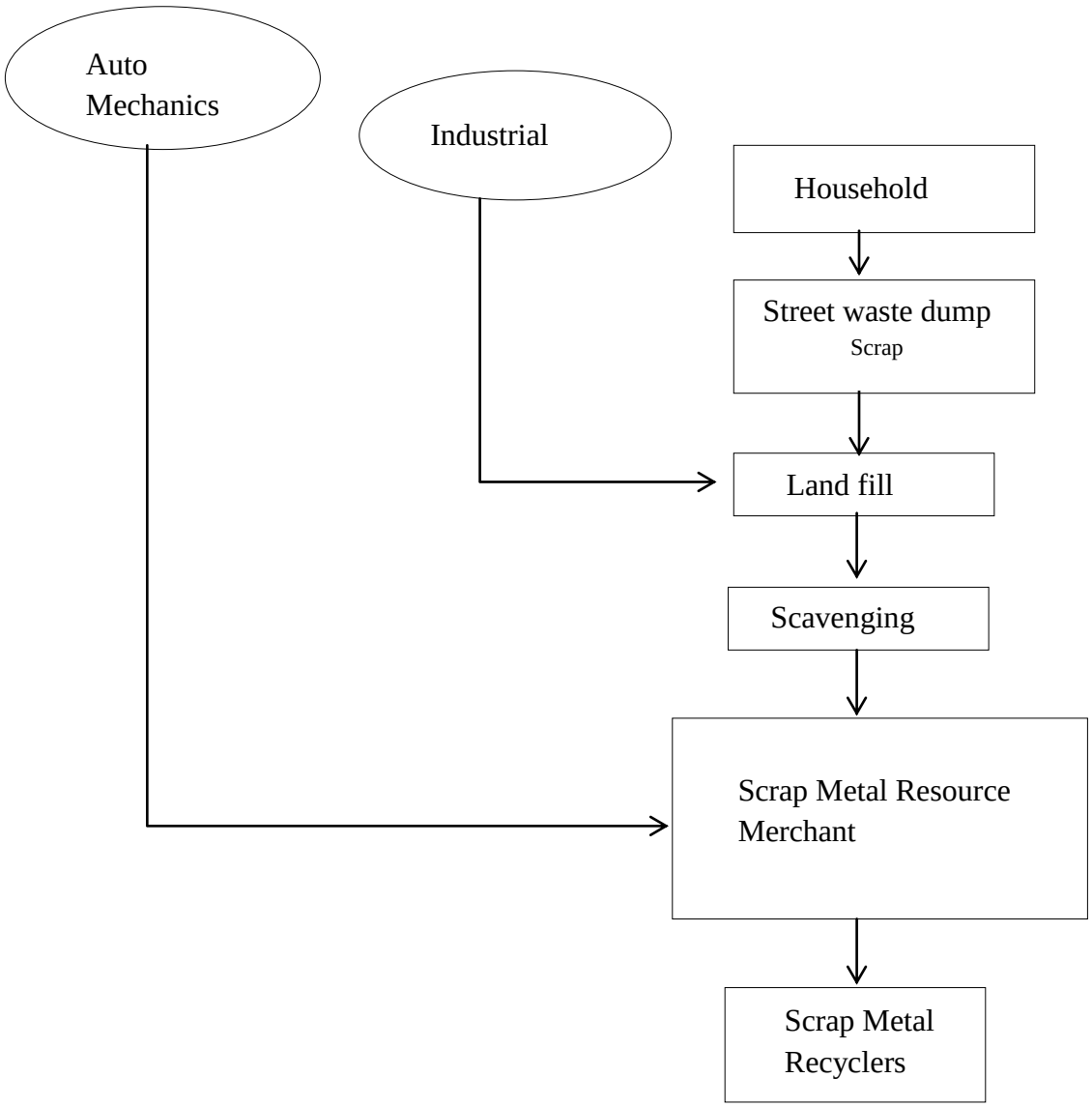

Figure 2.7: Scrap metal generation in Nigeria (Ohimain, 2013)

As part of the research, a field visit was made to a few of the Milling Companies to find out how the scrap metal is recycled. The few companies visited produces iron from basic raw materials and recycles scrap iron to new products for reuse. Scraps are typically brought to the point of reception by the heavy duty trucks (Plate 2.1). The scraps are sorted in two ways: namely, magnetic and manual separation. Non- ferrous metal is separated from the ferrous metal using magnetic separation devices. Manual separation is used to separate the ferrous metal into two phases, the low carbon iron and the high carbon iron. The high carbon metal takes longer time to melt and produce more waste (slag), while the low carbon iron produce less waste and melt faster. Figure 2.6presents the flow chart for the production of iron bars using 100% metal scraps. Less than 7% slag is produced in high quality scrap metal while 7 – 15% is produced in low quality metal scrap. Due to the shortage of iron ore, the companies and most of other rolling mills (not visited) are currently operating on 100% scrap iron for the production of new products.

Plate 2.1: Scrap Metal transportation to recycling centre (source: Fieldwork, 2014)

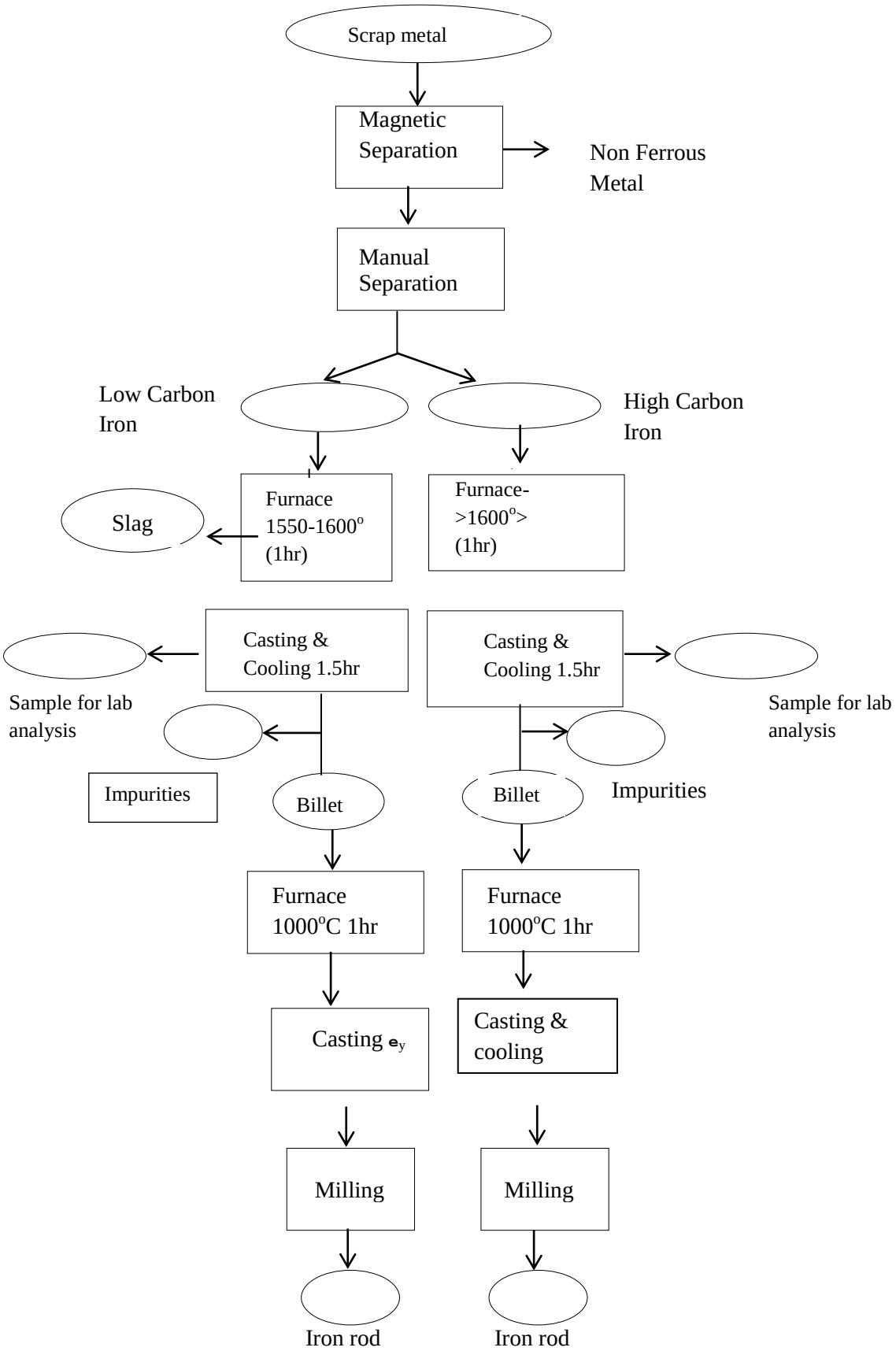

Figure 2.8: Scrap Metal recycling process (Ohimain, 2013)

2.8.2 Factors Affecting Ductility of Reinforced Concrete Beam

2.8.2.1 Confinement of the concrete Section

Ductility in reinforced beams can be enhanced either at the concrete, compressive or tensile steel section and several researchers have reported findings of works on them. One such way is confinement of the concrete section using closely spaced and stronger stirrups to achieve better concrete confinement which increases concrete strength and subsequently enhances both ductility and strength of concrete against compression in beams. It improves the flexural ductility of a beam in two ways: It increases the uni-axial strength of concrete and also increase ductility of the beam due to the increased ductility of the tri axially stressed concrete (Kwan et. al, 2004). Furthermore, the work of Hadi (2006) shows that utilizing confining reinforcement can achieve ductile behavior in HSC beams. Stirrups closely spaced were used to confine concrete in the over – reinforced beam; loaded to failure and load – deflection response recorded.

Test results show that ductility can be achieved by using confining reinforcement or confining reinforcing technique. The degree of ductility obtained is proportional to the confining pressure provided. The work of Kwan et al (2004) further showed that the flexural ductility, ultimate concrete strain and balanced steel ratio of high strength concrete (HSC) significantly increased for beams provided with confinement as compared with those without confinement. This is true because, HSC is relatively brittle and its use in a RC member result in unacceptable low flexural ductility. The work of Olivia and Mandal (2005) shows that with same the concrete strength and tensile steel but varying confinement at the section, the ultimate compressive strain and ductility is increased for HSC while for the work of Shin et al (1989) with the same concrete

strength, amount of tensile steel and compression steel but different confinement spacing shows that a closer spacing has a contribution to postpone the buckling of the compression steel and failure takes place in tension steel without any effect on ductility. The study further showed that the amount of confinement reinforcement in the concrete section of the beam, within the studied range, did not have appreciable effect on the load-deflection curves of the beams tested.

2.8.2.2 Tensile steel reinforcement ratio, (ρ)

ACI 318 (2005) has recommended that to ensure ductility in RC beams, the tensile steel ratio, ρ, in the beam should not exceed $0.75\rho_b$ where ρ_b is the steel ratio for a balanced section of a beam. Ashour (2000); Hadi and Schmidt (2002) have reported influence on ductility of beams due to varying tensile reinforcement ratio. In the work of Kumar et al (2006) on high performance concrete beams, varying concrete strength and tensile reinforcement ratio resulted in a displacement ductility index of 1.17 – 2.26. Also, the work of Elrakib (2013) has shown that for high strength concrete (HSC) beams, low tensile reinforcement ratio and varying concrete strength improves displacement ductility index up to a concrete strength of 75MPa and then decreases as concrete strength increases. The work of Shin et al, (1989), Peng *et al,* (2012) was able to establish that the parameter, ρ/ρ_b, which is the degree of beam section under reinforced or over reinforced ,$\rho \; and \; \rho_b \; are$ the tension and balanced steel ratios respectively, was found to be the controlling factor in determining the shape of the load-deflection curves, especially the post yield portion of the curve of the beams tested. Members with low values of ρ/ρ_b had large deformation with relatively long yield plateau in the load – deflection curve when

the steel yields and the drop in the load- carrying capacity was very gradual beyond the maximum indicating a ductile beam. On the other hand, beams with high values of ρ/ρ_b often exhibited a significant drop in load-carrying capacity immediately upon crushing of the concrete in compression that usually accompanied the attainment of the maximum load indicating brittleness.

The work of *Pam et al,* (2001) on six simply-supported RC beams containing various tension reinforcement areas and concrete strength shows that steel ratio, ρ and concrete strength, f_{cu}, are the deterministic factors affecting the flexural ductility of singly RC beams. Based on the tests results, a simple formula for estimating the flexural ductility of Normal strength concrete (NSC) beam was proposed. The maximum limits of tension steel ratio in singly RC beams to ensure minimum ductility has been proposed. The work of Iffat *et al,* (2011) shows that with a steel ratio of 0.0128, a ductility index less than 4.0 was obtained while those with less of steel ratio led to higher ductility index. This shows that in flexural ductility design of beams, tensile reinforcement should be minimal as much as possible.

2.8.3 Concrete strength (f_{cu})

Shin *et al.,* (1989), Pam et al, (2001), Siddique and Rouf (2008) in their separate works on normal strength concrete (NSC) and high strength concrete (HSC) beams showed that at a given steel ratio, ρ increase in concrete strength, f_{cu}, increases flexural ductility slightly for up to 80MPa when flexural ductility begins to decrease with further increase in concrete strength.

2.8.4 Yield Strength of Steel

Research results (Gravina, 2002) have also shown that properties of steel such as yield strength of steel, strain hardening ratio, manufacturing process do affect the ductility of reinforcing steel which in turn affect ductility indices of RC beams (Gravina 2002).The yield strength of steel affects ductility. High tensile strength invariably means increased brittleness. This indicates a reduced yield plateau and a very limited strain hardening region. This means that the yield region and its capacity to absorb energy through inelastic deformation is severely limited as shown in Figure 2.9.

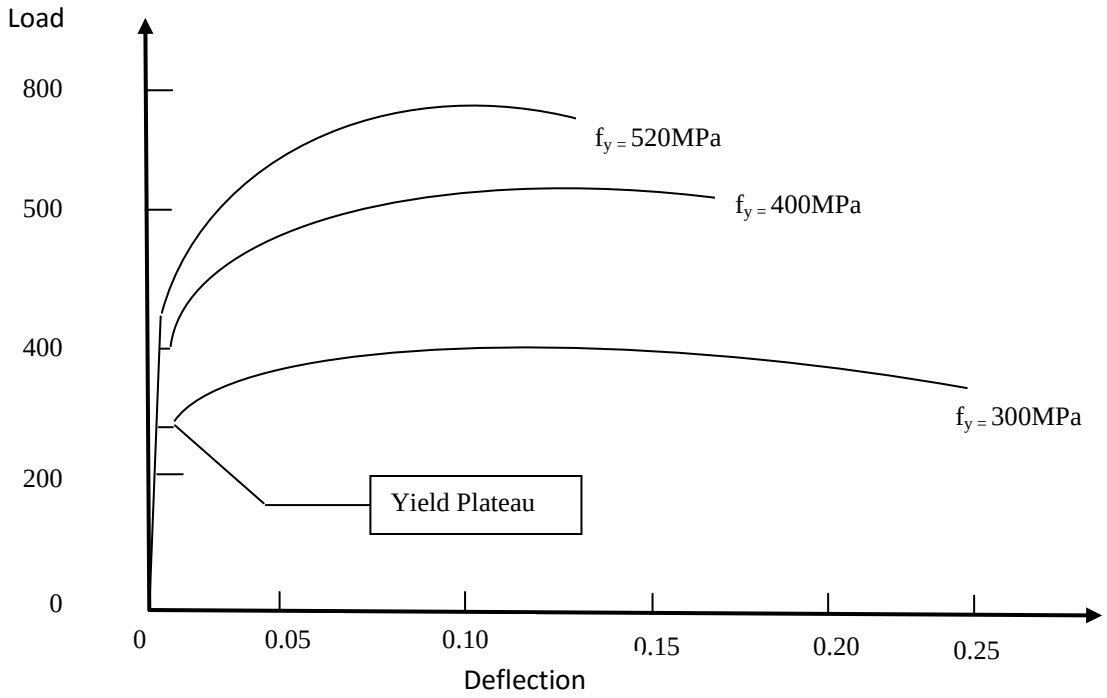

Figure 2.9: Effect of yield strength on ductility (Paulay and Priestly, 1992).

Figure 2.9indicates that ultimate strain and the length of the yield plateau decrease as the yield strength of steel increases. This development is not desirable because the steel stress

that may develop in a beam section may greatly exceed the yield stress leading to shear failure or unexpected flexural hinging. It is desirable to limit the steel grade used in construction. It has also been found by Kwan et al, (2003) that the flexural ductility will increase with an increase in compression steel, but reduce with an increase in tension steel yield strength. Moreover, the confinement reinforcement would also increase the beam's flexural ductility. Furthermore, Siddique and Rouf (2008) studied the effect of yield strength of steel on the curvature ductility of concrete beams. They used yield strength values of 276, 345 and 414 MPa for the study. Tests results show that as yield strength increases, curvature ductility of beams decreases.

Evaluation of deflection ductility indices of RC beams is not too complex. However, there is no simple method for direct evaluation of flexural ductility other than conducting experiment. To evaluate analytically the flexural ductility of a beam section, it is necessary to first analyze the complete Load- deflection relation of the section covering both the pre-peak and post-peak ranges and then calculate the amount of inelastic deflection that the section could sustain before complete failure. There is limited analysis of the load-deflection relation of concrete beams reinforced with rebars milled from metal ferrous scraps; hence there are a few data on the flexural ductility of such beams.

2.9 Summary of literature findings

Most code provisions for minimum ductility of beams requires that neutral axis depth does not exceed 0.5d, where d is the effective depth of the beam. ACI 318 requires that the maximum tensile steel ratio is $0.75\rho_b$, where ρ_b is the balanced steel ratio. The work of Preetha *et al,* (2013) showed that deflection ductility indices of beams was evaluated

on the basis of deflection computation which required accurate measurement of deflections throughout the loading history of the beams; the effective moment of inertia, (I_e) was utilized herein to measure the deflection, and stiffness of the beams for the study. For the test specimens to fail in flexure the beams were designed as under reinforced (steel ratio, $\rho < 0.75\rho_b$), where ρ_b is the balanced steel ratio. Deflection ductility index is the ratio of deflection at ultimate state of the beam to the deflection at yielding point of tensile steel. These were measured accurately.

The work of Pam *et al*, (2001) showed that the maximum flexural strength obtained for normal strength concrete beams was close to the theoretical prediction using the parabolic stress block given in BS 8110 (1997) and the ultimate concrete strain recommended by DG HSC (concrete society (1998). They also observed that the strength reserve that was normally available in NSRC beams gradually decreased as the concrete strength increased. The work of Shin *et al*, (1989), Pam *et al*, (2001), Siddique and Rouf (2006) showed that for a given steel ratio, increase in concrete strength, f_{cu} increases flexural ductility slightly for up to 80 MPa when flexural ductility decreases with further increase in concrete strength. Kwan *et al*, (2003) also showed that flexural ductility decreases with increase in steel ratio.

The work of Gravina (2002) showed that the yield strength of steel influences flexural ductility; increase in yield strength of steel lowers ductility. However, Peng *et al*, (2012) established that the Parameter, $\rho/\rho b$, which is the degree of beam section under-reinforced or over- reinforced is the controlling factor in determining the shape of the Load-deflection curve, especially the post yield portion of the curve of the beams tested.

Members with low values of $\rho/\rho b$ had large deformations with relative long yield plateau in the load-deflection curve when the steel yields and the drop in load- carrying capacity was very gradual beyond the maximum indicating a ductile beam. On the other hand, beams with high values of $\rho/\rho b$ exhibited a significant drop in load-carrying capacity and deformation.

To harmonize the work of kwan *et al*, (2003), Gravina (2002) and Peng *et al*, (2012), Beams were designed incorporating ACI 318 code provisions, produced with normal strength concrete, tensile steel ratios and yield strength values obtained from tensile strength test of rebars, analyzed and tested under a four –point loading to investigate the influence(s) of tensile steel ratio, concrete strength and yield strength of steel on deflection ductility of the beams. Details of materials and methods of the study are given in chapter three.

CHAPTER 3

MATERIALS AND METHODS

3.1Tests on aggregates and reinforcing bars

The constituent materials used in the concrete for casting of beams are Ordinary Portland cement with a specific gravity of 3.15, natural river sand of fineness modulus of 2.32. Crushed stones having maximum aggregate size of 19 mm served as coarse aggregate. Three concrete mixes were used in casting the test specimens. The mixes were designed to obtain concrete compressive strengths of 20, 25 and 30N/mm^2. The designed mix is in Table 3.1. Six standard 150 x 150 x 150 mm cubes were cast with each beam, cured in the same manner and kept under the same environmental conditions as the beams to obtain the aforementioned compressive strength. Two Prisms (100 mm x 200 mm x 500 mm) were also cast for each beam for the determination of modulus of rupture of the beam. The modulus of elasticity of concrete (E_c) was determined using the ultrasonic Pulse velocity (UPV) method (Plate 3.1).

Plate 3.1: Determination of modulus of elasticity of concrete, E_c, by the U.P.V method

Table 3.1 Design Mix for specimens

Target strength of concrete (N/mm^2) Materials Unit (kg/m^3)	20	25	30
Cement	340	380	409
Sand	554	556	559
Coarse aggregate	1388	1296	1187
Water	190	210	225

Reinforcing steel bars milled from ferrous metal scraps were used for the study. Samples of diameters 8mm and 10mm were obtained from the open market for example Dei-Dei market, Abuja, and tested for tensile strength. The test was conducted using universal testing machine (Plate 3.2) at the structures laboratory, Department of Civil Engineering, Kaduna Polytechnic, Kaduna, Nigeria. The samples were machined to standard shapes using the lathe machine (Plate 3.3). Plate 3.4 shows machined sample test specimens ready for tensile testing. Each specimen has a gauge length of 500mm. A sample was fixed into the jaw of the machine and as load was gradually applied it stretches the sample test bar until it failed. From the tensile strength test, yield and tensile strength, percentage elongation and modulus of elasticity were determined. The test was based on BS 4449 (2005) provisions. The result is as shown in table 3.3 and the stress-strain curves for the sample specimens are shown in figure 3.4.

Plate 3.2: Universal testing machine used for the study

Plate 3.3: Machined steel samples ready for testing

Plate 3.4: Sample test specimens being Machined using the Lathe Machine

Table 3.2: Yield strength and Modulus of Elasticity of steel samples used for the study

S/No	Market assumed diameter (mm)	Nominal diameter measured (mm)	Effective sectional area (mm^2)	Yield stress (N/mm^2)	Modulus of Elasticity (kN/mm^2)
1	8	7.45	43.59	400	200.00
2	8	7.68	46.32	360	180,00
3	10	9.48	70.58	400	200.00
4	10	9.72	74.20	360	180.00
5	8	7.62	45.60	387	193.50
6	8	7.79	47.66	353	176.50
7	8	7.88	48.77	390	195.00
8	8	7.69	46.45	350	175.00
9	10	9.78	75.12	395	197.00
10	10	9.88	76.67	355	178.00
11	8	8.02	50.52	390	195.00
12	8	8.04	50.76	355	178.00
13	8	7.92	49.27	385	193.00
14	8	7.89	48.89	355	178.00
15	10	9.68	73.59	395	197.50
16	10	9.72	74.20	355	178.00
17	8	7.88	48.77	390	195.00
18	8	7.61	45.48	355	178.00

3.2 Design of a beam

The beam is assumed to be a lintel supporting three courses of block work of a residential building subjected to large displacement. The beam design is the design of a structural element which means that the applied moment is known from structural analysis and it is required to compute the (beam section) dimensions of an adequate concrete section and the amount of steel reinforcement, given the material properties (concrete strength and yield strength of steel). The beam was designed based on the provisions of ACI 318(2005) so as to be able to sustain large inelastic deformation. Accordingly, the tensile steel ratio, $\rho \leq 0.75\rho_b$and the neutral axis depth/effective depth ratio (c_{max}/d) =0.5 was adopted. These provisions among others give desirable flexural behavior of the beam. In other words, this ratio predicts the failure mode of the beam, ductile failure when the ratio ≤ 0.5or at brittle failure when it is > 0.5. From Figure 3.1, the applied moment, M_a due to the loading is given as:

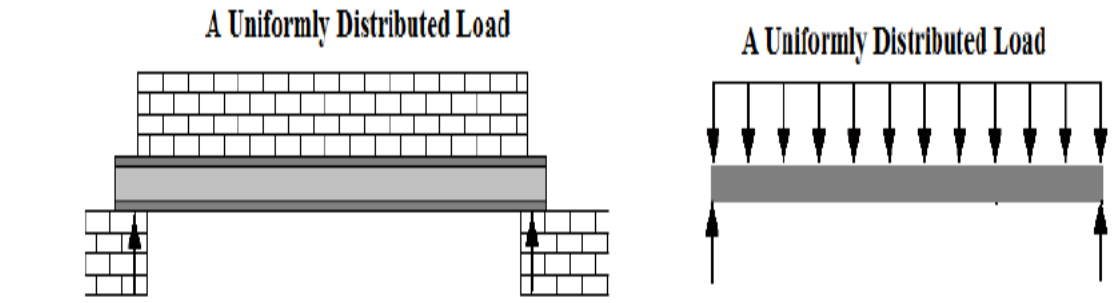

➢ The beam may be simply supported or built in.

Figure 3.1: Simply supported or built-in beam

$M_a = \frac{wl^2}{8}$ and (3.1)

$M_a = A_s f_y Z$ (3.2)

$A_s = \frac{M_a}{f_y . Z}$ (3.3)

Equation (3.3) was used to select flexural tensile steel requirements from steel tables.

To ensure that steel bars selected from steel tables produced a desirable ductile section, the balanced steel ratio, ρ_b, was determined using equation (3.4)

$\rho_b = \frac{0.85\beta}{f_y} f_{cu} \frac{(600)}{f_y + 600}$ (3.4)

The steel ratio, ρ for each beam was calculated using equation (3.5)

$\rho = \frac{A_s}{bd}$ (3.5)

The ductility design for each test specimen is in table 3.2

Moment of resistance, M_u of the beam is given by the relation:

$M_u = \rho b d^2 f_{st} \left[1 - 0.59\rho \frac{f_{st}}{f_c}\right]$ (3.6)

Compare $M_a \leq M_u$ for adequacy of design and final adoption of beam cross section.

Design of beam details is shown in appendix C.

3.3 Experimental Program

In the experimental program, eighteen RC beams (100 x 200 x 1000 mm) were produced. All the beams were produced in the Structures Laboratory, Department of Civil Engineering, Kaduna Polytechnic, Kaduna, Nigeria and tested under a four point bending arrangement (Kumar, *et al*, 2006). Beam set-up and details are shown in Figure 3.1 and 3.2 respectively. Since very low ratios of flexural reinforcement were used, the flexural

capacity of all test specimens was lower than the diagonal cracking capacity. Therefore, no shear cracks were expected. However, steel stirrups, R06 @ 150mm for minimum shear reinforcement which was obtained from S_y = V/0.002ht was provided. Also, Φ6 mm bars were provided as hanger bars to hold the stirrups in position.

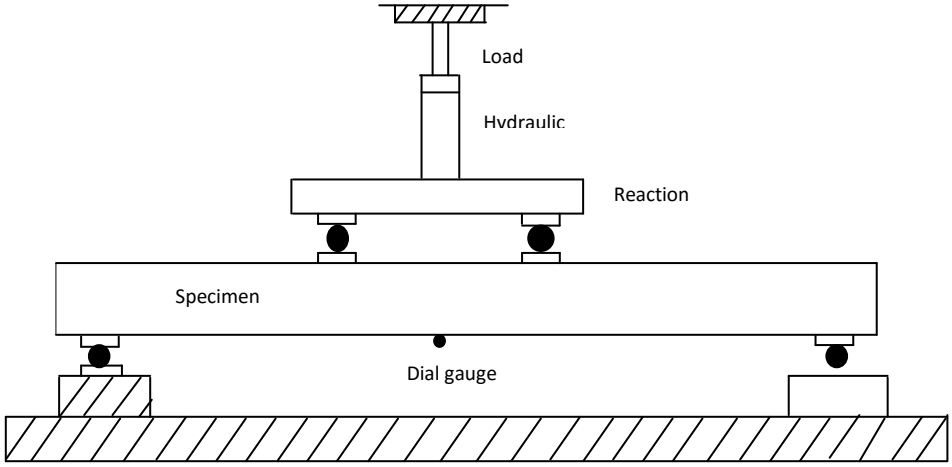

Figure 3.2: Beam set-up (Kumar *et al*, 2006)

Test specimens were grouped into three series according to their compressive target strengths (20, 25 and 30N/mm^2). Each series consists of six beams. In each series, three different reinforcement ratios were used; That is, the test specimens in each series have the same concrete compressive strengths but varying steel ratios. This is to determine the effect of steel ratios on the ductility indices of the beams. Similarly the beams in one series is compared with beams in another series, the effect of concrete strengths on ductility indices of the beam is also determined. The specimens and the experimental design are in Table 3.2. Concrete clear cover of 20 mm was provided for all beams.

The longitudinal reinforcements were placed in the mould. The mix of the constituent materials was designed and mixed using a rotating drum mixer. The fresh homogeneous mix was poured into the beam mould and compacted using a needle vibrator. The beams

were de molded after 24hrs and cured in a curing tank for 28 days. After 28 days of curing, they were white washed so as to observe crack patterns during testing.

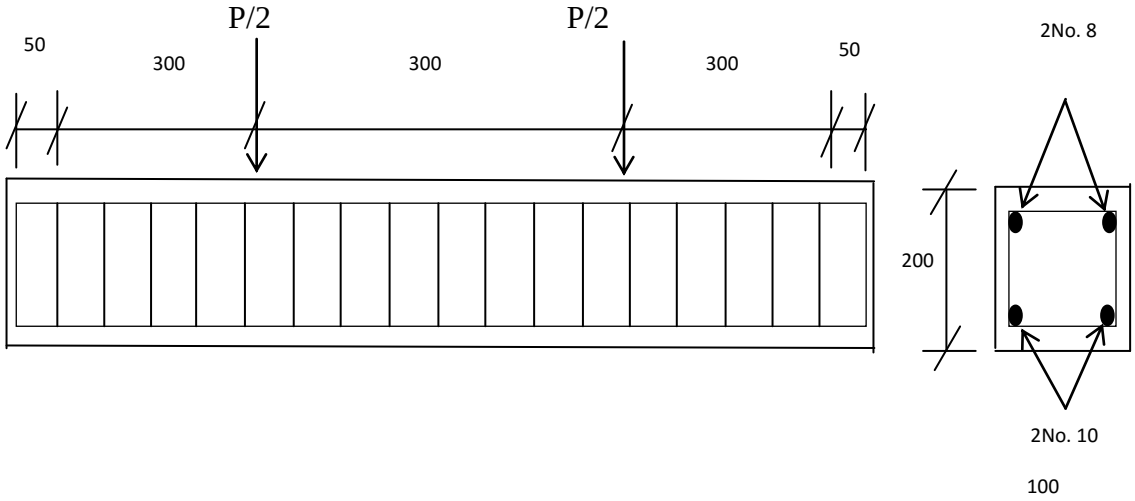

Figure 3.3: Reinforcement details for beam

Plate 3.5: Universal testing machine used for the study

Table 3.3 Ductility designed details of test specimens

s/no	Beam ID	Comp. strength f_{cu} (N/mm^2)	steel ratio (ρ)	Bal. steel ratio (ρ_b)	Area of steel A_s (mm^2)
1	BM 1	21.33	0.012	0.0268	201.06
2	BM 2	21.33	0.012	0.0231	201.06
3	BM 3	21.33	0.0092	0.0268	157.08
4	BM 4	21.33	0.0092	0.0231	157.08
5	BM 5	21.33	0.0058	0.0268	100.53
6	BM 6	21.33	0.0058	0.0231	100.53
7	BM 7	26.71	0.012	0.0335	201.06
8	BM 8	26.71	0.012	0.0287	201.06
9	BM 9	26.71	0.0092	0.0349	157.08
10	BM 10	26.71	0.0092	0.0301	157.08
11	BM 11	26.71	0.0058	0.0349	100.53
12	BM 12	26.71	0.0058	0.0301	100.53
13	BM 13	30.00	0.012	0.0335	201.06
14	BM 14	30.00	0.012	0.0289	201.06
15	BM 15	30.00	0.0092	0.0335	157.08
16	BM 16	30.00	0.0092	0.0287	157.08
17	BM 17	30.00	0.0058	0.0349	100.53
18	BM 18	30.00	0.0058	0.03014	100.53

3.3.1 Determination of modulus of elasticity of concrete (E_c)

This is required as an input in Equation (2.5) for the determination of moment of inertia (I_{cr}) of the cracked section of the beam. The Ultrasonic Pulse velocity test equipment consists essentially of an electrical Pulse generator, a pair of transducers, an amplifier and an electronic timing device for measuring the time interval between the initiation of a Pulse generated at the transmitting transducer and its arrival at the receiving transducer. The Pulse velocity was carried out using cylindrical specimens in accordance with the requirements of EN12504-4. A Pulse of longitudinal vibrations is produced by an electro-acoustic transducer held in contact with one face of the cylindrical concrete (Plate 3.1), transmitted through the concrete and received by the receiving transducer. The time of transmission is recorded. Longitudinal Ultrasonic Pulse velocity is given by:

U.P.V = $\frac{D}{T}$ m/s (3.7)

The U.P.V is related to the dynamic modulus, E_d , by the relation;

E_d = U.P.$V^2 \rho c \frac{(1+\square)(1-2\square)}{(1-\square)}$ where μ is Poisson ratio (3.8)

$E_c = 1.2E_d$ (3.9)

The modulus of elasticity of concrete, E_c, for grade 20, 25 and 30N/mm^2 were determined.

3.4 Theoretical Measurement of Ductility Indices

The ductility indices were measured from an analytical approach using an iterative procedure. Each beam was analyzed using strain compatibility approach in order to satisfy the section equilibrium. The approach is based on the use of Hognestad Model

(modified by Macgregor, 1997) for concrete and steel, which utilizes the material characteristics of the concrete and reinforcement. The model is shown in Figure 3.4.

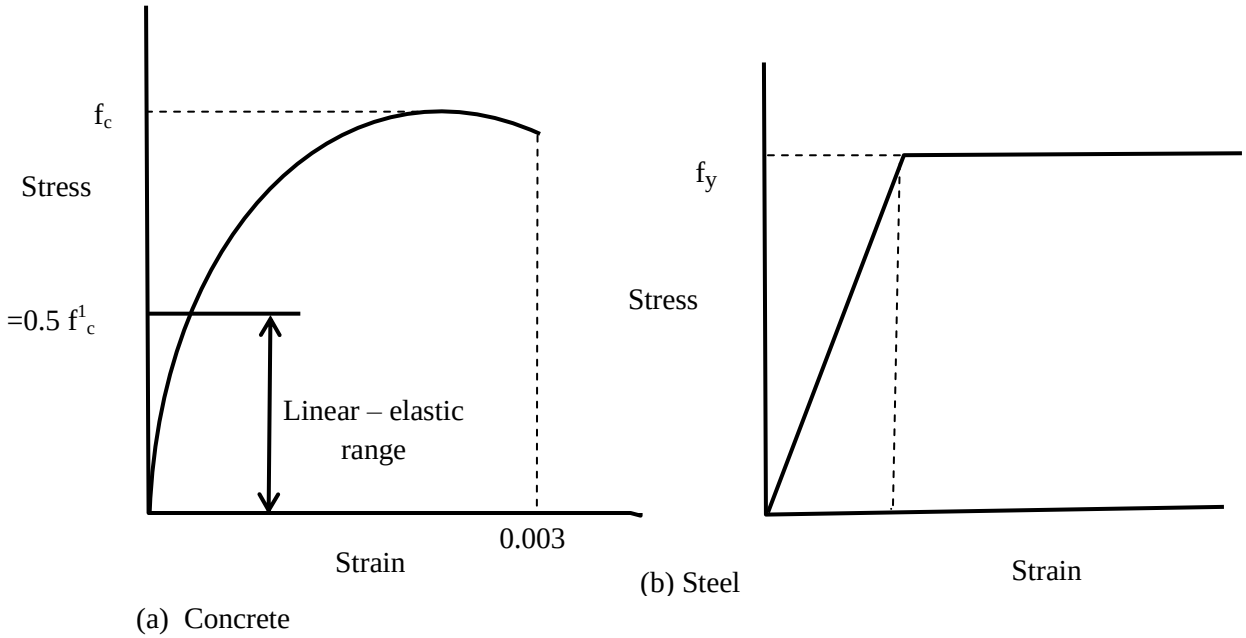

Figure 3.4: Hognestad's stress-strain Models for concrete and steel as modified by Magregor (1997).

The following assumptions were made for the study:

(i) Plane sections remain plane before and after bending.

(ii) There is strain compatibility between compressive and tensile sections of the beam.

(iii) The beam section obeys Hognestad Models for concrete and steel.

(iv) There is linear strain distribution throughout the full depth of the beam and tensile strength of concrete is neglected.

(v) Failure at beam section occurs by compressive concrete crushing at ultimate concrete strain, $\varepsilon_{cu} = 0.003$.

Parallel to experimental investigation, an iterative non - linear analytical procedure was derived for predicting the load-deflection response of a rectangular under reinforced concrete beam reinforced with rebars milled from scrap metals. The four point bending arrangement (fig 3.2) is considered. This configuration generates tension along the bottom fibers of the beam and constant bending moment at mid-span. Figure 3.5 shows the beam cross-section dimensions, strain-stress profiles across the depth of the beam with tensile steel only. In developing the analytical model, Bernoulli's hypothesis of strain compatibility, that plane sections remain plane before and after bending which requires perfect bonding between steel and concrete is employed. This give rise to linear strain distribution throughout the full depth of the beam; and tensile strength of concrete is neglected. Behavior of concrete in compression is modeled using Hognestand model (Fig 3.4a) for concrete as modified by Macgregor (1997). Behavior of reinforcing steel in both compression and tension assumed to be bilinear was defined using Hognestad model for steel (Fig 3.4b) as modified by Macgregor (1997). The constitutive behavior of the beam section is shown in Figure 3.5 from which the strain compatibility and section equilibrium equations were derived for the model. The model assumed beam failure by compressive concrete crushing at ultimate concrete strain, $\varepsilon_{u,}$ of 0.003. In order to define the section geometry and materials models, the beam section was subdivided into a series of very thin layers. A computer Program using MATLAB version 2013 was written to predict the load-deflection behavior of rectangular concrete beams under monotonic loading. The script of the program is in Appendix H. From the load-deflection values, the ductility indices for the beams were evaluated. The key steps in the prediction algorithm are as follows:

(i) An assumed value of strain in the range of 0.0001 to 0.003 (failure strain) acts on the extreme concrete fiber of the beam.

(ii) The neutral axis depth, c, was estimated such that the compressive force (Fc) due to the concrete section and due to the steel section, (F_s), are in equilibrium; that is (F_c= F_s).

$$F_c = bcf_{cu} -\left[\frac{\varepsilon_{cm}}{\varepsilon_0} - \sqrt[3]{\frac{(\varepsilon_{sm})^2}{\varepsilon_0}}\right] \quad (3.10)$$

$$F_S = Es\ \varepsilon_{cm}\left[\frac{d-c}{c}\right]A_S \quad (3.11)$$

(iii) The moment (M_{cc}) due to the concrete section was determined using the relation;

$$M_{cc} = bc^2 f_{cu}\left[\frac{\varepsilon_{cm}}{\varepsilon_0}\right]\left[\frac{2}{3} - \frac{1}{4}\frac{\varepsilon_{sm}}{\varepsilon_0}\right] \quad (3.12)$$

(iv)The Moment (M_s) due to the steel section is given by the relation:

$$M_s = f_s\ (d-c) \quad (3.13)$$

(v) The total moment, M = M_{cc}+ $M_s$which gave rise to the curvature (Φ) of the beam section was determined: (3.14)

(vi) Load was determined from the moment using the relation; $P = 6\frac{M}{L}$ (3.15)

(vii) The deflection,δ, due to the load: $\delta = \frac{23Pl^3}{1296EI}$ (3.16)

(sample calculated values is in appendix B).

(viii) Increase the strain value, ε_{cm} and repeat step (ii) to (vii) until the strain value, ε_{cm} attains the failure strain, ε_{cu}. This resulted to a series of load-deflection values.

(viii) The deflection ductility index, μ_Δ, for the beam was determined as the ratio of deflection at failure to the deflection at yield point of steel as expressed in Equation (3.17):

$$\mu_\Delta = \frac{\Delta\mu}{\Delta\gamma} \quad (3.17)$$

The load – deflection response curve of the beam which defines its behavior when loaded from inception to failure point is plotted and compared with experimental values. In other words, a computer program was written incorporating all the test variables of constituent materials attained in the Laboratory to predict the behavior of the beams which was compared with experimental values. The MATLAB Programme list is in Appendix H.

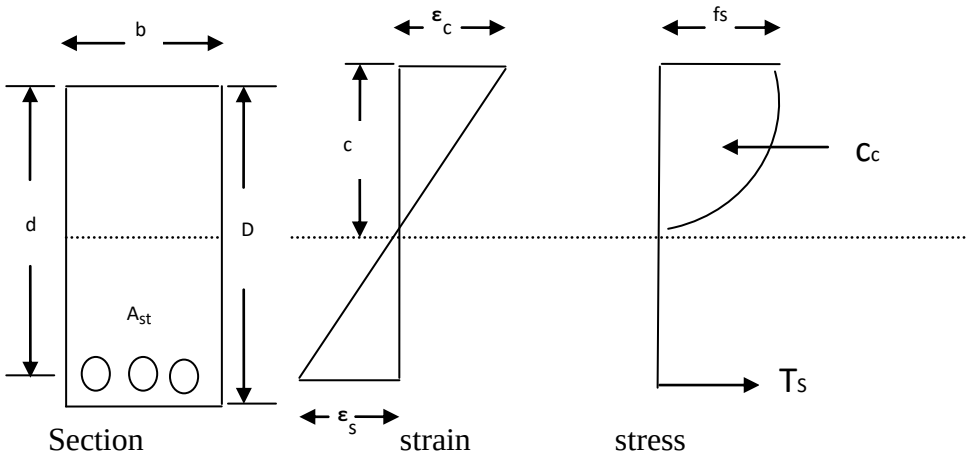

Figure 3.5: Stress- strain distribution of beam section

The results obtained from both the experimental, theoretical modeling and the discussions arising therein are given in chapter four.

CHAPTER 4

RESULTS AND DISCUSSION

4.1 Tests on Aggregates

Table 4.1shows particle size distribution of fine aggregates as percentage by weight passing sieve sizes; while Table 4.2 shows the distribution for course aggregate. Figures 4.1 and 4.2 show grading curves of fine and coarse aggregate sample used for the study respectively. The curves show well graded aggregate sample and the cumulative percentage fines values are within BS 882 limit values. The fineness modulus (f_m) for fine aggregate is 2.96 while that for course aggregate is 3.22.

Table 4.1 Sieve Analysis test for Fine Aggregate

Sieve size (mm)	Wt. Ret. (kg)	Cum. Wt Passing (kg)	Cum. % Finer	Cum. % Ret (kg)	BS Limit % Finer
10	0	10.36	100	0	100 - 100
5	0.18	10.18	98.26	1.74	89 - 100
2.36	0.72	9.46	91.51	8.69	65 - 100
1.18	3.14	6.32	61.00	37.00	45 - 100
600µm	3.98	2.34	22.59	79.42	25 - 100
300µm	1.96	0.38	3.67	96.34	5 - 48
150µm	0.3	0.08	0.77	99.24	0 - 15
Pan	0.06				

Fineness modulus (f_m) = 3.22

Table 4.2 Sieve Analysis test for Coarse Aggregate

Sieve size (mm)	Wt. Ret. (kg)	Cum. Wt Passing (kg)	Cum. % Finer	Cum. % Ret (kg)	BS Limit % Finer
19	1.4	13.6	90.67	9.33	100 - 100
10	11.76	1.84	12.27	87.73	85 - 100
5	1.67	0.17	1.13	98.86	0 - 25
2.36	0.12	0.05	0.33	99.67	0 - 5
Pan				295.59	0

F_m = 2.96

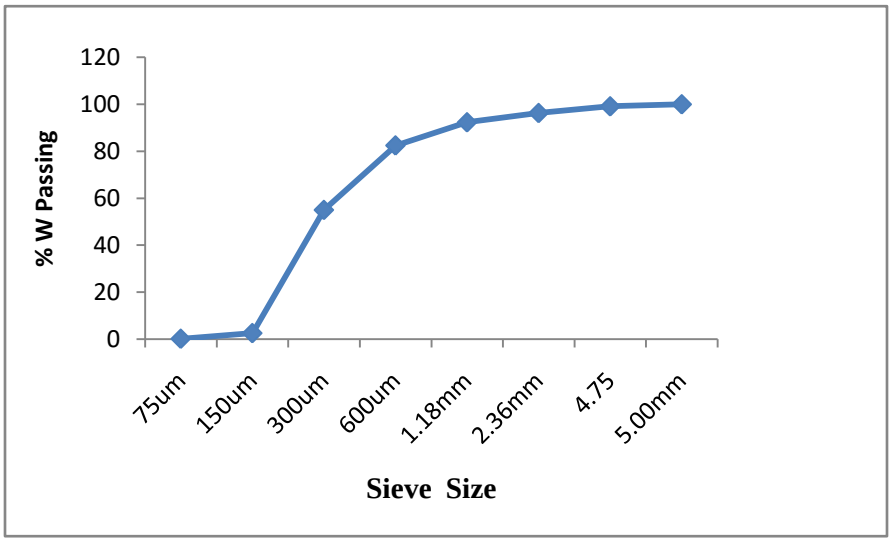

Figure 4.1; Grading Curve for Fine Aggregate

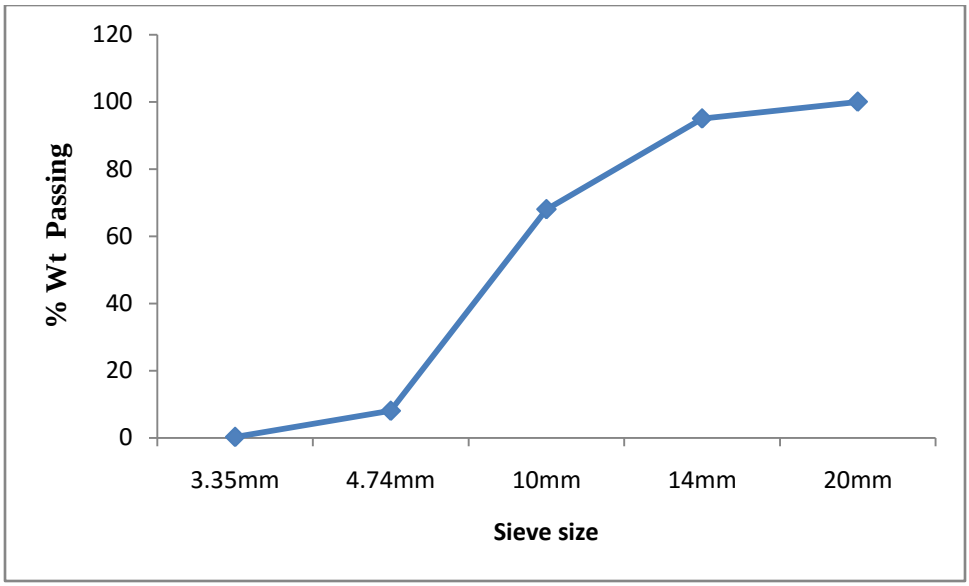

Figure 4.2: Grading Curve for Coarse Aggregate

4.2 Tensile Strength Tests on Reinforcing Bars Milled

The stress-strain curve for a particular material provides information on the yield strength, tensile strength, Young modulus, and percentage elongation. These variables give reasons for such mechanical behavior. Figure 4.3 to 4.6 show the average stress-strain curves of steel reinforcing bars produced from ferrous metal scraps by eight Companies in Nigeria. The yield strength was determined by drawing a line from an off set of 0.2% (0.002) on the strain axis, parallel to the elastic portion of the curve. The point at which the line meets the curve is the yield strength of the steel sample. The modulus of elasticity, E_s for the steel sample is the ratio of stress to strain which is the slope of the elastic portion of the stress-strain curve.

Figures 4.3 to 4.6 indicated that the yield stress (f_s) ranged from 360 to 480N/mm^2. Also, the modulus of elasticity, E_s, ranged from 175,000 to 220,000N/mm^2. For the

analytical study, a yield stress, f_y = 360 and 400N/mm^{2}and a modulus of elasticity, E_s = 200000N/mm^2 was adopted and the result is presented in Table 4.3.

Table 4.3: Result of yield strength and modulus of elasticity of steel samples used for the study

S/No	Market assumed diameter (mm)	Nominal diameter measured (mm)	Effective sectional area (mm^2)	Yield stress (N/mm^2)	Modulus of Elasticity (kN/mm^2)
1	8	7.45	43.59	400	200.00
2	8	7.68	46.32	360	180.00
3	10	9.48	70.58	400	200.00
4	10	9.72	74.20	360	180.00
5	8	7.62	45.60	387	193.50
6	8	7.79	47.66	353	176.50
7	8	7.88	48.77	390	195.00
8	8	7.69	46.45	350	175.00
9	10	9.78	75.12	395	197.00
10	10	9.88	76.67	355	178.00
11	8	8.02	50.52	390	195.00
12	8	8.04	50.76	355	178.00
13	8	7.92	49.27	385	193.00
14	8	7.89	48.89	355	178.00
15	10	9.68	73.59	395	197.50
16	10	9.72	74.20	355	178.00
17	8	7.88	48.77	390	195.00
18	8	7.61	45.48	355	178.00

Apart from the stress-strain curve of sample A, in Figure 4.3 which has a fairly smooth plateau, the rest curves have sharp triangular plateau. This is the extent of ductility of the steel sample. The stress-strain curves for the steel samples differ from each other. This is reasoned to be due to the chemical composition of its constituents (obsolete scrap metal), could fluctuates widely depending on its origin and which affects the mechanical properties of the reinforcing bars.

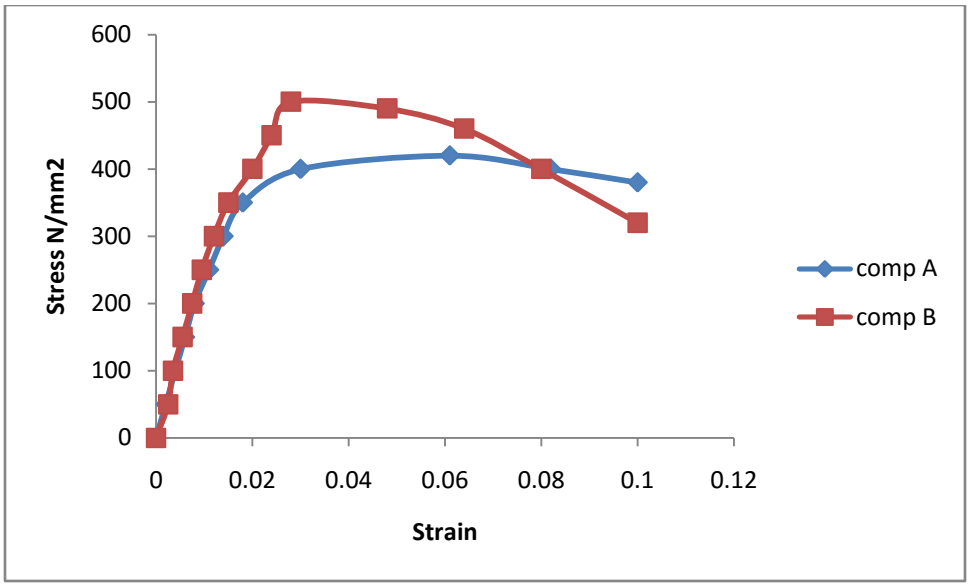

Figure 4.3: Average stress- strain curve of bars milled from ferrous metal scrap (Company A and B)

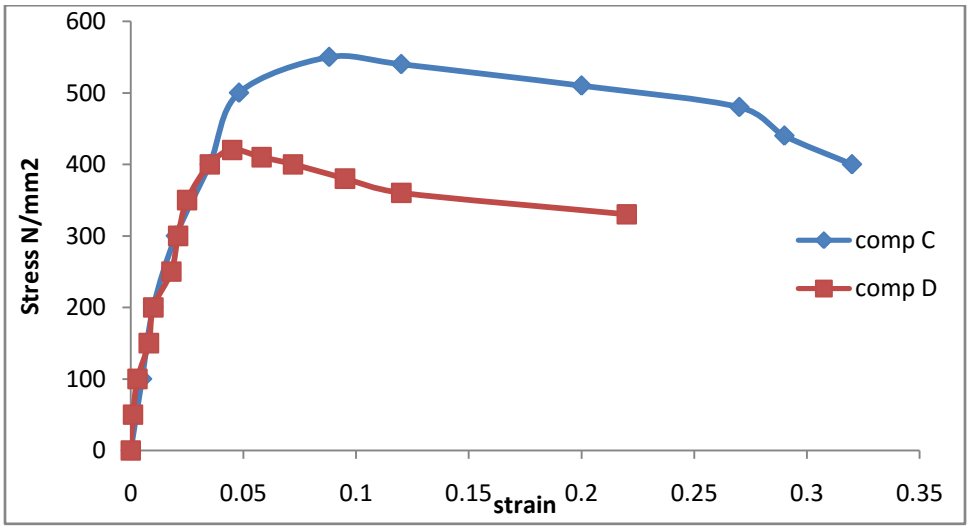

Figure 4.4 Average stress – strain curve for bars milled from ferrous metal scrap (Company C and D)

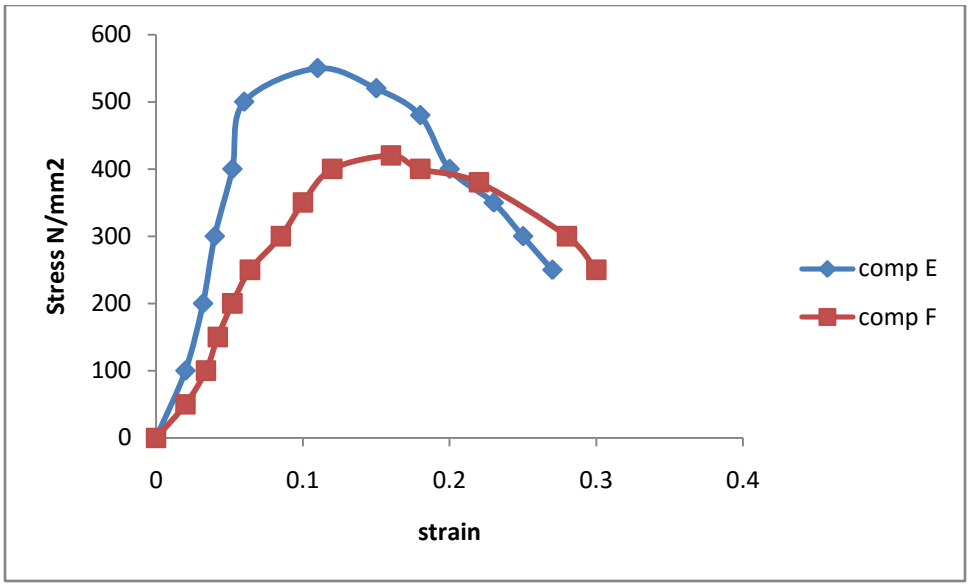

Figure 4.5: Average stress-strain curve for bars milled from ferrous metal scrap (Company E and F)

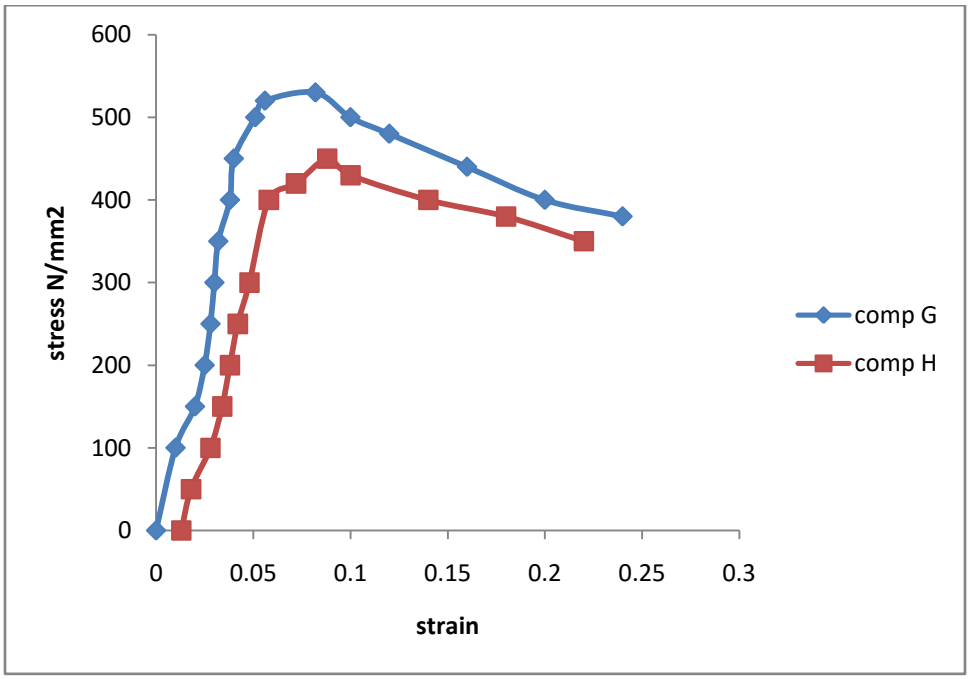

Figure 4.6: Average stress-strain curve for steel bars milled from ferrous metal scrap (Company G and H)

4.3 Load-Deflection Response of Beams

Figures 4.7 to 4.24 show the analytical and experimental load- deflection response of the beams tested. The deflection was measured at the mid span with detailed results in Appendix A and B. As can be seen from the figures, the curves exhibit a tri-linear response defined by elastic concrete cracking to steel yielding and steel yielding to failure stage. From inception of testing to cracking point, the resistance of the beam section is proportional to the applied load. This accounts for the linearity of the portion of the curve. From cracking to steel yielding, linearity of the curve was still observed but with reduction in slope of the curve. This is because, on cracking the concrete section lost its tensile strength and moment of inertia of the cracked beam section is less than that of the un- cracked section. This also accounts for the reduction in stiffness of the beam. At this stage, the tensile steel wholly resists the applied bending stress. At steel yielding to failure stage, there is a further reduction in slope of the curves because steel has yielded. This caused sharp increase in deflections with little or no increases in applied load. The curve becomes asymptotic to the horizontal axis as failure point is reached. A typical behavior of under-reinforced concrete beam is observed from these curves; that is, the stiffness is reduced after concrete cracking which leads to increase in deflection. The mean value of the ratio of the predicted deflection to the actual deflection across all the beams is 1.50, with a standard deviation of 0.28 and a coefficient of variation of 0.184. Statistically, the deflection values of the beams measured experimentally and theoretically has low variation. Similarly, the average value of the ratio of the predicted ultimate load to the actual ultimate load (observed in experiment) across all the beams is 0.91 with a standard deviation of 0.091 and a coefficient of variation of 0.10. This value

suggests that the theoretical approach predicts the load-deformation behavior of the beams within reasonable limits.

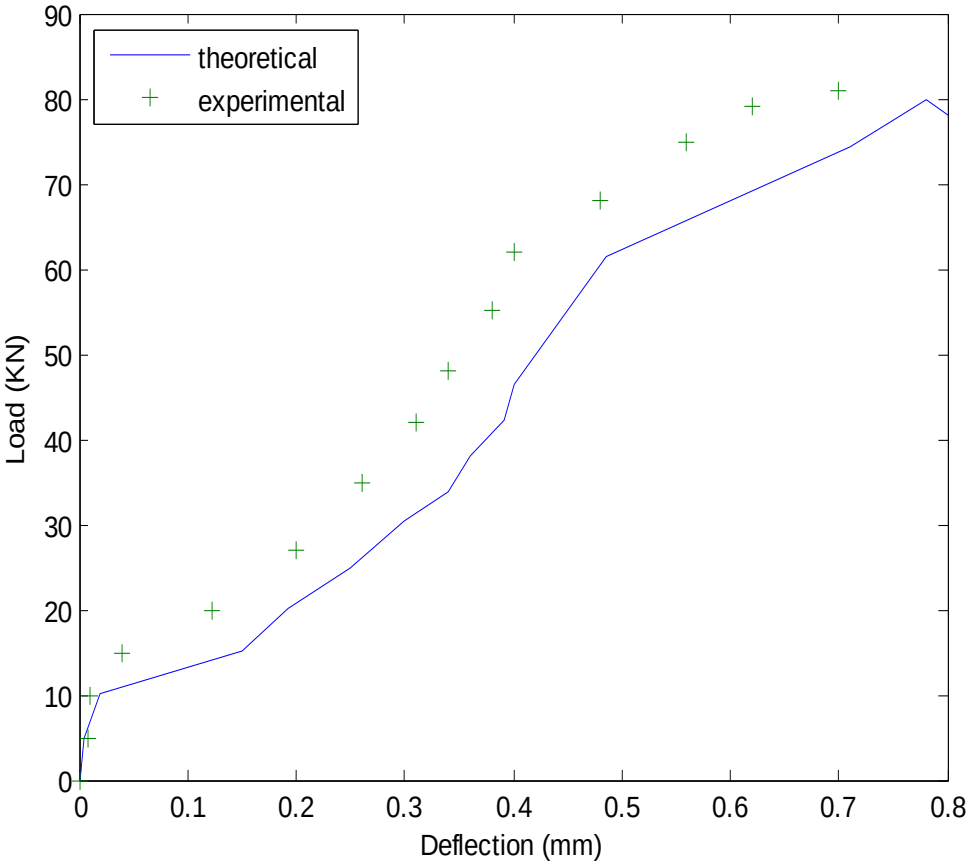

Figure 4.7: Load – deflection response of experimental and theoretical values for BM 1

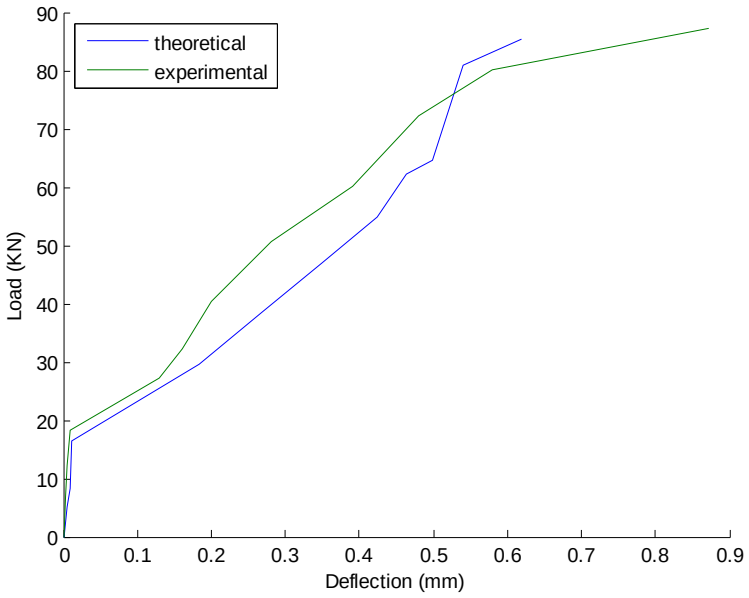

Figure 4.8: Load – deflection response values for BM 2

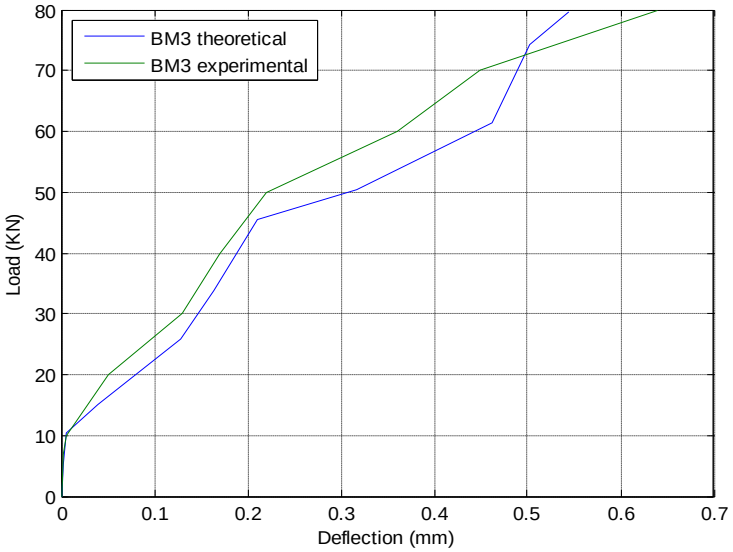

Figure 4.9: Load – deflection response values for BM 3

For Beams 1, 2 & 3, there is good agreement of load-deformation response between experimental and theoretical values up to yield point of steel and fairly good up to failure point of beam.

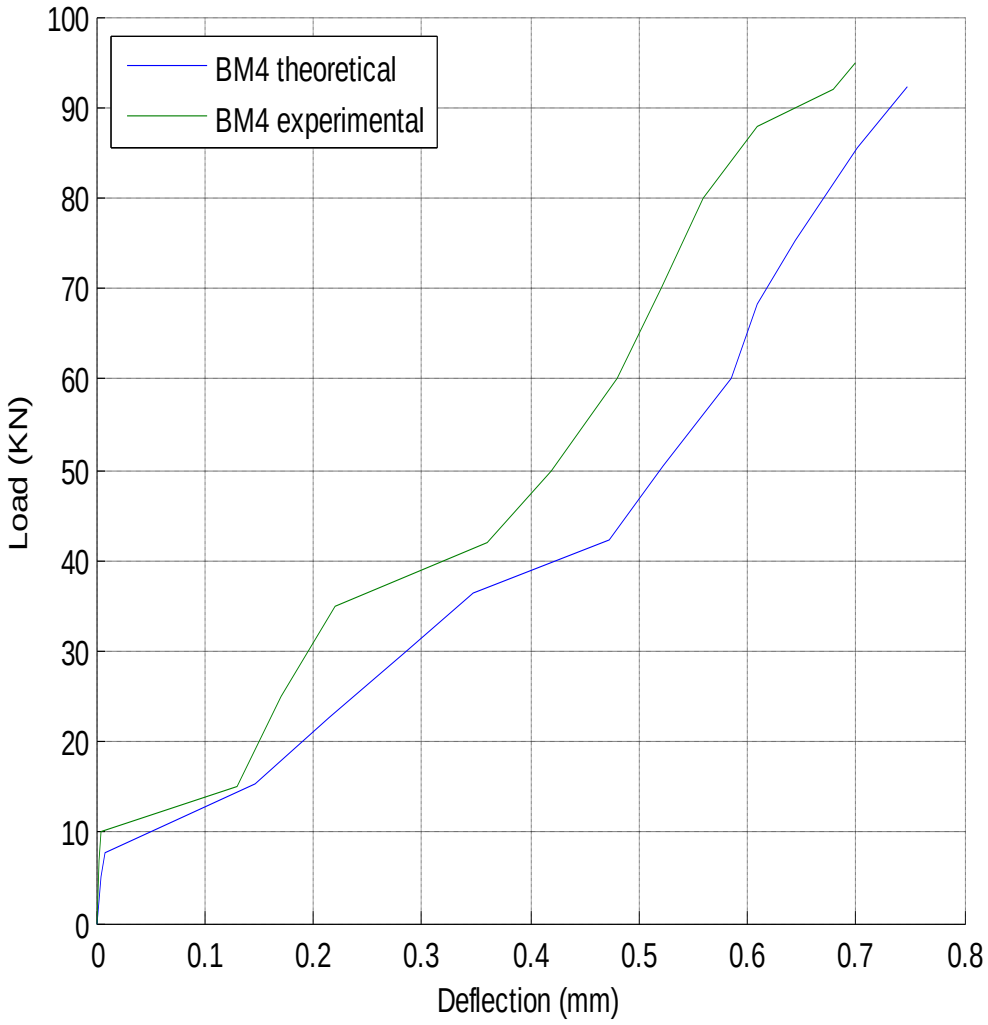

Figure 4.10: Load-deflection response of beam 4

Good agreement between observed and predicted load-deformation response of the beam up to failure point.

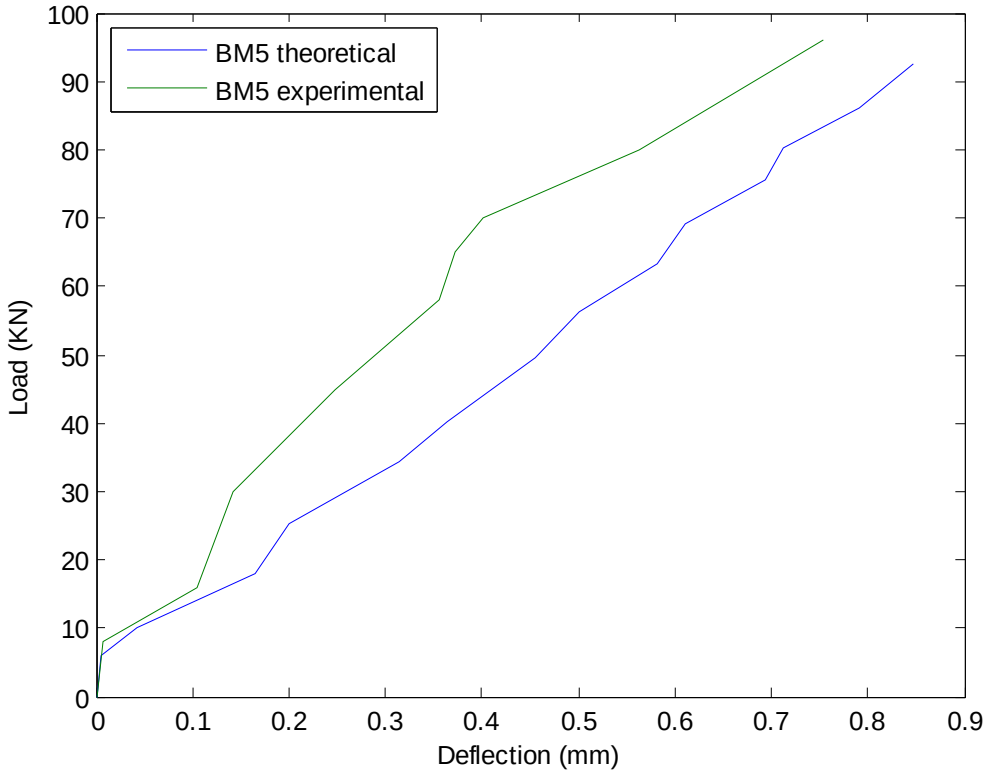

Figure 4.11: Load-deflection response of Beam 5

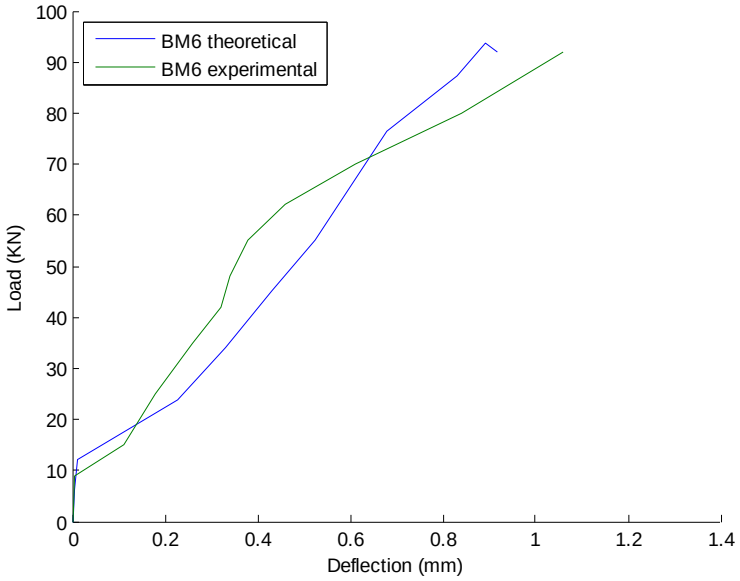

Figure 4.12: load-deflection response of Beam 6

For Beams 5, 6 & 7, there is agreement of load-deformation response between experimental and theoretical values.

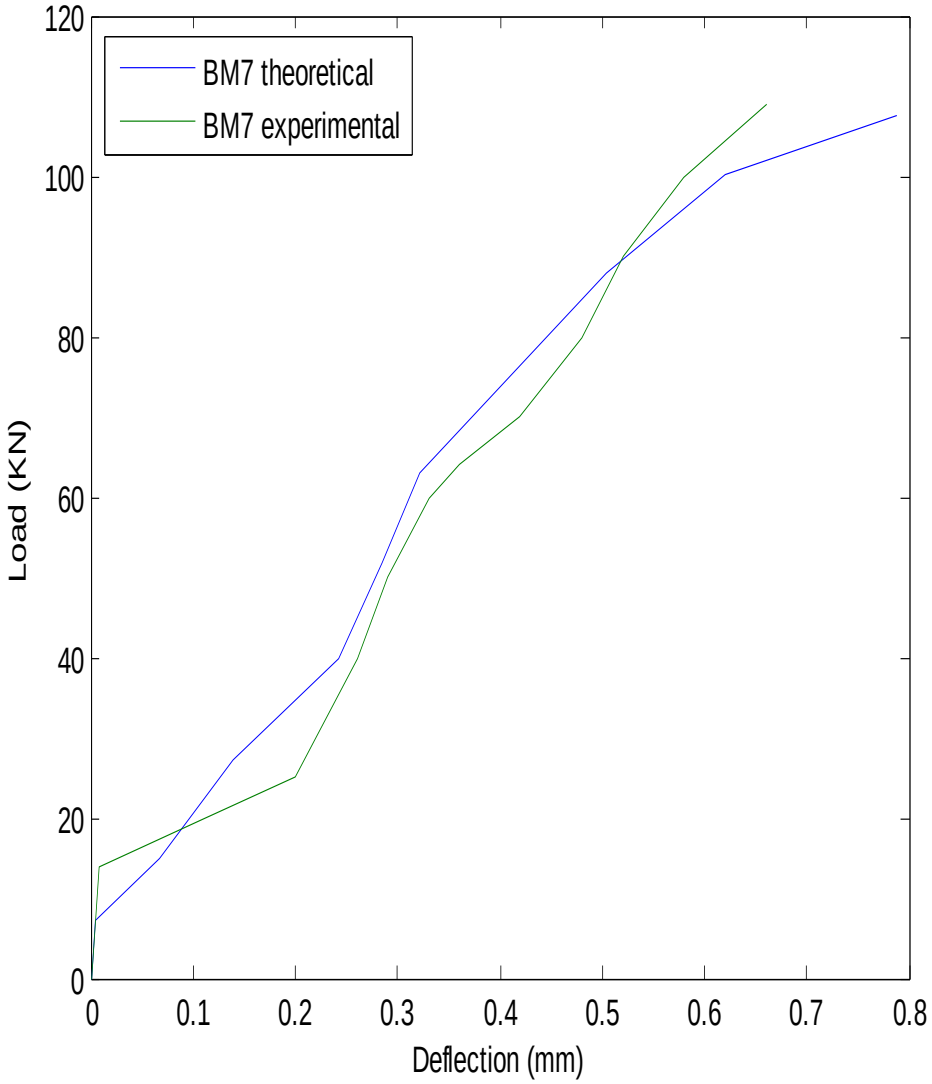

Figure 4.13: Load-deflection response of Beam 7

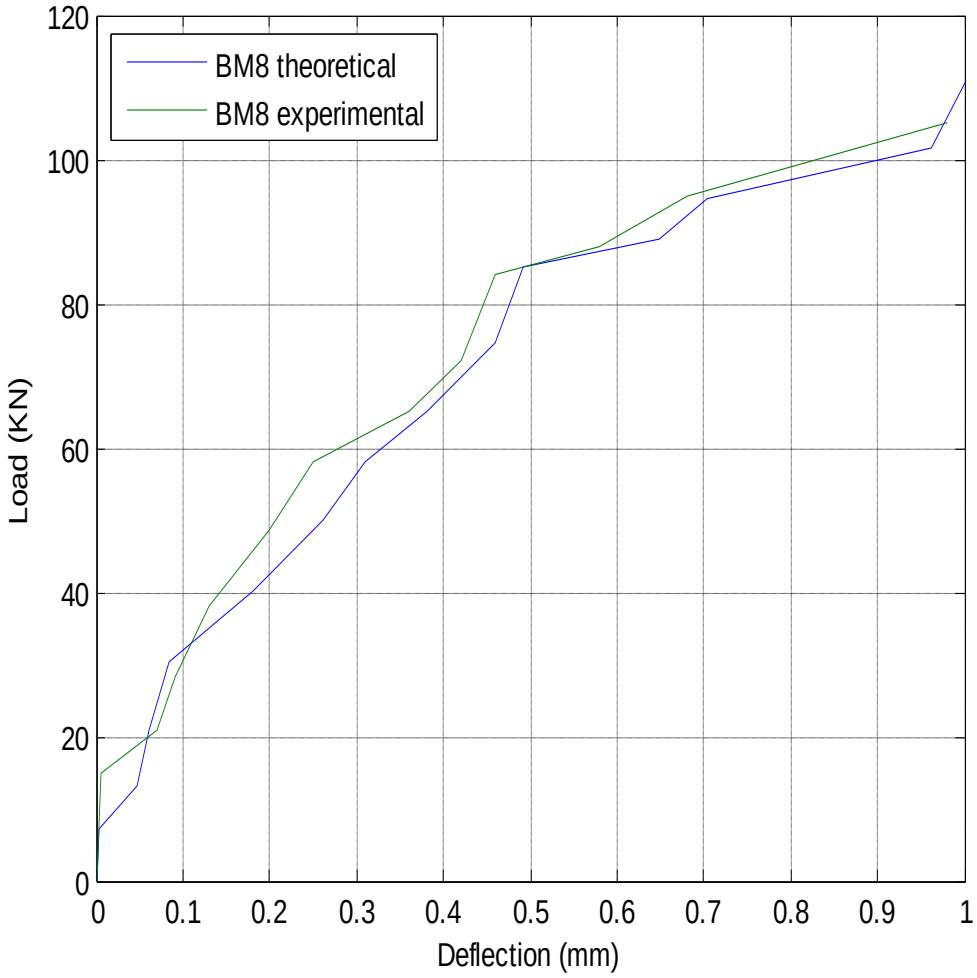

Figure 4.14: Load-deflection response of Beam 8

Good agreement of load-deformation response between observed and predicted values.

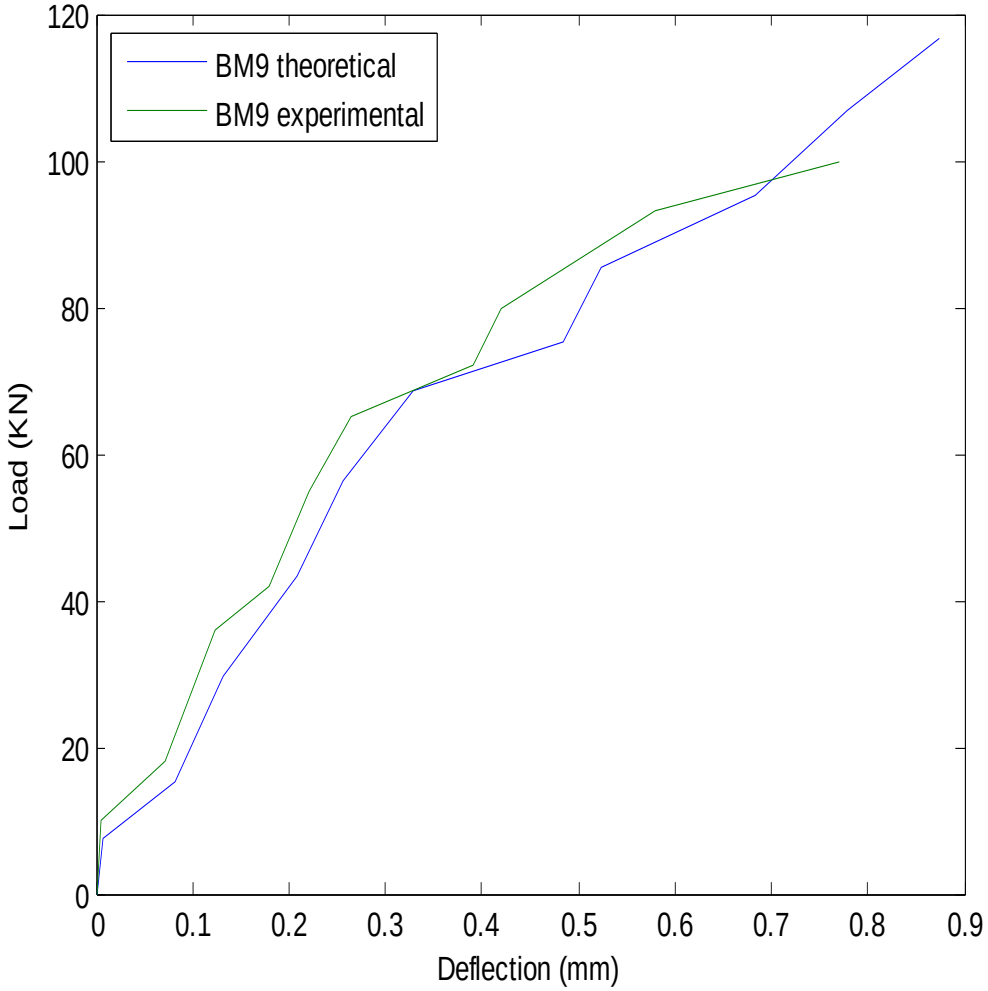

Figure 4.15: Load-deflection response of Beam 9

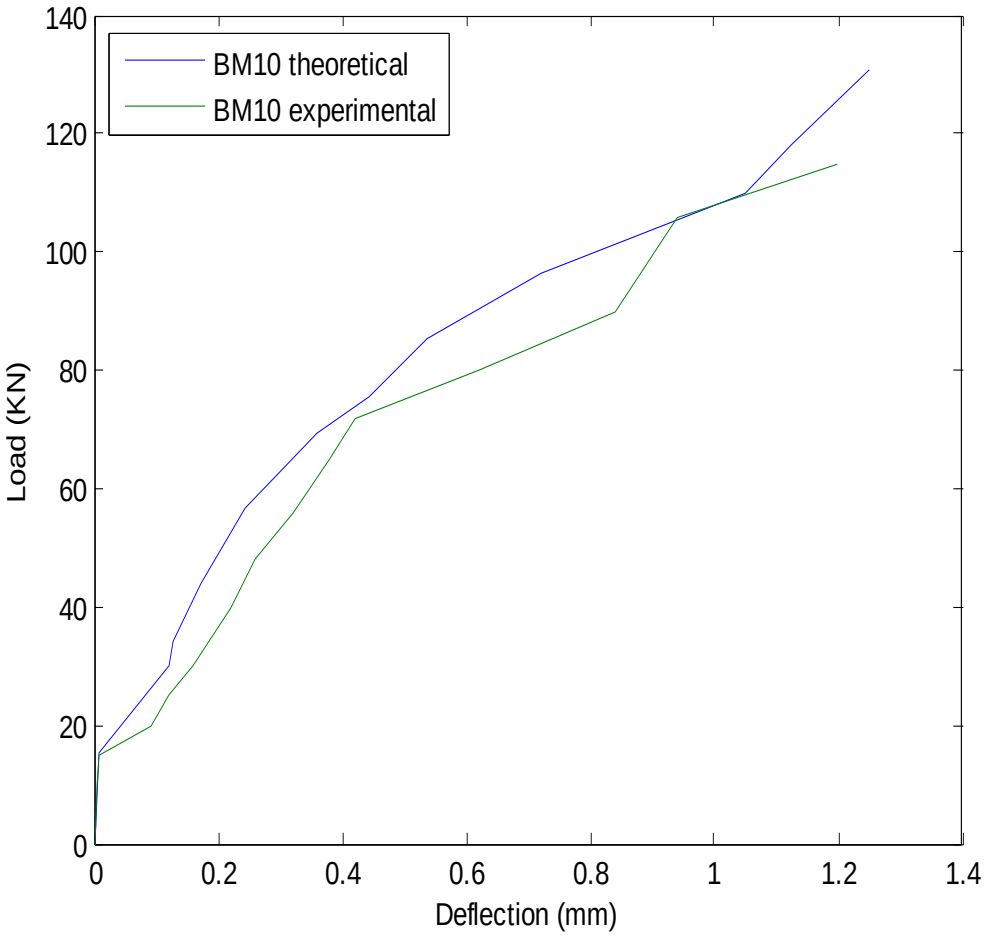

Figure 4.16: Load-deflection response of Beam 10

Good agreement of load-deformation response between observed and predicted values for Beams 9, 10 and 11 respectively.

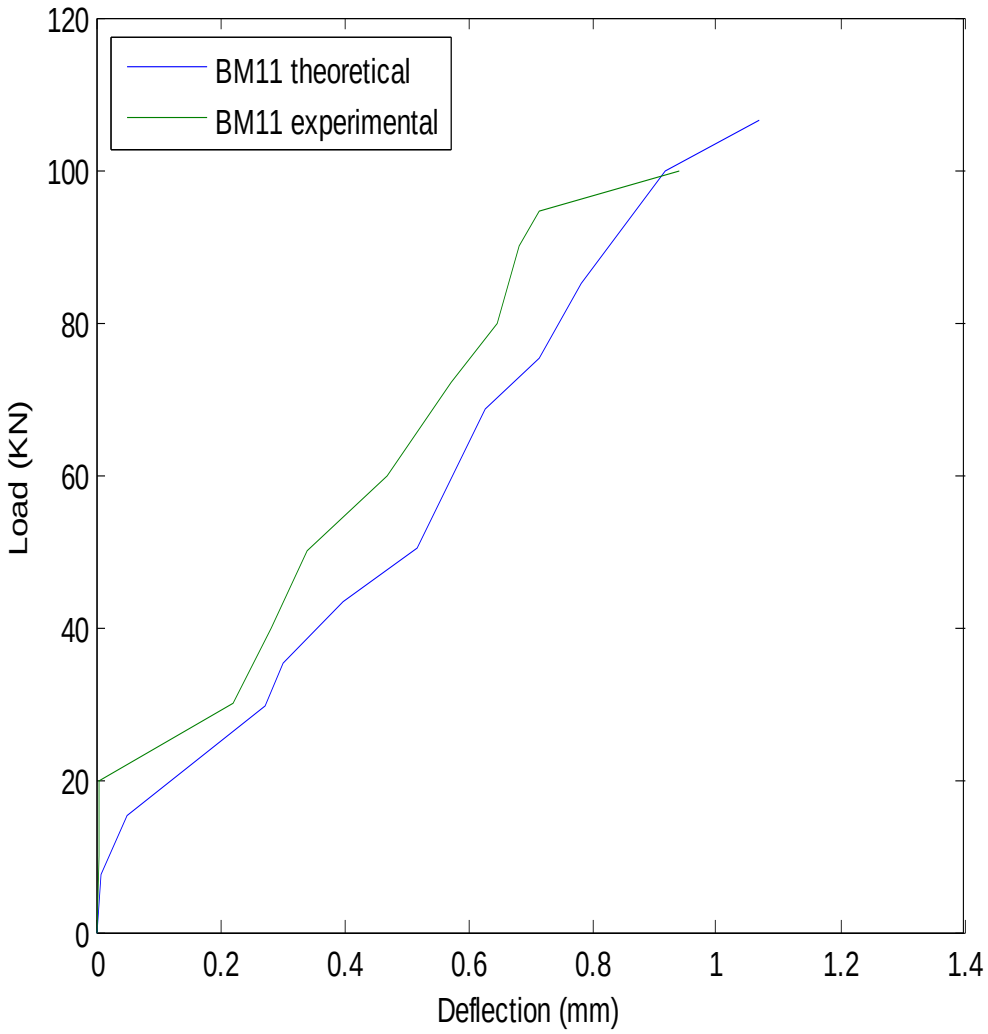

Figure 4.17: Load-deflection response of Beam 11

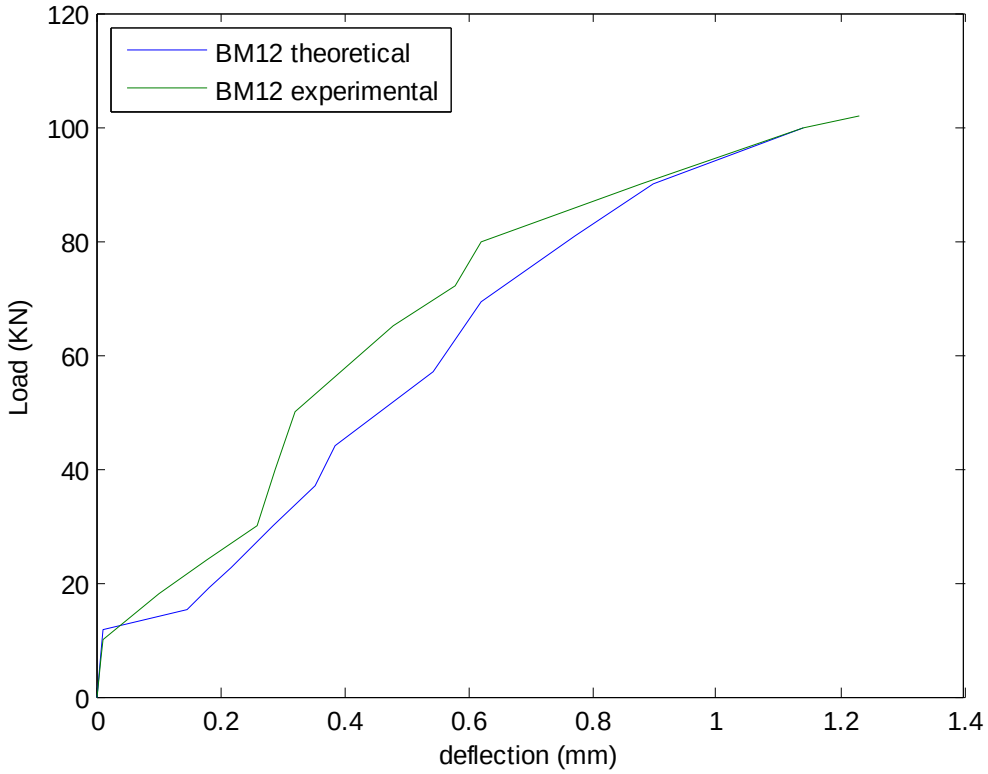

Figure 4.18: Load-deflection response of Beam 12

Fairly good agreement of load-deformation response between experimental and theoretical values for Beams 12, 13 & 14 while there is good agreement for Beam 15 values. Beam 16 to 18 has fairly good agreement of load-deformation response between experimental and theoretical values.

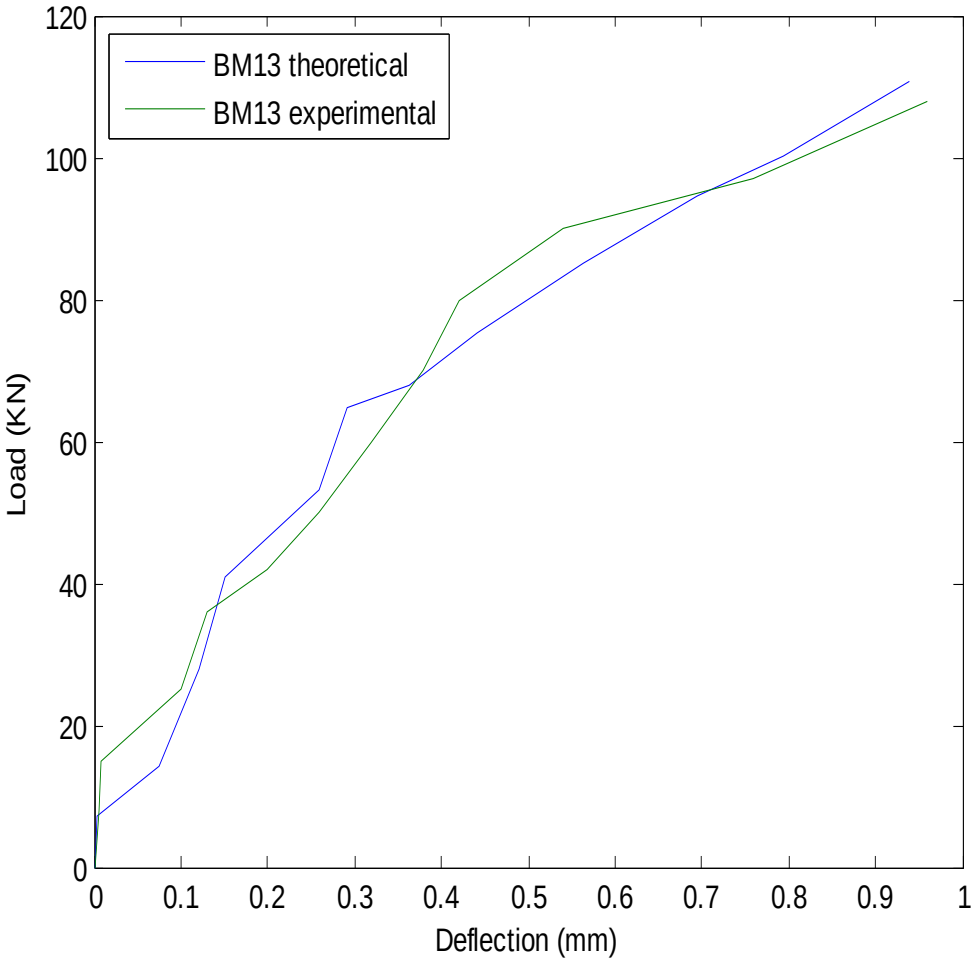

Figure 4.19: Load-deflection response of Beam 13

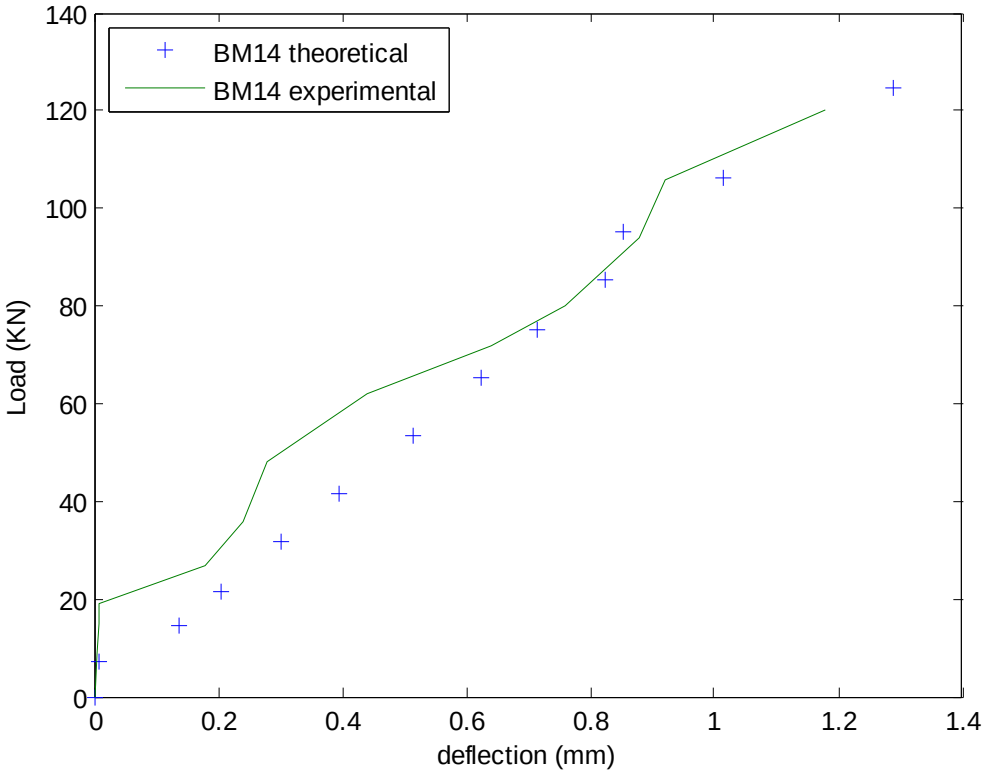

Figure 4.20: Load-deflection response of Beam 14

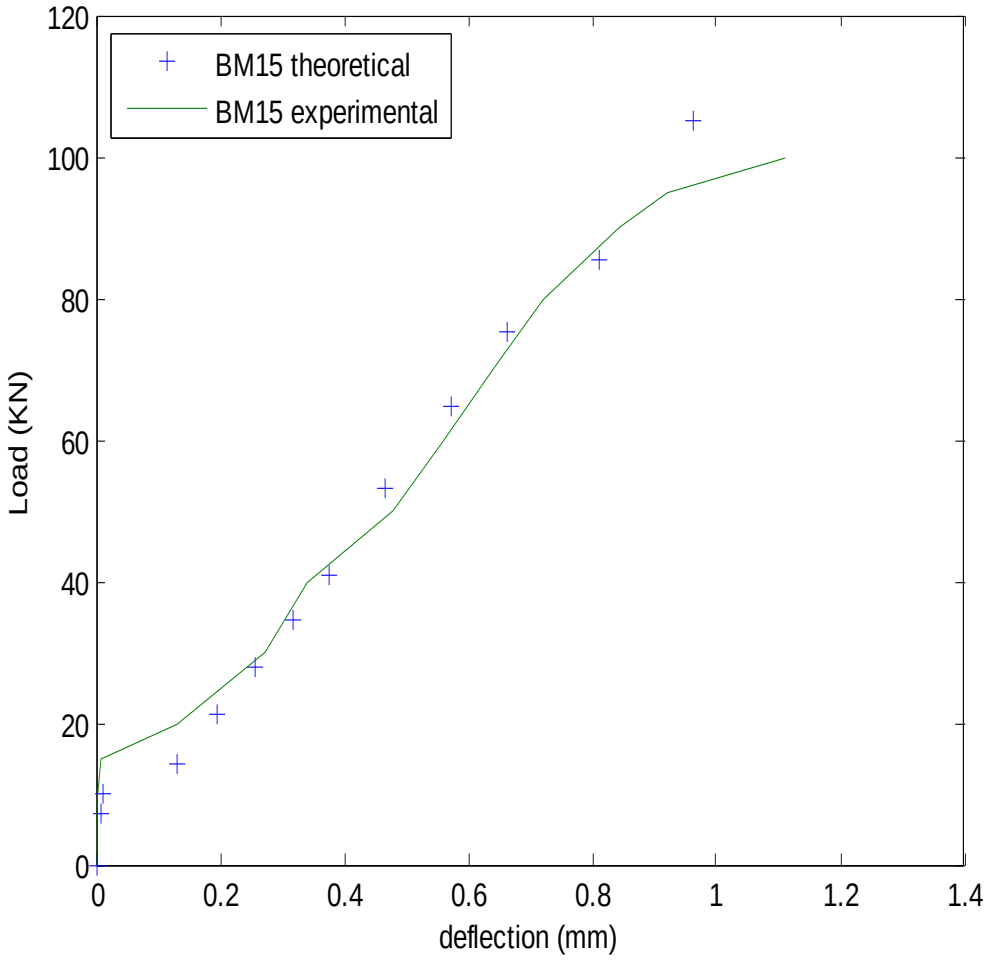

Figure 4.21; Load-deflection response of Beam 15

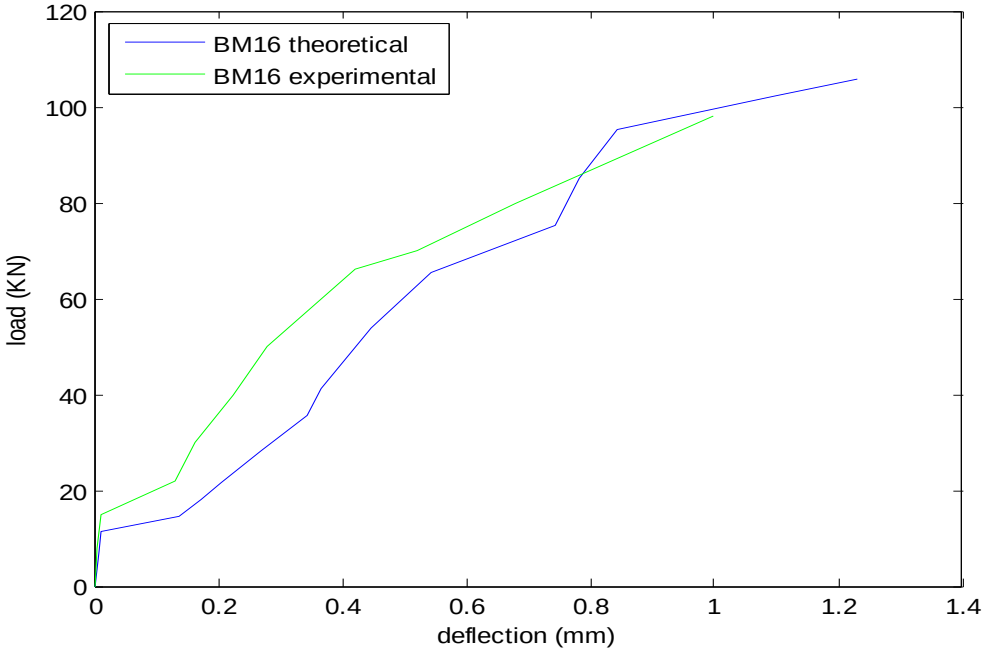

Figure 4.22: Load-deflection response of Beam 16

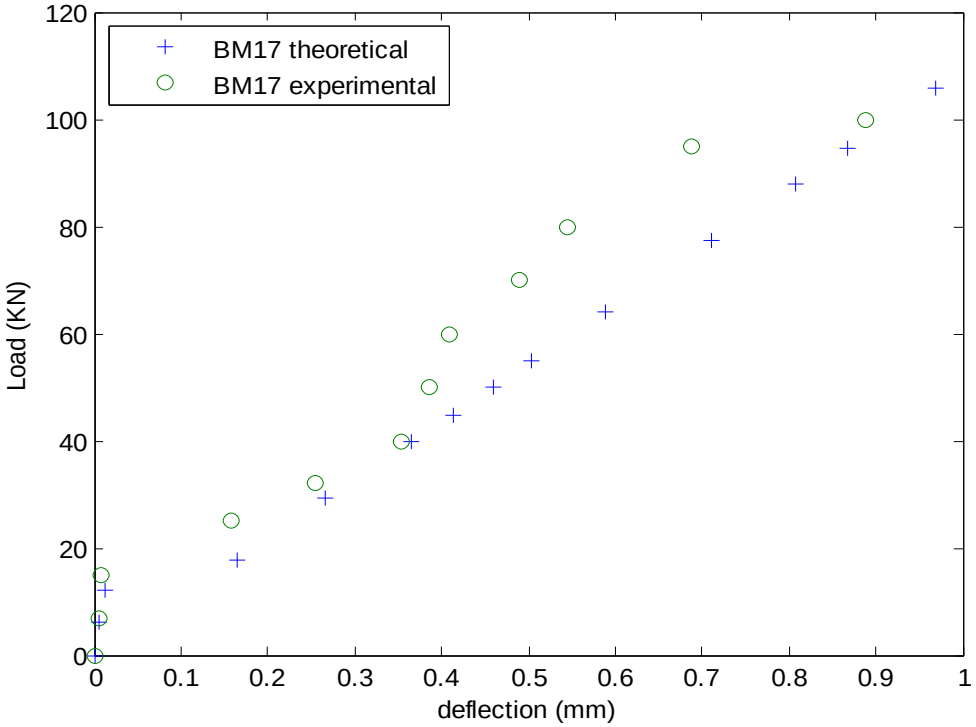

Figure 4.23: Load-deflection response of Beam 17

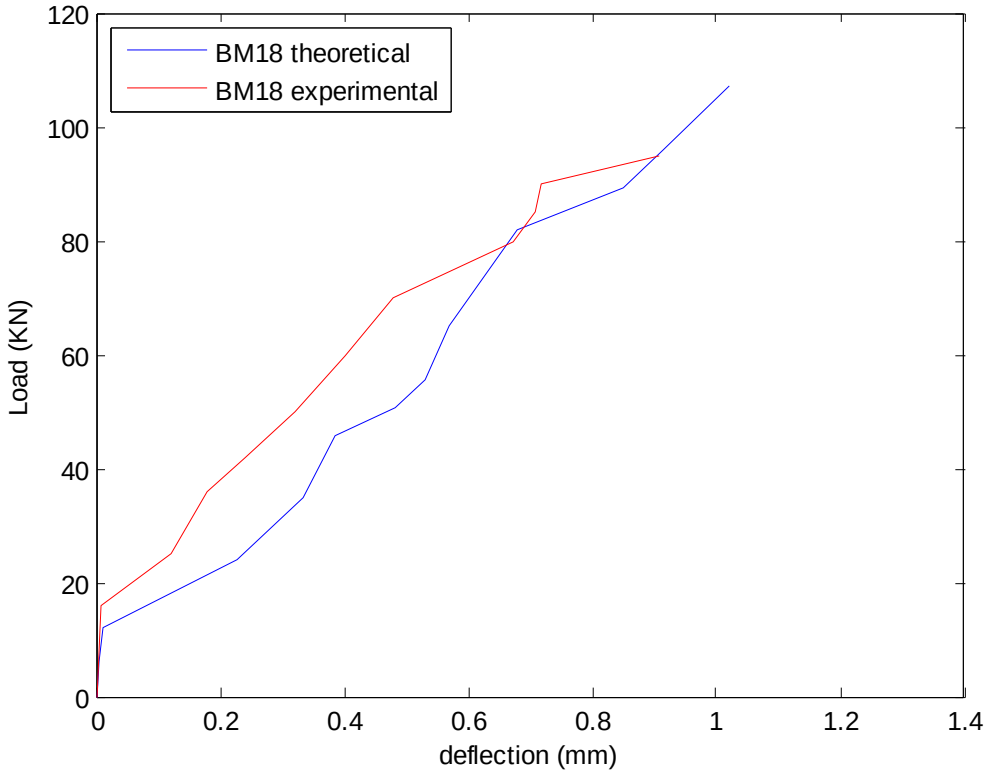

Figure 4.24: Load-deflection response of Beam 18

4.3.1 First cracking and ultimate moment

The theoretical first cracking moment is calculated in accordance with ACI 318(2008) provisions as stated in Equation (4.1).

$$M_{cr} = \frac{fr\ I}{yt} \tag{4.1}$$

Also, the theoretical ultimate moment capacity of the beam is calculated in accordance with ACI 318-08 Provisions as stated in equation (4.2).

$$M_n = \frac{\rho fyb\ d^2\ (1 - 0.59\rho fy)}{f_{cu}} \tag{4.2}$$

Table 4.4 shows the theoretical first cracking load and ultimate flexural capacity of the beams tested. From the table, first theoretical crack load ranged from 12.32kN to 15.59kN and from 14.00 kN to 18.00 kN for experimental values. The cracking strength was observed to be varying with the compressive strength of the concrete. There is no significant difference in first crack load for theoretical and experimental values. This is because prior to cracking, load on a beam is resisted by the concrete section only which is dependent on concrete grade. This trend can be seen especially in the theoretical values. However, for flexural capacity of the beams, an average of 42% increase is noticed in beams with steel ratio, $\rho = 0.012$ compared with beams with steel ratio, $\rho = 0.0058$ while beams with a steel ratio, $\rho = 0.0092$ has about 33% increase in flexural capacity compared with beams that has steel ratio, $\rho = 0.0058$. This result show that flexural capacity of beam increases with increases in steel ratio.

Theoretical comparison of ultimate loads computed based on Equation (4.2) shows that the values are in the range of 72 to 97% of the measured experimental ultimate load which is in very good agreement. The difference between the theoretical values and the measured results can be attributed to the fact that all beams failed by crushing of concrete between the points of load application with concrete strain higher than 0.003 which is assumed to be the ultimate theoretical strain in concrete at top fibers.

Table 4.4: First cracking load and flexural capacity of beams

Beam ID	First crack Load (theo) kN	First crack Load (exp) kN	Flexural Capacity (kN) (theo)	(exp)
BM 1	12.32	15.81	83.33	88.25
BM 2	12.73	14.32	76.48	82.00
BM 3	12.45	15.00	66.37	79.00
BM 4	12.97	15.90	60.94	64.40
BM 5	12.60	18.00	43.76	55.70
BM 6	13.25	16.00	39.90	52.75
BM 7	14.04	14.00	86.30	87.25
BM 8	14.25	21.00	78.88	79.55
BM 9	14.14	15.20	68.15	69.45
BM 10	14.25	15.40	61.93	65.00
BM 11	14.21	15.20	44.42	58.75
BM 12	14.44	15.40	40.25	55.15
BM 13	14.40	14.30	86.83	87.15
BM 14	15.48	14.50	80.14	82.25
BM 15	14.48	14.30	68.43	72.10
BM 16	15.51	14.50	62.72	66.25
BM 17	15.20	18.00	44.72	50.00
BM 18	15.59	15.00	40.52	43.25

4.3.2 Cracking and failure mode

Cracking within the critical region of the concrete beam was the first significant event of the load-deflection response of the beam. The cracks were vertical and propagated upwards. As load increases, more cracks were formed and extended to the shear span of the beam. They were measured with a digital Vernier Caliper. Plate 4.1 to 4.4 depicts the crack patterns within the test zone of the beam. They are similar for most of the beams and this indicates ductile failure. Crack width at initial stages of loading varies from 0.06

mm to 0.08 mm and at ultimate stages between 0.198 to 0.32 mm which are within ACI 318 (2008) code specifications.

Plate 4.1: Crack pattern at mid span of beam

Plate 4.2: Crack pattern at critical section of beam at ultimate loading stage

Plate 4.3: Crack Pattern at section of beam at ultimate stage of loading

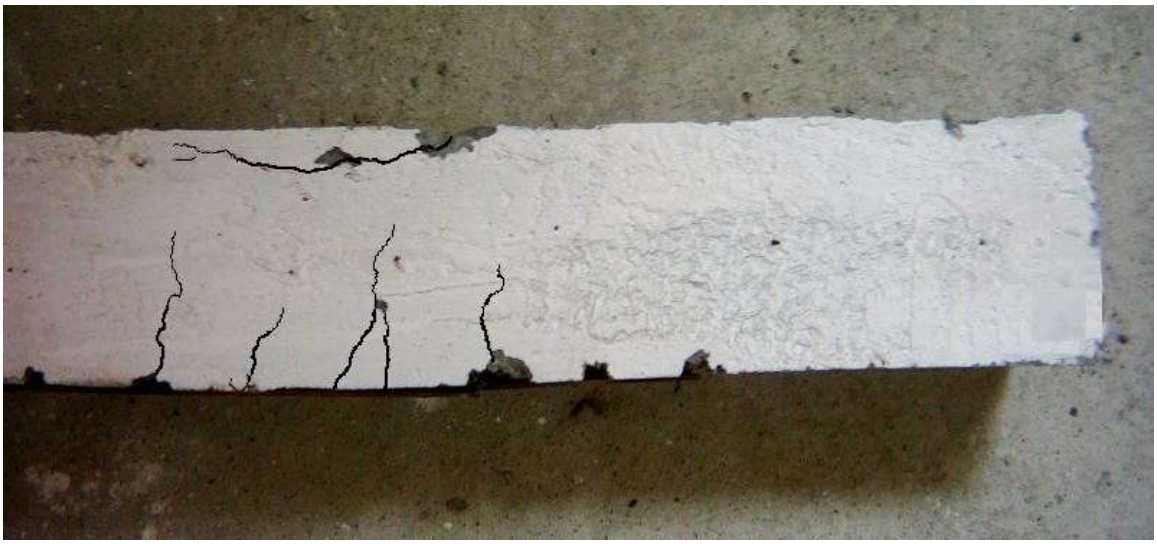

Plate 4.4: Crack pattern of beam showing flexural failure at ultimate load

Plate 4.5: Measurement of crack width with digital Vernier Caliper.

4.3.3 Measurement of crack width

Formation of flexural cracks in beams is detrimental to structural safety as it affects the serviceability of the beam. Excessive crack width can impair corrosion resistance. Therefore, control of cracking helps improve serviceability. Crack width, (w_{cr}), was measured using a digital Vernier Calliper (Plate 4.5) and predicted using equation (4.3) as stated in ACI 224 R-01. Results are as presented in Table 4.4. Experimental results were compared with theoretical values. The experimental values have a mean value of 0.253, a standard deviation of 0.036 and coefficient of variation of 14.23%. Similarly, the predicted values have a mean value of 0.151, a standard deviation of 0.021and coefficient of variation of 13.88%. These statistics are closely related, thus, there is a good correlation between measured and calculated values.

$$W_{cr} = (11\ x\ 106)[dc(A\text{c/n})\beta]^{1/3} f_{st} \qquad (4.3)$$

Table 4.5: Experimental and Predicted crack width of sample beams used for the study

S/No	Beam ID	Average crack width measured w_{cr}(mm)	Predicted Crack width w_{cr}(mm)	$W_{cr}exp/w_{cr}$ Ratio
1	BM 1	0.320	0.181	1.76
2	BM 2	0.290	0.170	1.71
3	BM 3	0.282	0.181	1.56
4	BM 4	0.220	0.163	1.35
5	BM 5	0.272	0.182	1.60
6	BM 6	0.240	0.167	1.44
7	BM 7	0.282	0.182	1.55
8	BM 8	0.250	0.164	1.52
9	BM 9	0.210	0.143	1.47
10	BM 10	0.230	0.131	1.76
11	BM 11	0.210	0.141	1.49
12	BM 12	0.198	0.128	1.55
13	BM 13	0.275	0.180	1.53
14	BM 14	0.260	0.166	1.57
15	BM 15	0.230	0.146	1.58
16	BM 16	0.200	0.132	1.52
17	BM 17	0.280	0.176	1.59
18	BM 18	0.280	0.160	1.75

4.4 Stiffness is based on the elastic deformation theory. It is the resistance of structural element (beam) against Load. It was obtained using Equation (4.4):

$$EI_{exp} = \frac{23PL^3}{1296\Delta exp} \qquad 4.4$$

Detailed calculation is in appendix F.

Figures 4.23 to 4.26 present the stiffness – load characteristics of the test beams for the study. The stiffness- load plot indicated that for all the test beams, the stiffness of the member at the initial stages of loading prior to the cracking is governed by the gross section properties of the member. The post cracking stiffness of all the beams being affected by the amount of longitudinal reinforcement. Steel bar with high steel ratio has

high stiffness and less slip with respect to the surrounding concrete matrix hence the beams has high post cracking stiffness. As load increased initially, stiffness remained fairly constant and decreased after the onset of cracking. Further decrease occurred upon yielding of steel. It was noticed that stiffness is higher for beams with high reinforcement ratios compared to beams with low reinforcement ratios.

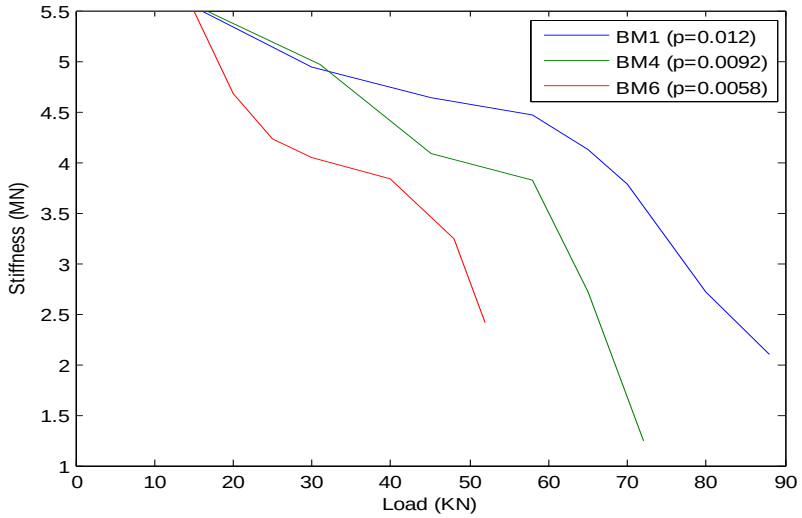

Figure 4.25: Relationship of stiffness to loading and steel ratio in beams

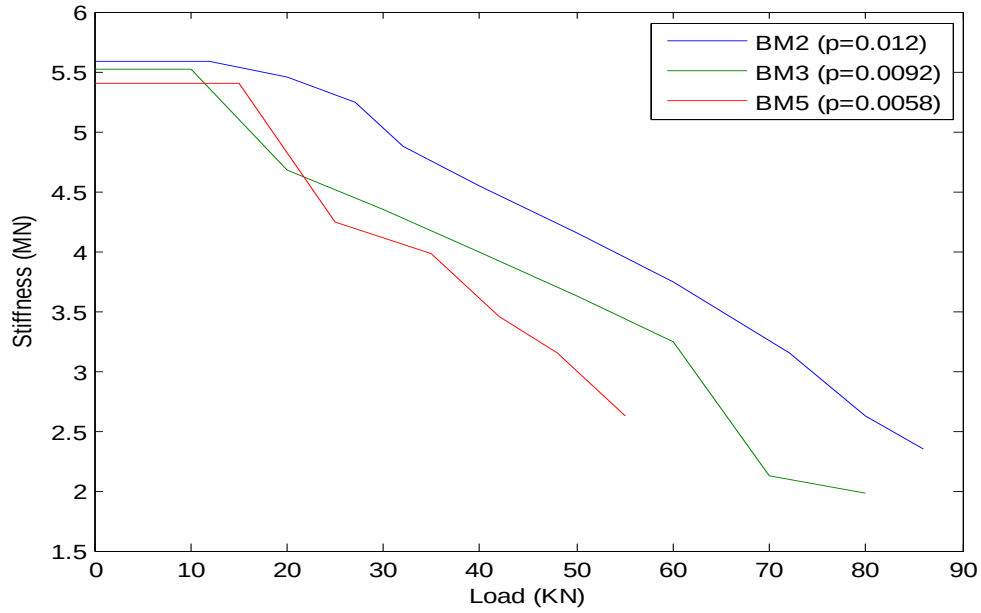

Figure 4.26: Relationship of stiffness to loading and steel ratio in beams

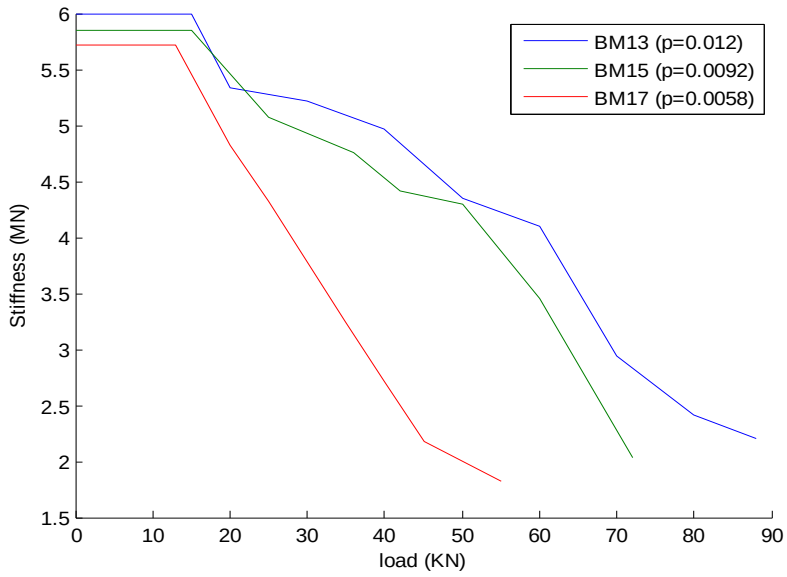

Figure 4.27: Relationship of stiffness to loading and steel ratio in beams

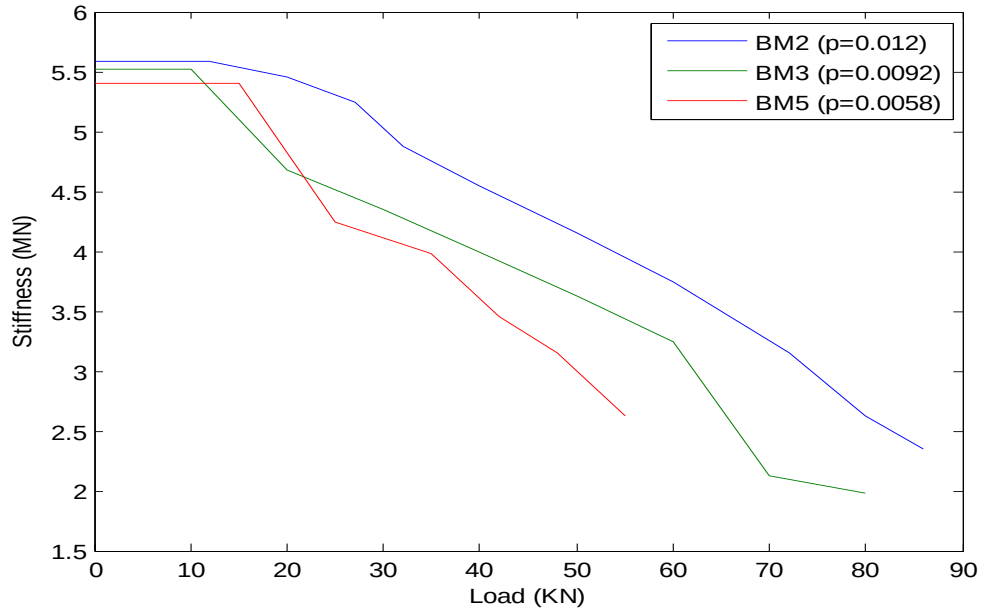

Figure 4.28: Relationship of stiffness to loading and steel ratio in beams

4.5 Ductility Index

The ductility of a beam is its ability to sustain inelastic deformation without loss in load carrying capacity, prior to failure. It is usually calculated for conventional reinforced concrete structures as the ratio of curvature, deflection or rotation at ultimate to yielding of steel. The ductility index in this study is obtained based on deflection computation, and is defined as the mid-span deflection at ultimate load, divided by the mid-span deflection at the point when the tensile steel starts yielding. Table 4.6 show the values for ductility indices for all the beams computed from experimental and analytical values.

Generally, a high ductility index indicates that a structural member is capable of undergoing large deflections prior to failure. From Table 4.6, the ductility index of beams computed analytically ranged from 1.72 to 3.19 while for the experimental values, it ranged from 1.73 to 3.24. From these values only two beams have ductility index above

3.0. Most values for the beams are below 3.0.**It has been mentioned in literature that the displacement ductility indices in the range of 3 to 5 are considered imperative for adequate ductility especially in the areas of seismic design and redistribution of moments** (Ashour 2000; Kumar, 2008; Rashid and Mansur, 2005;Iffat *et al*, 2011). Hence, beams with ductility indices up to 3.0 and above have adequate ductility, can redistribute moment and be considered as structural members that can withstand large displacement, while those whose ductility indices are less than 3.0 lack adequate ductility, cannot redistribute moments nor are they considered as structural members capable of being subjected to large displacements.

Table 4.6 Results of theoretical and experimental values of ductility index of beams

S/No	Beam ID	DI(exp)	DI(theo)	Exp/Theo
1	BM 1	1.73	1.72	1.01
2.	BM 2	2.26	2.31	0.98
3.	BM 3	1.78	2.10	0.85
4.	BM 4	2.28	2.32	0.98
5.	BM 5	1.87	1.85	1.01
6.	BM 6	2.72	2.73	0.99
7.	BM 7	1.82	1.91	0.95
8.	BM 8	2.72	2.85	0.95
9.	BM 9	1.98	1.92	1.03
10.	BM10	3.16	3.00	1.05
11.	BM 11	1.86	1.76	1.06
12.	BM 12	3.24	3.19	1.02
13.	BM 13	1.99	2.03	0.98
14.	BM 14	2.89	2.59	1.12
15.	BM 15	1.93	1.90	1.02
16.	BM 16	2.78	2.74	1.01
17.	BM 17	1.83	1.85	0.98
18.	BM 18	2.38	2.35	1.01

4.6 Theoretical versus Experimental Values

The load at ultimate stage of concrete beams reinforced with rebars milled from ferrous metal scraps was predicted using the Hognestad model which is an analytical approach. The predicted first crack load and the load at ultimate stage using the analytical model was compared with experimental values. The average value of the ratio of the predicted first crack load to the experimentally observed first crack load for all the beams was found to be 0.91, standard deviation of 0.12 and a coefficient of variation of 13%. Similarly, the average value of the ratio of the predicted ultimate load to the actual ultimate load (observed in experiment) for all the beams was found to be 0.91 with a standard deviation of 0.091 and a coefficient of variation of 10%. These statistics are closely related which indicates that the analytical approach can predict the load in concrete beams reinforced with rebars milled from ferrous metal scraps at various stages of loading quite accurately.

In the same vein, the ductility indices of concrete beams reinforced with rebars milled from ferrous metal scraps were predicted using the analytical approach and compared with experimental values. The average value of the ratio of the predicted ductility indices to the experimental ductility indices for all the beams was found to be 1.003 with a standard deviation of 0.056 and a coefficient of variation of 5.60%. This indicates that the analytical approach can predict the ductility indices in concrete beams reinforced with rebars milled from ferrous metal scraps quite accurately since it has a variation of about 5.60%.

4.7 Effect of Concrete Strength and Tensile Steel Ratio on Ductility Indices

A parametric study was conducted on the effect of concrete strength and tensile steel ratio on ductility indices of the beams. Figure 4.29 and 4.30 show the effect of these parameters on the ductility indices of the beams. In figure 4.29, increase in concrete strength increases ductility index for varying steel ratios. For beams with steel ratio, ρ = 0.0058, an increase in concrete strength from 21N/mm^2 to 30N/mm^2 increased ductility index from 1.87 to 3.24 for example. Similarly, for beams with steel ratio, ρ= 0.0092, as concrete strength increased from 20N/mm^2 to 30N/mm^2, ductility index increased from 1.78 to 2.78; while for beams with steel ratio, ρ = 0.012, ductility index increased from 1.72 to 1.99. These results show that increase in ductility indices due to increase in concrete strength is highest in beams with lowest steel ratios, ρ = 0.0058 with 42%, 36% in beams with steel ratio, ρ = 0.0092 and 13% in beams with steel ratio, ρ = 0.012 respectively.

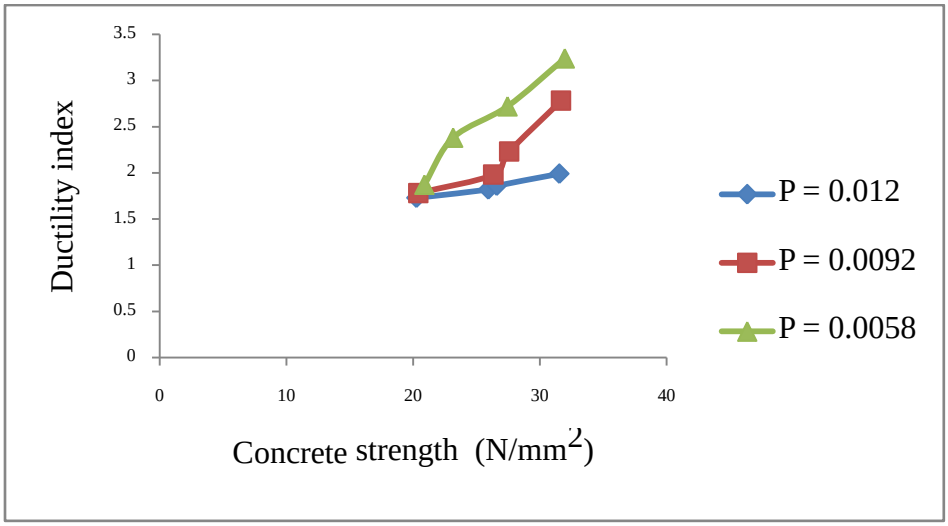

Figure 4.29: Concrete strength versus ductility index

The effect of tensile steel ratios on ductility indices is outstanding. Figure 4.30 shows the effect of steel ratio on ductility index for varying concrete strengths. Decrease in steel ratio from 0.012 to 0.0058 increased ductility indices from 1.73 to 2.72 or (36%) increase for beams with concrete strength of 20N/mm^2. For beams with concrete strength of 25N/mm^2, a decrease in steel ratio from 0.012 to 0.0058 increased ductility index from1.98 to 3.24 or (39%) increase and for beams with concrete strength of 30N/mm^2, a decrease in steel ratio from 0.012 to 0.0058 increased ductility indices from 1.83 to 2.89or (36%) increase. These results show that for a particular concrete strength of beams, decreases in steel ratio improved ductility indices between 31 and 39% respectively. The works of Siddique and Rouf (2006) and Lim *et al*, (2006) showed similar trend.

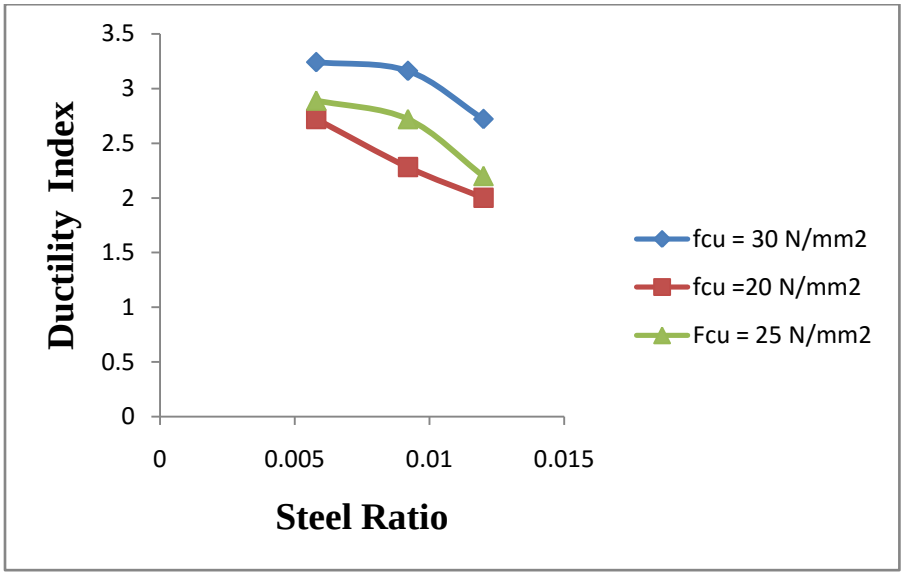

Figure 4.30: Relationship of steel ratio to ductility indices

4.8 Model for Predicting Beam Ductility

One of the objectives of this study is to develop an empirical model that predicts ductility indices of beams reinforced with rebars produced from ferrous metal scraps. Equation (4.5) gives the relationship between the variables under study. From the results of the experimental and analytical studies on ductility indices indicated in Table 4.4, a multivariate data analysis approach was used to estimate the parameters of the model as expressed in equations (4.5) to (4.8) and subsequent development of the model (Equation 4.9).

$$\boldsymbol{\mu = b_0 + b_1 f_{cu} + b_2 \rho} \quad (4.5)$$

Where:

$$b_1 = \frac{\sum x_2^2 \sum x_1 y - \sum x_1 x_2 \sum x_2 y}{\sum x_1^2 \sum x_2^2 - (\sum x_1 x_2)^2} \quad (4.6)$$

$$b_2 = \frac{\sum x_1^2 \sum x_2 y - \sum x_1 x_2 \sum x_1 y}{\sum x_1^2 \sum x_2^2 - (\sum x_1 x_2)^2} \quad (4.7)$$

$$b_0 = \bar{Y} - b_1 x_1 - b_2 x_2 \quad (4.8)$$

$$\boldsymbol{\mu = 1.101 + 0.047 f_{cu} + 0.12 \rho} \quad \textbf{(4.9)}$$

Where:

μ = dependent variable (ductility index)

f_{cu} = independent variable (concrete strength)

ρ = independent variable (tensile steel ratio)

The model shows that a unit change in concrete strength of the beam results in a 0.047 change in the ductility indices of the beam. It also shows that a decrease in tensile steel improves ductility indices of beams for given concrete strengths and verse versa (Siddique and Rouf, 2006; Lim *et. al*, 2006).This shows that tensile steel ratios have

greater influences on ductility indices. This is why the value is fixed in most concrete design codes to ensure that structural elements especially beams are ductile and under- go ductile failures rather than brittle failures. The intercept of the model (1.101) is the mean ductility index for the beams in this study.

Table 4.7: Data for development of model

Beam ID	Compressive Strength (N/mm^2)	Tensile steel ratio (ρ)	Ductility Index (μ_Δ)
BM 1	20.25	0.012	1.73
BM 2	21.33	0.012	2.26
BM 3	20.40	0.0092	1.78
BM 4	22.12	0.0092	2.28
BM 5	20.89	0.0058	1.87
BM 6	23.16	0.0058	2.72
BM 7	25.92	0.012	1.82
BM 8	26.72	0.012	2.72
BM 9	26.32	0.0092	1.98
BM 10	26.71	0.0092	3.16
BM 11	26.58	0.0058	1.86
BM 12	27.45	0.0058	3.24
BM 13	27.29	0.012	1.99
BM 14	31.52	0.012	2.89
BM 15	27.57	0.0092	1.93
BM 16	31.66	0.0 092	2.78
BM 17	30.40	0.0058	1.83
BM 18	31.97	0.0058	2.38

CHAPTER 5

SUMMARY, CONCLUSION AND RECOMMENDATIONS

5.1 Summary of Findings

The summary is as follows:

(a) Rectangular concrete beams reinforced with rebars produced from ferrous metal scraps are less ductile with ductility index in the range of 1.73 to 2.75.

(b) Rectangular concrete beams reinforced with rebars milled from scrap metals has crack width ranged from 0.198 mm to 0.320 mm which is within ACI 224-01 specification of 0.41mm maximum value for beams exposed to open dry air (Table 2.1).

(c) Hognestad Models for concrete and steel, theoretical equations for beam section based on strain compatibility and equilibrium of forces can be used to evaluate the deflection ductility index of rectangular concrete beams reinforced with rebars milled from scrap metals.

(d) The ductility index of rectangular concrete beams reinforced with rebars milled from scrap metals is dependent on concrete strength and steel ratio.

(e) Reduction in stiffness of concrete beams with rebars milled from scrap metals is dependent on steel ratio.

(f) Concrete beams reinforced with rebars milled from scrap metals have inadequate deflection ductility index (1.73 to 2.75) and thus a structural member not capable of sustaining large inelastic displacement.

(g) The theoretical and experimental values of deflection ductility index of the beams were in good agreement.

(f) An empirical model developed for predicting the deflection ductility indices of rectangular concrete beams singly reinforced with rebars produced from scrap metals conforms with the work of other researchers (El Tahawawy, *et.al*., 2009; Peng Jun, 2012).

5.2 CONCLUSION

Based on experimental, theoretical results and observations, the following conclusions were drawn:

The study has shown that singly reinforced rectangular beams reinforced with rebars produced from ferrous metal scraps are less ductile. The ductility index of the beams are inadequate, as such may not redistribute moment effectively and thus cannot be considered a structural member capable of resisting large displacements.

The analytical and experimental values of deflection of the beams at yield point of steel and failure point of the beam gives an appreciation of the difficulties in attaining the deflection ductility index of the beam. The ratio of deflection value at failure point of beam to the deflection at yield point of steel is the extent of ductility index of the beam. This could be attributed largely to the behaviour of the steel bars due to its constituents

(carbon equivalent) of the steel bars. This effectively means that the deflection ductility improved with better characteristics (low carbon equivalent) of steel bars which warrant higher deformations without loss of strength.

The computational approach to determine the deflection ductility index of concrete beams reinforced with rebars milled from ferrous scrap metals proved to be good, and efficient in the prediction of experimental values. The results generally showed that all computational models presented in this study performed well for the prediction of experimental values.

The load - deflection curves of the beams obtained theoretically is in good agreement with experimental values. This means that Hognestad models for concrete and steel and theoretical equations based on strain compatibility and equilibrium of forces for a beam section can be used to evaluate the deflection ductility index of a rectangular concrete beam reinforced with rebars produced from scrap metals. The study further showed that there is no significant difference in initial stiffness of the beams. However, the effective stiffness for the beams is significant at the inelastic range of deformations. It is dependent on the steel ratio.

The deflection ductility index of rectangular beams reinforced with rebars milled from ferrous scrap metals is dependent on concrete strengths and steel ratios. The range of steel ratios used (0.0058 to 0.012) is compatible with that of other researchers. Though the range of concrete strengths used in this study is narrow (20 N/mm^2 to 30 N/mm^2), results from other studies revealed that normal concrete strength up to 40 N/mm^2 influences deflection ductility indices positively.

5.3 RECOMMENDATIONS

The recommendations arising from this work are as follows:

(1) The result obtained herein is recommended for the prediction of ductility indices of singly reinforced rectangular concrete beams reinforced with rebars produced from ferrous scrap metals.

(2) Rebars milled from scrap ferrous metal can be used for rectangular reinforced concrete beams but such beams lack adequate ductility, neither redistribute moment(s) (when used as continuous beam) nor can they be considered as structural members capable of sustaining large displacements. However, such rebars should be produced at acceptable standard. Such rebars requires as little as 26% of energy required to produce steel from raw materials extracted from natural source. Also, in the production of rebars, milled from scrap metals, there is a reduction of carbon dioxide (co_2) emission by 56%.

(3) The deflection ductility index of concrete beams reinforced with steel bars milled from ferrous metal scraps is dependent on yield point of steel. It is a function of the steel characteristics especially the carbon equivalent (C_{eq}). There is need to investigate the effect of carbon content (C_{eq}) of steel on the deflection ductility indices of concrete beams reinforced with rebars milled from scrap metals.

REFERENCES

ACI Committee 318, Building code requirements for structural concrete (ACI 318-08)

and commentary, an ACI standard, American concrete Institute, Detroit, MI, 2008.

ACI 224R-01: Causes, mechanism and control of cracking in concrete structures, A

report of ACI Committee 224.

Alabi , A.G.F and Onyeji, L.I (2010). Analysis and comparative Assessment of locally produced reinforcing steel bars for structural purposes. Journal of research information in Civil Engineering Vol. 7, (2) 49 -60.

Apeh, J.A. (2013): Assessment of mechanical properties of reinforcing steel used in construction works at F.C.T Abuja, Nigeria. International Journal of Engineering and Technology (IJERT), 2, 6, 2346-2358.

Appa, G.R; Vijayanand, I. and Eligehansen R.: Studies on ductility of RC beams in flexure and size effect; Available at http;//francos.org/francos – 6/329.pdf.

Arivalagan, S,(2004). Flexural behavior of Reinforced Fly Ash concrete beams. International Journal of structural and civil engineering, 1, 1,

Ashour, S. A; (2000). Effect of compressive strength and tensile reinforcement ratio on flexural behavior of high – strength concrete beams. Engineering structures, Vol. 22, 5, 413 – 423,

Balogun, S, David, E, Samson, A; andOlatunde S (2009): Challenges of producing quality construction steel bars in west Africa. Case study of Nigeria steel Industry. Journal of minerals and materials characterization and engineering, 8, 4, 283 – 292.

BS 8110, Part I; 1997 code of practice for design and construction, British Standard institute, London, 1985.

BS 4449 (2005): Hot rolled steel bars for the reinforcement of concrete, London, British Standards Institution, 2005.

Brooke, N; Megget, L; and Ingham, J; (2005) Factors to consider in the use of grade 500E longitudinal reinforcement in beams of ductile moment resisting frames; SESOC Journal, 18; 1, 14-22.

Carillo, J; Giovanni, G; Astrid, R. (2004): Displacement ductility for Seismic design of RC walls for Low-rise Housing. Latin American Journal of Solids and structures, 11, 725 – 737.

CEB-FIP (1993): European model code for concrete structures; European committee for concrete structures; European committee for concrete international and Federation of prestressed concrete.

Chen, M.T; and Ho, J.C.M. (2014): Concurrent flexural strength and ductility design of RC beams via strain gradient dependent concrete stress-strain curve. The structural design of Tall and special Buildings.

Ejeh, S.P and Jibrin, M.U (2012). Tensile tests on reinforcing steel bars in the Nigerian Construction Industry. IOSR Journal of mechanical and Civil engineering, 4, 2, 06 – 12.

Elrakib, T.M; (2013). Performance evaluation of High Strength Concrete beams with low flexural reinforcement. HBRC Journal, 9, 1, 48-59.

EC 1992, 'European committee for standardization, Euro code 2: design of concrete structures, Part 1-1; general rules and rules for building concrete structures.

EN 12504-4 9 (2004); Testing co 4. Concrete – Part 4. 'Determination of pulse velocity' European community for standardization, CEN.

Grimaldi, A and Rinaldi, Z; (2000).Influence of steel properties on the ductility of RC structures; (12WCEE) World Conference on earthquake engineering,pp 1175 – 1183.

Hadi, M.N.S and Schmidt, R.C; (2002).Use of Helixes in Reinforced concrete beams, ACI Structural Journal, 99, 2, 191 – 198.

Holmberg,A; Lindgren, S. (1970) Crack spacing and crack width due to normal force or bending moment. Document D2, National Swedish Council for Building research, Stockholm, pg 37.

Iffat, S;Maina, K and Munaz A.N; (2011).Member ductility experiment with high strength steel and concrete, 4th annual Paper meeting and 1st civil engineering Congress, December 22 – 24, Dhaka, - Bangladesh.

ISRI (2015) Institute of scrap recycling Industry, 1615L street, NW, suite 600, Washington DC 20036, pg 1-16.

Jibrin, M.U and Ejeh, S.P: (2013) A Comparative Assessment of the bent, chemical and Tensile properties of reinforcing steel bars in the Nigerian Construction Industry. International Journal of engineering research and Technology, Vol. 2, (3), pp 1 – 19.

Kankam, C.K and Adom – Asamoah, M; (2002). Strength and ductility Characteristics of reinforcing steel bars milled from scrap metals. Materials and design, 23, 537 - 545.

Kumar P.S; Mannan, M.D. A and Kurian, U.J; (2008).High Performance Reinforced Concrete beams made with sandstone reactive aggregates. The Open Civil Engineering Journal, 2, 15 – 24.

Kumar P.S; Mannan, M.A; Kurian, V.I; Achuytha H; (2006).Ductility of high Performance Concrete beams using sandstone aggregates, Proceedings of the 6th Asia Pacific structural Engineering and construction conference (APSFC0 2006), 5 – 6 September 2006, Kuala Lumpur, Malaysia.

KS 573; Kenya bureau of standards specification for high yield steel bars for reinforcement of concrete (second edition) 1986.

Kwan, A.K.H; Ho, J.C.M; Pam, H.J. (2004): Effects of concrete grade and steel yield strength on flexural ductility of reinforced concrete beams. Australian Journal of structural engineering, 6(2), 119- 138.

Kwam, A.K.H, Au, F.T.K and Chu S.L; Effects of confinement on flexural strength and ductility of HSC beams. The structural engineer, 38 – 44, 2004.

Lim, H.S, Wee, T.H, Mansur M.A, and Kong, K.H.(2006) Flexural behavior of reinforced lightweight aggregate concrete beams. Proceedings of the 6th Asia–Pacific structural engineering and construction conference (APSEC, 2005), 5-6 September, 2006, Kuala Lumpa, Malaysia.

Leonhardt, F. (1997): Crack control in concrete structures, IABSE Surveys no s4/77, International Association for bridges and structural engineering, Zurich, 26pp

Macgregor, J.G and Wright, J.K; 'Reinforced concrete Mechanics and Design' New Jersey, Pearson Prentice Hall, 2005.

Macgregor, J.G. and Ibrahim, H.H.H. (1997): Modification of the ACI Rectangular stress-strain block for high strength concrete beams. ACI Structural Journal, 94(1), 40-48.

Mantai, Cl and Johnny, C. M.H; (2014) Flexural strength design of Reinforced Concrete beams with consideration of strain gradient effect. Structures and Buildings, 165, (SB 16).

MCA- Metal Construction Association: Recycled content of Metal Roofing and siding Panels; Technical Bulletin. 470004. Lake Avenue, Glenview; www.metalconstruction.org. Technical Bulletin #04 – 0004.

Ndiaye, M.B; Sandrine, B; Bernard, C. and Ibrahima K.C. (2009). Evaluation and improvement of the quality of Senegalese reinforcing steel bars produced from scrap metals, Journal of Materials and design, 30, 804-809,

Ng S.C; and Lee, S; (2002) A study of flexural behavior of Reinforced Concrete beam strengthened with Carbon Fiber Reinforced Plastic (CFRP).Journal of reinforced Plastics and Composites, 21, 919 – 938.

NZS 3101 (1995), New Zealand standards. Concrete structures standard, New Zealand, Wellington.

Ohimain, E.I. (2013): Scrap Iron and steel recycling in Nigeria. Greener Journal of Environmental management and public safety, 2(1), 001 - 009.

Olivia, M; and Mandal, P. (2005): Curvature ductility of reinforced concrete beam. Teknick Sapili, 6 (3), 1-13.

Paulay, T; and Priestly, M.J.N (1992) Seismic design of Reinforced Concrete and Masonry Buildings; John Wiley & Sons, Inc, U.S.A 114.

Peng, J; Ho, J.C.M; Pam; H.J; Wong Y.L. (2012): Equivalent stress block for normal-Strength concrete incorporating strain gradient effect. Magazine of concrete Research, 64(1), 1 – 17.

Preetha, R; Joanna, P. S; Jessy, Roobu; Pillai, C.S. (2013): Ductility behavior of reinforced high Volume fly-ash Concrete Beams. International journal of scientific & Engineering research, 4(5), 123 – 126.

Rashid, M.A; Mansur, M.A; (2005). Reinforced high – strength concrete beams in flexure, ACI Structural journal, vol. 102, no 3, pp 462 – 471.

Rai. D.C; Jain S.K, Chakrabarti, I, (2012). Evaluation of properties of steel reinforcing bars for Seismic design. 15thWorld conference of Earthquake Engineering (WCEE), Lisboa.

Shin, S; Ghosh, S.K; and Moreno, J. Flexural ductility of Ultra – high strength concrete members. ACI Structuraljournal, 1989, 86, no 6, 394 – 400.

Shunichi H, and Morifumi, N; 'Effect of Microalloying elements on Mechanical properties of reinforcing bars', ISIJ International, vol. 46, no 10, pp 1510 – 1515, 2006.

Siddique, M.A and Rouf M.A. (2006). Effect of material properties on behavior of over-reinforced concrete beams. Journal of Civil engineering, no 2, vol. 7, pp 195-204.

Sofi, A, Phanikumar, B.R (2015): An experimental investigation on flexural behavior of fibre- reinforced pond ash-modified concrete.AinSharms engineering Journal (6), 1133- 1142.

Teo, D.C.L, Mannan M.A, Kurian J.V; (2006). Flexural behavior of reinforced Lightweight concrete beams made with oil palm kernel shell (OPS). Journal of advanced concrete Technology, 4,(3) 1-10.

Torok, T. I. Kekesi, T; Kabelik, G. (2000): Extraction of Tin from scrap by Chemical and electrochemical methods in alkaline media, Hydrometallurgy, 55, 213 – 222.

Towl, K and Burrel, G; (2005) Reinforcing steel in New Zealand – pacific steel future product range and design issues, SESOC Journal, Vol. 18; (1) pp 24 – 28.

Wight, J.K; and Magregor, J.G. (2012): Reinforced concrete mechanics and design. Pearson Education, Inc, Saddle river, New Jersey 07458, 6th edn.

Yang, E.I; Morita, S; Seong, T.Y; (2000).Effect of axial restraint on Mechanical behavior of high – strength concrete beams, ACI Structural Journal,pp 751 – 756.

Zaki, S.I; Ibrahim, M.M; Sameh, (2011) A.E; Flexural behavior of reinforced High – Performance concrete beams made with steel slag coarse aggregate; international scholarly Research network (ISRN Civil engineering;

APPENDIX A: SAMPLE CALCULATION OF THEORETICAL LOAD-DEFLECTION RESPONSE OF A BEAM

Beam 1: Data

Fiber 1; b = 100mm, d = 171mm, ε_{cm} = 0.0001, fcu = 21.33N/mm^2, c = 51.09 mm, E_s = 192500N/mm^2, A_s = 100.53mm^2

$$F_c = b_c f_{cu} \left[\frac{\varepsilon cm}{\varepsilon o} - 1/3 \left(\frac{\varepsilon cm}{\varepsilon o}\right)^2\right] \quad (3.7)$$

$$= 100 \text{ x } 51.09 \text{ x } 21.33 \left[\frac{0.0001}{0.002} - ⅓(\frac{0.0001}{0.002})^2\right]$$

$$= 4541.53\text{N}$$

$$f_s = E_s \text{ x } \varepsilon_{cm} \left[\frac{d-c}{c}\right] A_s \quad (3.8)$$

$$= 192500 \text{ x } 0.0001\left[\frac{171-51.09}{51.09}\right] 100.53$$

$$= 4541.99 \text{ N}$$

Determine Moment

$$M_{cc} = bc^2 f_{cu} \frac{\varepsilon_{cm}}{\varepsilon_0}\left[⅔ - ¼\frac{\varepsilon_{cm}}{\varepsilon_0}\right] \quad (3.9)$$

$$= 100 \text{ x } (51.09)2 \text{ x } 21.33\left[\frac{0.0001}{0.002}\right]\left[⅔ - ¼ \frac{0.0001}{0.002}\right]$$

$$= 183032.59 \text{ Nmm}$$

$$M_s = F_s[\text{d} - \text{c}] \quad (3.10)$$

= 4541.99 (171 – 51.09)

= 544630.021 Nmm

$M = M_{cc} + M_s$ (3.11)

= 183032.59 + 544630.021

= 727662.611 Nmm

= 0.728 kNM

M_1 = 0.728 kNM

Load, P due to M_1, $P = \frac{6M}{L}$ (3.12)

$= \frac{0.728 \ x \ 106 \ x \ 6}{900}$ = 4853.33 N

= 4.853 kN

Deflection, δ_1 due to P_1:

$\delta_1 = \frac{23PL^3}{1296 \ EI}$ (3.13)

$I = \frac{bh^3}{12} = \frac{100 \ x \ 200^3}{12}$ = 6.67 x 10^7 mm^4

E_S = 192500 N/mm^2

$\delta_1 = \frac{23 \ x \ 485 \ x \ 9003}{1296 \ x \ 192500 \ x \ 6.67 \ x \ 107}$

= 0.00531mm

Thus for fiber 1 of beam 1

Fiber	N.A depth	strain value	Moment	Load	Deflection
1	51.09 mm	0.0001	0.728kNM	4.85kN	0.00531mm

Table 1: Theoretical Load-deflection response values forBeam1

Fiber No	**N.A Depth (mm)**	**Strain**	**Moment (kNM)**	**Load (kN)**	**Deflection (mm)**
1	47.70	0.0001	0.728	4.85	0.00531
2	48.035	0.0002	1.536	10.24	0.0103
3	48.392	0.0003	2.2774	15.183	0.145
4	48.75	0.0004	3.002	20.013	0.191
5	49.117	0.0005	3.710	24.733	0.236
6	49.4927	0.0006	4.3964	29.31	0.279
7	49.8772	0.0007	5.066	33.773	0.322
8	50.272	0.0008	5.718	38.12	0.363
9	50.677	0.0009	6.3499	42.333	0.404
10	51.092	0.001	6.9632	46.4210	0.443
11	52.8683	0.0014	9.22	61.47	0.586
12	54.8576	0.0018	11.14	74.27	0.706
13	55.9462	0.002	11.962	79.75	0.760

Table 2: Theoretical Load-deflection response values for BEAM 2

Fiber No	N.A Depth (mm)	Strain	Moment (kNM)	Load (kN)	Deflection (mm)
1	48.47	0.0001	0.788	5.253	0.0053
2	48.814	0.0002	1.25	8.333	0.0084
3	49.531	0.0004	3.045	20.45	0.194
4	50.283	0.0006	4.459	29.73	0.283
5	51.072	0.0008	5.7983	38.66	0.369
6	51.902	0.001	7.061	47.073	0.449
7	52.776	0.0012	8.2434	54.96	0.524
8	53.699	0.0014	9.344	62.213	0.594
9	55.7102	0.0018	9.697	64.65	0.616
10	56.811	0.002	12.121	80.81	0.770
11	61.0838	0.0024	12.813	85.42	0.814
12	67.5012	0.003	13.252		

Table 3: Theoretical load-deflection response values for BEAM 3

Fiber No	N.A Depth (mm)	Strain	Moment (kNM)	Load (kN)	Deflection (mm)
1	47.698	0.0001	0.7764	5.176	0.0050
2	48.372	0.0003	2.2774	15.182	0.139
3	49.117	0.0005	3.8914	25.942	0.238
4	49.8172	0.0007	5.0663	33.78	0.310
5	50.677	0.0009	6.825	45.50	0.417
6	51.5182	0.0011	7.557	50.38	0.462
7	52.8683	0.0014	9.2172	61.45	0.564
8	54.8576	0.0018	11.13614	74.241	0.681
9	55.9462	0.002	11.962	79.75	0.732
10	64.987	0.003	13.6671	91.12	

Table 4: Theoretical load-deflection response values for BEAM 4

Fiber No	N.A Depth (mm)	Strain	Moment (kNM)	Load (kN)	Deflection (mm)
1	48.47	0.0001	0.7876	5.251	0.0053
2	48.64	0.00015	1.175	7.833	0.0079
3	49.169	0.0003	2.31011	15.4	0.147
4	49.716	0.00045	3.383	22.533	0.215
5	50.283	0.0006	4.459	29.73	0.283
6	50.8713	0.00075	3.471	36.473	0.348
7	54.18	0.9915	9.862344	65.75	0.627
8	55.7102	0.0018	11.286	75.24	0.717
9	56.811	0.002	12.121	80.81	0.770
10	61.0838	0.0024	12.813	85.42	0.815
11	67.5012	0.003	13.252		

Table 5: Theoretical Load-deflection response values for BEAM 5

Fiber No	N.A Depth (mm)	Strain	Moment (kNM)	Load (kN)	Deflection (mm)
1	57.265	0.0001	0.913	6.087	0.006
2	58.057	0.0003	2.6753	17.84	0.164
3	59.313	0.0006	5.155	34.37	0.315
4	60.6612	0.0009	7.431	49.54	0.455
5	62.113	0.0012	9.4938	63.292	0.581
6	63.6833	0.0015	11.333	75.553	0.693
7	65.3893	0.0018	12.9366	86.244	0.791
8	66.6127	0.002	13.868	92.453	0.848
9	73.7643	0.0024	13.65		
10	81.9882	0.003	13.526		

Table 6: Theoretical load-deflection response values BEAM 6

Fiber No	N.A Depth (mm)	Strain	Moment (kNM)	Load (kN)	Deflection (mm)
1	58.143	0.0001	0.92953	6.197	0.0063
2	58.54	0.0002	1.829	12.193	0.0123
3	59.358	0.0004	3.571	23.81	0.227
4	60.2132	0.0006	5.223	34.0	0.332
5	61.11	0.0008	6.783	45.22	0.431
6	65.0514	0.001	8.248	54.987	0.524
7	64.6262	0.0015	11.475	76.5	0.279
8	66.3479	0.0018	13.0951	87.34	0.832
9	67.582	0.002	14.0353	93..57	0.892
10	74.79	0.0024	13.802	13.802	0.879
11	83.064	0.003	13.659		

Table 7: Theoretical load- deflection response values for Beam 7

Fiber No	N.A Depth (mm)	Strain	Moment (kNM)	Load (kN)	Deflection (mm)
1	52.282	0.0001	1.0552	7.035	0.0071
2	52.65	0.0002	2.0865	13.91	0.128
3	53.408	0.0004	4.0762	27.18	0.249
4	54.203	0.0006	5.967	39.78	0.365
5	55.037	0.0008	7.75521	51.701	0.474
6	55.913	0.001	9.4384	62.923	0.577
7	58.3153	0.0015	13.1632	87.754	0.805
8	59.9264	0.0018	15.0471	100.314	0.920
9	61.0833	0.002	16.1427223	107.65	0.988
10	64.3806	0.0024	17.582		
11	70.9669	0.003	18.1396		

Table 8: Theoretical Load-deflection response values for Beam 8

Fiber No	N.A Depth (mm)	Strain	Moment (kNM)	Load (kN)	Deflection (mm)
1	53.106	0.0001	1.0699	7.133	0.0072
2	53.857	0.0003	3.1365	20.91	0.199
3	55.0488	0.0006	6.049	40.33	0.384
4	56.329	0.0009	8.727	58.18	0.555
5	57.71	0.0012	11.1597	74.40	0.709
6	59.2053	0.0015	13.336	88.91	0.848
7	60.8328	0.0018	15.241	101.61	0.963
8	62.0013	0.002	16.61	110.73	1.06
9	64.574	0.0024	18.17024		
10	69.1785	0.003	19.781		

Table 9: Theoretical load-deflection response values for Beam 9

Fiber No	N.A Depth (mm)	Strain	Moment (kNM)	Load (kN)	Deflection (mm)
1	57.769	0.0001	1.1521	7.68	0.007
2	58.162	0.0002	2.2774	15.183	0.139
3	58.976	0.0004	4.447	29.65	0.272
4	59.8287	0.0006	6.504	43.36	0.398
5	60.7216	0.0008	8.447	56.313	0.517
6	61.659	0.001	10.272	68.48	0.628
7	64.22306	0.0015	14.29322	95.29	0.874
8	67.1676	0.0018	16.0085	106.723	0.979
9	67.1676	0.002	17.486	116.573	1.07
10	69.8682	0.0024	19.387		
11	74.681	0.003	21.0152		

Table 10: Theoretical load-deflection response values for Beam 10

Fiber No	N.A Depth (mm)	Strain	Moment (kNM)	Load (kN)	Deflection (mm)
1	58.653	0.0001	1.1675	7.783	0.0078
2	59.05	0.0002	2.308	15.39	0.147
3	59.873	0.0004	4.505	30.033	0.286
4	60.734	0.0006	5.161	34.161	0.328
5	61.636	0.0008	8.5301	56.91	0.542
6	62.5824	0.001	10.4034	69.36	0.661
7	65.1712	0.0015	14.471	96.473	0.920
8	66.9016	0.0018	16.5121	110.08	1.049
9	68.1416	0.002	17.696	117.97	1.125
10	70.864	0.0024	19.61113	130.74	1.25
11	75.713	0.003	21.24214		

Table 11: Theoretical Load-deflection response values for Beam 11

Fiber No	N.A Depth (mm)	Strain	Moment (kNM)	Load (kN)	Deflection (mm)
1	57.769	0.00001	1.1521	7.68	0.0074
2	58.162	0.0002	2.2774	15.162	0.019
3	58.976	0.0004	4.4463	29.642	0.272
4	59.828	0.0006	6.504	43.36	0.398
5	60.7216	0.0008	8.447	56.31	0.517
6	61.659	0.001	10.272	68.48	0.628
7	63.1566	0.0013	12.78	85.20	0.782
8	64.7788	0.0016	15.001	100.00	0.918
9	67.167	0.002	17.486	116.57	1.07
10	69.8682	0.0024	19.387		
11	74.68	0.003	21.016		

Table 12: Theoretical load-deflection response values for Beam 12

Fiber No	N.A Depth (mm)	Strain	Moment (kNM)	Load (kN)	Deflection (mm)
1	58.653	0.0001	1.1675	7.783	0.0078
2	58.85	0.00015	1.741	11.61	0.012
3	59.05	0.0002	2.308	15.39	0.147
4	59.252	0.00025	2.86744	19.12	0.182
5	59.457	0.0003	3.42024	22.8	0.218
6	59.873	0.0004	4.501	30.01	0.286
7	60.2988	0.0005	5.5612	37.074	0.354
8	60.734	0.0006	6.5888	43.93	0.419
9	61.636	0.0008	8.5561	57.041	0.544
10	62.5824	0.001	10.4034	69.36	0.662
11	68.1416	0.002	17.6958	80.85	0.771
12	75.713	0.003	21.24214		

Table 13: Theoretical load-deflection response values for Beam 13

Fiber No	N.A Depth (mm)	Strain	Moment (kNM)	Load (kN)	Deflection (mm)
1	51.422	0.0001	1.0826	7.22	0.007
2	51.786	0.0002	2.141	14.28	0.131
3	52.535	0.0004	4.1828	27.89	0.256
4	53.3206	0.0006	6.1234	40.823	0.375
5	54.1448	0.0008	7.95964	53.064	0.487
6	55.0108	0.001	9.6884	64.59	0.593
7	57.3858	0.0015	10.2025	68.02	0.624
8	60.123	0.002	16.588	110.59	1.02
9	62.6459	0.0024	18.447	122.98	1.13
10	67.167	0.003	20.1126		

Table 14: Theoretical load-deflection response values for Beam 14

Fiber No	N.A Depth (mm)	Strain	Moment (kNM)	Load (kN)	Deflection (mm)
1	52.238	0.0001	1.0978	7.32	0.0074
2	52.604	0.0002	2.171	14.473	0.138
3	52.978	0.0003	3.21854	21.46	0.205
4	53.567	0.00045	4.74242	31.62	0.301
5	54.156	0.0006	6.20782	41.39	0.395
6	54.987	0.0008	8.0685	53.29	0.513
7	55.865	0.001	9.8197	65.46	0.624
8	61.0323	0.002	15.941	106.27	1.013
9	63.597	0.0024	18.676	124.57	1.19
10	66.5043	0.0028	19.9533	133.02	1.27
11	68.1411	0.003	20.3474		

Table 15; Theoretical load-deflection response values for Beam 15

Fiber No	N.A Depth (mm)	Strain	Moment (kNM)	Load (kN)	Deflection (mm)
1	51.422	0.0001	1.0826	7.22	0.007
2	51.604	0.00015	1.615	10.77	0.0104
3	51.786	0.0002	2.141	14.273	0.131
4	52.156	0.0003	3.1743	21.162	0.194
5	52.535	0.0004	4.183	27.89	0.256
6	52.923	0.0005	5.18933	34.60	0.317
7	53.3204	0.0006	6.1234	40.823	0.375
8	54.1448	0.0008	7.9577	53.064	0.487
9	55.0108	0.001	9.6884	64.59	0.593
10	60.1238	0.002	15.7542	105.03	0.964
11	67.167	0.003	20.113		

Table 16: Theoretical load-deflection response values for Beam 16

Fiber No	N.A Depth (mm)	Strain	Moment (kNM)	Load (kN)	Deflection (mm)
1	52.236	0.0001	1.0962	7.31	0.0074
2	52.42	0.00015	1.694	11.293	0.0114
3	52.604	0.0002	2.171	14.473	0.138
4	52.7892	0.00025	2.698	17.99	0.171
5	52.978	0.0003	3.219	21.46	0.205
6	53.362	0.0004	4.241	28.27	0.270
7	54.156	0.0006	6.208	41.39	0.395
8	54.9893	0.0008	8.0685	53.79	0.513
9	55.865	0.001	9.8197	65.47	0.624
10	61.0323	0.002	15.0393	100.26	0.956
11	62.2638	0.0022	17.80912	118.73	1.132
12	64.9885	0.0026	19.3931	129.29	1.23
13	68.1411	0.003	20.3474		

Table 17: Theoretical load-deflection response values for Beam 17

Fiber No	N.A Depth (mm)	Strain	Moment (kNM)	Load (kN)	Deflection (mm)
1	42.624	0.0001	0.938	6.253	0.0061
2	42.938	0.0002	1.809	12.06	0.012
3	43.258	0.0003	2.684	17.893	0.164
4	43.9227	0.0005	4.3724	29.15	0.267
5	44.6196	0.0007	5.978	39.853	0.366
6	44.981	0.0008	6.749	44.993	0.413
7	45.353	0.0009	7.498	49.99	0.459
8	45.7342	0.001	8.225	54.833	0.503
9	46.528	0.0012	9.6112	64.074	0.588
10	47.367	0.0014	11.604	77.36	0.710
11	49.1994	0.0018	13.20	88.0	0.807
12	50.2042	0.002	14.193	94.62	0.868
13	52.4265	0.0024	15.85	105.67	0.970
14	56.4406	0.003	17.42		

Table 18: Theoretical load-deflection response values for Beam 18

Fiber No	N.A Depth (mm)	Strain	Moment (kNM)	Load (kN)	Deflection (mm)
1	43.329	0.0001	0.9281	6.19	0.0062
2	43.646	0.0002	1.8361	12.24	0.012
3	44.3022	0.0004	3.591	23.94	0.228
4	44.9919	0.0006	5.2622	35.08	0.334
5	45.7159	0.0008	6.848	45.653	0.435
6	46.092	0.0009	7.6075	50.72	0.483
7	46.478	0.001	8.345	55.633	0.530
8	47.282	0.0012	9.7503	65.00	0.620
9	49.0312	0.0016	12.274	81.83	0.780
10	49.9004	0.0018	13.386	89.24	0.851
11	51.0033	0.002	14.391	95.94	0.915
12	53.2518	0.0024	16.065	107.10	1.021
13	57.3106	0.003	17.64543		

APPENDIX B. EXPERIMENTAL DATA OF LOAD-DEFLECTION RESPONSEOF BEAMS

Table 1: Experimental load-deflection response values for BEAM 1

LOAD (kN)	DEFLECTION (mm)
0	0
5	0.0072
10	0.0108
15	0.041
20	0.122
27	0.20
35	0.26
42	0.31
48	0.34
55	0.38
62	0.40
68	0.48
75	0.56
82	0.70

Table 2: Experimental load-deflection response values for BEAM 2

LOAD (kN)	DEFLECTION (mm)
0	0
7	0.003
12	0.005
20	0.10
27	0.13
32	0.16
40	0.20
50	0.28
60	0.39
72	0.48
80	0.58
86.5	0.872

Table 3: Experimental load-deflection response values for BEAM 3

LOAD (kN)	DEFLECTION (mm)
0	0
7	0.003
10	0.005
20	0.05
30	0.13
40	0.17
50	0.22
60	0.36
70	0.45
80	0.64

Table 4: Experimental load-deflection response values for BEAM 4

LOAD (kN)	DEFLETION (mm)
0	0
7	0.004
10	0.006
25	0.11
35	0.18
42	0.22
50	0.26
60	0.29
70	0.364
80	0.44
90	0.52
95	0.83

Table 5: Experimental load-deflection response values for BEAM 5

LOAD (kN)	DEFLECTION (mm)
0	0
8	0.007
16	0.105
30	0.142
45	0.247
58	0.35
65	0.37
70	0.40
80	0.56
96	0.75

Table 6: Experimental load-deflection response values for BEAM 6

LOAD (kN)	DEFLECTION (mm)
0	0
9	0.004
15	0.1123
25	0.18
35	0.26
42	0.32
48	0.34
55	0.38
62	0.46
70	0.61
80	0.84
92	1.06

Table 7: Experimental load-deflection response values for **Beam 7**

LOAD (kN)	**DEFLECTION (mm)**
0	0
7	0.0084
14	0.084
20	0.11
25	0.20
30	0.22
40	0.26
50	0.29
60	0.33
64	0.36
90	0.46
100	0.58
109	0.66

Table 8: Experimental load-deflection response values BEAM 8

LOAD (kN)	DEFLECTION (mm)
0	0
8	0.0036
18.75	0.07
31	0.13
45	0.20
58	0.25
65	0.36
72	0.42
84	0.46
88	0.58
91	0.68
96	0.98

Table 9:Experimental Load-deflection response values for BEAM 9

LOAD (kN)	DEFLECTION (mm)
0	0
10	0.005
18	0.07
36	0.17
42	0.20
55	0.22
65	0.26
72	0.39
80	0.42
93	0.58
100	0.77

Table 10: Experimental Load-deflection response values for BEAM 10

LOAD (kN)	DEFLECTION (mm)
0	0
10	0.0035
15	0.007
20	0.092
25	0.12
30	0.16
40	0.22
48	0.26
56	0.32
65	0.38
72	0.42
80	0.52
90	0.64
96	0.84
97.5	1.2

Table 11: Experimental Load-deflection response values BEAM 11

LOAD (kN)	DEFLECTION (mm)
0	0
10	0.005
20	0.0085
30	0.11
40	0.15
50	0.30
60	0.35
72	0.43
80	0.48
90	0.58
94.5	0.63
100	0.80

Table 12: Experimental Load-deflection response values for BEAM 12

LOAD (KN)	DEFLECTION (mm)
0	0
7	0.008
10	0.01
18	0.10
24	0.18
30	0.26
40	0.29
50	0.32
65	0.38
72	0.48
80	0.62
90	0.88
100	1.14
110	1.23

Table 13: Experimental load-deflection response values for BEAM 13

LOAD (kN)	DEFLECTION (mm)
0	0
8	0.005
15	0.085
25	0.10
36	0.13
42	0.20
50	0.26
60	0.32
70	0.38
80	0.42
90	0.54
97	0.76

Table 14: Experimental load-deflection response values for BEAM 14

LOAD (kN)	DEFLECTION (mm)
0	0
9	0.004
15	0.007
19	0.092
27	0.18
36	0.24
48	0.28
60	0.38
72	0.64
80	1.10

Table 15: Experimental load-deflection response values for BEAM 15

LOAD (kN)	DEFLECTION (mm)
0	0
9	0.006
15	0.008
20	0.03
30	0.072
40	0.14
50	0.18
60	0.22
70	0.30
80	0.34
90	0.46
95	0.58

Table 16: Experimental Load-deflection response values for BEAM 16

LOAD (kN)	DEFLECTION (mm)
0	0
8	0.006
15	0.082
22	0.096
30	0.14
40	0.18
50	0.24
60	0.36
70	0.42
80	0.68
90	1.00

Table 17: Experimental load-deflection response values for BEAM 17

LOAD (kN)	DEFLECTION (mm)
0	0
7	0.006
15	0.0072
25	0.133
32	0.195
40	0.53
50	0.282
60	0.309
70	0.36
80	0.48
95	0.66

Table 18: Experimental Load-deflection response values for BEAM 18

LOAD (kN)	DEFLECTION (mm)
0	0
8	0.0045
16	0.0082
25	0.12
36	0.18
42	0.24
50	0.32
60	0.346
70	0.38
80	0.674
85	0.708
84	0.718

APPENDIX C: CALCULATION OF EFFECTIVE MOMENT OF INERTIA (Ie) OF BEAM SECTION

$$I_e = \left[\frac{Mcr}{Ma}\right]^3 I_g + \left[1 - \left[\frac{Mcr}{Ma}\right]^3\right] I_{cr}$$

Where

$$M_{cr} = \frac{f_r I_g}{y_t}; \quad f_r = 0.62\sqrt{f_{cu}}$$

$$M_a = M_u = \rho f y b d^2 \left(1 - \frac{0.59\rho f_y}{f_{cu}}\right)$$

$$I_{cr} = 0.18\ (\text{n}\rho)0.25 \ \text{x}\ \frac{bd^3}{12}$$

Where

$$\text{n} = \frac{E_s}{E_c}; \quad \rho = \frac{A_{st}}{bd}$$

For Beam 1:

b = 100mm, d = 176mm, f_{cu} 21.33N/mm^2, y_1 =100mm

$f_r = 0.62\sqrt{21.33} = 2.063$ N/mm^2

$I_g = \frac{bd^3}{12} = \frac{100\ x\ 176^3}{12} = 6.67$ x 10^7 mm^4

$\text{P} = \frac{A_{st}}{bd} = \frac{201}{100\ x\ 171} = 0.01175$; $\text{n} = \frac{E_s}{E_c} = \frac{200000}{23000} = 8.7$

$I_{cr} = 0.18\ (8.7 \text{ x } 0.01175)\ 0.25 \text{ x } 100 \text{ x } \frac{100\ x\ 176^3}{12}$

$= 0.18 \text{ x } 0.5654 \text{ x } 6.67 \text{ x } 10^7 = 6.79 \text{ x } 10^6$ mm^4

M_a = 2.2774kNM = 2.2774 x 10^7Nmm

M_{cr} = 2.068 kNM = 2.068 x 10^6Nmm

$I_e \left[\frac{2.068\ x\ 106}{2.2774\ x\ 106}\right]^3$ x 6.67 x 10^6 + 1 - $\left[\left[\frac{2.068\ x\ 106}{2.2774\ x\ 106}\right]^3 6.67 \text{ x } 10^6\right]$

= 0.9081^3 x 6.67 10^6 + $[1 - (0.9081)^3]$6.79 x 10^6

= 0.748822 x 6.67 x 10^6 + $[1 - 0.748861]$6.67 x 10^6

= 4994642. 74 + 1675097.13

= 6.67 x 10^6 mm^4

I_e = 6.67 x 10^6 mm^4 for BM 1 to 6

I_e = 6.598 x 10^6 mm^4 for BM 7 to 13

APPENDIX D: DETERMINATION OF YIELD POINT OF TENSILE STEEL FOR DEFLECTION VALUES

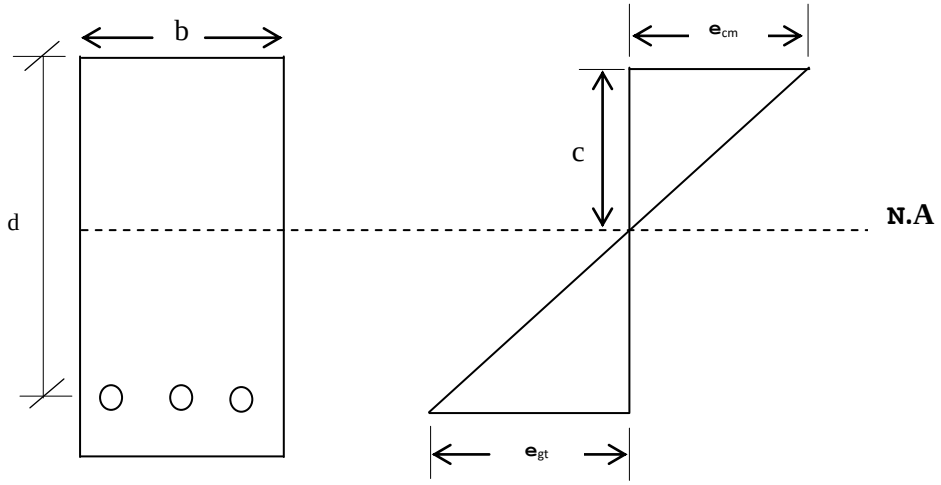

Strain distribution at beam section

From similar triangles:

$\frac{\varepsilon_{cm}}{c} = \left[\frac{\varepsilon_{st}}{d-c}\right]$

$\varepsilon_{st} = \varepsilon_{cm}\left[\frac{d-c}{c}\right]$

Beam 1

At ε_{cm} = 0.0009, c = 50.272mm

$\varepsilon_{st} = \varepsilon_{cm}\left[\frac{d-c}{c}\right]$ = 0.0009 $\left[\frac{171-50.272}{50.272}\right]$= 0.002137

This implies steel has yield.

Beam 2

At ε_{cm} = 0.001, c = 51.902mm

ε_{st}= $\varepsilon_{cm}\left[\frac{d-c}{c}\right]$ = 0.001 $\left[\frac{171-51.902}{51.902}\right]$ = 0.0022947

This implies steel has yield

Beam 3

Atε_{cm} = 0.009, c = 50. 679mm

$\varepsilon_{st} = \varepsilon_{cm}\left[\frac{d-c}{c}\right]$ = 0.009 $\left[\frac{171-50.679}{50.679}\right]$= 0.00213676

This implies steel has yield

Beam 4

Atε_{cm} = 0.0015, c = 54.18mm

ε_{st}= $\varepsilon_{cm}(\frac{d-c}{c})$ = 0.0015 $(\frac{171-54.18}{54.18})$ = 0.0032342

Steel has yield

Beam 5

Atε_{cm} = 0.0012, c = 62.113 mm

ε_{st} = $\varepsilon_{cm}\left[\frac{d-c}{c}\right]$ = 0.0012 $\left[\frac{171-62.113}{62.113}\right]$= 0.00210366

This implies steel has yield.

Beam 6

Atε_{cm} = 0.0015, c = 64.6262 mm

$\varepsilon_{st} = \varepsilon_{cm}\left[\frac{d-c}{c}\right]$ = 0.0015 $\left[\frac{171-64.6262}{64.6262}\right]$= 0.00247

This implies steel has yield

Beam 7

At ε_{cm}= 0.001, c = 55.913mm

ε_{st} = $\varepsilon_{cm}\left[\frac{d-c}{c}\right]$ = 0.001 $\left[\frac{171-55.913}{55.913}\right]$= 0.002058

This implies steel has yield

Beam 8

At ε_{cm}= 0.0012, c = 57.71mm

$\varepsilon_{st} = \varepsilon_{cm}\left[\frac{d-c}{c}\right] = 0.0012\left[\frac{171-57.71}{57.71}\right] = 0.00236$

This implies steel has yield.

Beam 9

At ε_{cm} = 0.0015, c = 64.22306mm

$\varepsilon_{st} = \varepsilon_{cm}\left[\frac{d-c}{c}\right] = 0.0015\left[\frac{171-64.22306}{64.22306}\right] = 0.002494$

This implies steel has yield

Beam 10

At ε_{cm} = 0.0015, c = 65.1712

$\varepsilon_{st} = \varepsilon_{cm}\left[\frac{d-c}{c}\right] = 0.0015\left[\frac{171-65.1712}{65.1712}\right] = 0.00244$

This implies steel has yield

Beam 11

At ε_{cm} = 0.0013, c = 63.1566mm

$\varepsilon_{st} = \varepsilon_{cm}\left[\frac{d-c}{c}\right] = 0.0013\left[\frac{171-63.1566}{63.1566}\right] = 0.00222$

This implies steel has yield

Beam 12

At ε_{cm} = 0.002, c = 68.1476mm

$\varepsilon_{st} = \varepsilon_{cm}\left[\frac{d-c}{c}\right] = 0.002\left[\frac{171-68.1476}{68.1476}\right] = 0.003$

This implies steel has yield.

Beam 13

At ε_{cm} = 0.001, c = 55.0108mm

$\varepsilon_{st} = \varepsilon_{cm}\left[\frac{d-c}{c}\right] = 0.001\left[\frac{171-55.0108}{55.0108}\right] = 0.00211$

This implies steel has yield.

Beam 14

At ε_{cm} = 0.001, c = 55.865 mm

$\varepsilon_{st} = \varepsilon_{cm}\left[\frac{d-c}{c}\right] = 0.001\left[\frac{171-55.865}{55.865}\right] = 0.002061$

This implies steel has yield

Beam 15

At ε_{cm} = 0.001, c = 55.0108mm

$\varepsilon_{st} = \varepsilon_{cm}\left[\frac{d-c}{c}\right] = 0.001\left[\frac{171-55.0108}{55.0108}\right] = 0.0021$

This implies steel has yield

Beam 16

At ε_{cm} = 0.001, c = 55.865mm

$\varepsilon_{st} = \varepsilon_{cm}\left[\frac{d-c}{c}\right] = 0.001\left[\frac{171-55.865}{55.865}\right] = 0.002061$

This implies steel has yield

Beam 17

At ε_{cm} = 0.0008, c = 44.9818mm

$\varepsilon_{st} = \varepsilon_{cm}\left[\frac{d-c}{c}\right] = 0.008\left[\frac{171-44.9818}{44.9818}\right] = 0.00224123$

This implies steel has yield

Beam 18

At ε_{cm} = 0.0008, c = 45.7159mm

$\varepsilon_{st} = \varepsilon_{cm}\left[\frac{d-c}{c}\right] = 0.0008\left[\frac{171-45.7159}{45.7159}\right] = 0.002192394$

This implies steel has yield.

APPENDIX E: DATA FOR STIFFNESS VERSUS LOAD RESPONSE OF BEAMS

Table 1: Stiffness –Load response values for BEAM 1

EI (MN)	LOAD (k N)
5.52	0
5.41	8
5.27	16
4.94	30
4.64	45
4.47	58
4.12	65
3.78	70
2.72	80
2.10	88

Table 2: Stiffness-load response values for BEAM 2

EI (MN)	LOAD (k N)
5.52	0
5.33	7
5.12	12
4.82	20
4.11	27
3.98	32
3.85	40
3.67	50
3.25	60
2.88	72
2.42	80
1.98	86

Table 3: Stiffness – load response values for BEAM 3

EI (MN)	LOAD (kN)
5.50	0
5.463	7
5.073	10
4.683	20
4.35	30
3.80	40
3.623	50
3.25	60
2.13	70
2.03	80

Table4: Stiffness – load response values for BEAM 4

EI (MN)	**LOAD (kN)**
5.35	0
5.29	8
5.15	16.75
4.97	31
4.09	45
3.82	58
2.72	65
1.25	72

Table5: Stiffness-load response values for BEAM 5

EI (MN)	LOAD (kN)
5.46	0
5.35	9
5.12	15
4.85	25
3.98	35
3.45	42
3.15	48
2.82	55

Table 6: Stiffness –load response values for BEAM 6

EI (MN)	LOAD (kN)
5.25	0
5.09	10
4.94	15
4.68	20
4.23	25
4.05	30
3.83	40
3.24	48
2.42	52

Table 7; Stiffness - load response values for BEAM 7

EI (MN)	LOAD (kN)
0	0
5.92	7
5.84	14
5.53	20
5.35	25
5.15	30
4.90	40
4.78	50
4.65	60
3.72	70
2.25	80
1.93	88

Table 8: Stiffness – load response values for BEAM 8

EI (MN)	LOAD (kN)
5.68	0
5.61	7
5.53	10
4.61	15
4.3	25
4.0	35
3.71	42
3.25	50
2.64	60
2.25	70
2.0	80

Table 9: Stiffness-Load response for BEAM 9

EI (MN)	LOAD (kN)
5.59	0
5.53	10
5.22	18
4.98	36
4.57	42
4.18	55
3.65	60
3.22	65
1.98	70

Table10: Stiffness – Load response for BEAM 10

EI (MN)	LOAD (kN)
0	0
5.33	7
5.29	10
5.17	18
4.57	24
3.67	30
3.15	40
2.75	50
2.28	58
1.98	65

Table 11: Stiffness –load response values for BEAM 11

EI (MN)	LOAD (kN)
5.52	0
5.43	7
5.15	15
4.75	25
4.32	32
3.85	40
3.22	48
2.84	55
2.44	60

Table 13: Stiffness-Load response values for BEAM 13

EI (MN)	LOAD (kN)
5.88	0
5.83	9
5.71	15
5.53	20
5.22	30
4.97	40
4.35	50
4.10	60
2.94	70
2.42	80
1.84	88

Table 14: Stiffness – load response values for BEAM 14

EI (MN)	LOAD (kN)
5.55	0
5.44	10
5.27	20
5.07	30
4.35	40
4.05	50
3.78	60
3.18	70
2.72	80
2.34	85

Table 15: Stiffness – load response values for BEAM 15

EI (MN)	LOAD (kN)
5.48	0
5.42	9
5.37	15
5.07	25
4.76	36
4.41	42
4.29	50
3.46	60
2.53	72

Table 16: Stiffness – load response values for BEAM 16

EI (MN)	LOAD (kN)
0	0
5.55	8
5.31	14
4.96	20
4.35	26
4.05	30
3.85	40
3.28	50
2.82	60
2.18	68

Table 17: Stiffness- load response values for BEAM 17

EI (MN)	LOAD (kN)
5.55	0
5.53	7
5.27	13
4.82	20
4.32	25
3.78	30
3.24	35
2.72	40
2.18	45
1.82	55

Table 18: Stiffness-Load response values for BEAM 18

EI (MN)	LOAD (kN)
5.58	0
5.53	8
5.05	15
4.62	20
4.24	25
3.22	30
2.72	35
2.46	40
2.18	45
1.72	50

APPENDIX F

Table 1: Mid-span deflection at Yield point of steel and ultimate state of beam (Theoretical Values)

Bm ID	Deflection at Yield point of steel (mm)	Deflection at ultimate state (mm)	Deflection ductility index
Bm1	0.443	0.760	1.72
Bm 2	0.320	0.720	2.31
Bm 3	0.300	0.630	2.10
Bm 4	0.310	0.720	2.32
Bm 5	0.400	0.850	1.85
Bm 6	0.330	0.900	2.73
Bm 7	0.517	0.988	1.91
Bm 8	0.302	0.860	2.85
Bm 9	0.395	0.760	1.92
Bm 10	0.340	1.020	3.00
Bm 11	0.450	0.780	1.73
Bm 12	0.354	1.130	3.19
Bm 13	0.320	0.650	2.03
Bm 14	0.363	0.940	2.59
Bm 15	0.300	0.570	1.90
Bm16	0.290	0.740	2.74
Bm17	0.292	0.540	1.85
Bm 18	0.310	0.720	2.35

Table 2: Mid-span deflection at Yield point of steel and ultimate state of beam (Experimental Values)

Bm ID	Deflection at Yield point of steel (mm)	Deflection at ultimate state (mm)	Deflection ductility index
Bm1	0.400	0.690	1.73
Bm 2	0.385	0.870	2.26
Bm 3	0.360	0.640	1.78
Bm 4	0.364	0.830	2.28
Bm 5	0.400	0.750	1.87
Bm 6	0.390	1.06	2.72
Bm 7	0.360	0.660	1.82
Bm 8	0.360	0.980	2.72
Bm 9	0.390	0.770	1.98
Bm 10	0.380	1.20	3.16
Bm 11	0.430	0.800	1.86
Bm 12	0.380	1.230	3.24
Bm 13	0.380	0.755	1.99
Bm 14	0.380	1.10	2.89
Bm 15	0.300	0.580	1.93
Bm16	0.360	1.00	2.78
Bm17	0.360	0.660	1.83
Bm 18	0.340	0.990	2.38

APPENDIX G

Design of Singly RC Beam

The beam is assumed to carry three (3Nos) courses of block-work over an opening (figure below).

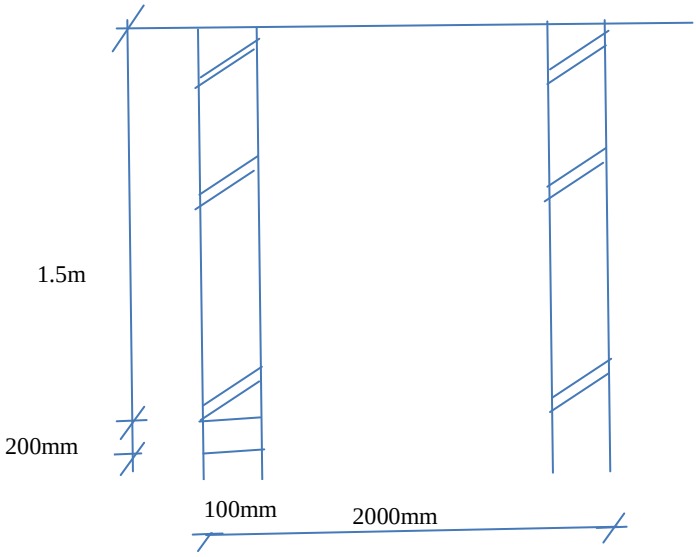

Unit Weights

150mm block – 2.15kN/m

Wall finishes – 0.60kN/m^2

Loading:

Wall = 2.15x0.765x1.4

= 2.3038kN/m

Finisher = 0.60x0.765x14

= 0.672

Total load = 3.62kN/m

Life load = 3.0kN/m

Design load, w = 1.4gk + 1.6gk

= 3.62 + 1.6 x 3 = 3.62 + 4.8 = 8.42kN/m

M = $\frac{wl^2}{8} = \frac{8.42\times2^2}{8} = 4.21kNm = 1.0325 \times 10^2$Nmm

= 1.0525kNm

Mu = $0.156fcubd^2$ = 0.156x25x100x176 = 12080640Nmm

= 12.081kNm

Since M < Mu, design beam for tensile reinforcement only.

K = $\frac{m}{f_{cu}\,bd^2}$ = 0.14l $Z_a = d\left(0.5 + \sqrt{0.25 - \frac{0.14}{0.9}}\right) = 0.307$

Z = $176(0.5 + 0.307) = 142.032mm$

M = $A_s . f_y Z; A_s = \frac{M}{f_y Z} = \frac{4.21 \times 10^6}{250 \times 142.032} = 124.81mm^2$

As required = $124.81mm^2$; from tables, provide 4Φ08mm

= $\frac{4 \times 64}{4} \times 3.142 = 201.08mm^6$

APPENDIX H: MATLAB LIST PROGRAMME FOR EVALUATION OF DEFLECTION DUCTILITY INDEX AND LOAD-DEFLECTION RESPONSE OF BEAMS

% Program written for load-deflection behavior of concrete beams

% reinforced with rebars milled from scrap metal

% written for Bldr J.A. Apeh, Dept of Building, F.U.T. Mx

% Date: 09/12/2015, email: apehjoe@futminna.edu.ng

% define variables

f_{cu} = 21.33; 26.74; 30.00

f_y = 410

b = 100

d_e = 176; y_t = 200/2; l = 900; d = 200

E_s = 200000; E_c = 5700*sqrt(f_{cu})

n = E_s/E_c

e_{cm} = 0.0001; 0.003

E_{cu} = 0.003; e_0 = 0.002; d_1 = 23*P*l^3/1296*E_s*I_g

A_s = 100. 53: 201.01

rho = 0.0058: 0.012; rho = A_s/bd

c = 47.71:83.06

I_g = b*(d^3)/12;

f_r = 7.5*sqrt(f_{cu})

M_{cr} = f_r*I_g/y_t

I_e = (M_{cr}/M) * I_g + [1 - (M_{cr}/M)]^3*I_{cr}

I_{cr} = 0.18*(n*rho)*0.25*b*d^3/12

F_s = E_s*e_{cm}(d – c/c)*A_s

% obtain value for beta (b_1)

if f_{cu} = [21.33 26.71 30.00];

B_1 = 0.85;

else if 21.33 < f_{cu} < 30.00

B_1 = 0.85*(f_{cu} – 20)

else

B_1 = 0.65;

end

% initialize load - deflection matrix

M_{cc} = b*c^2f_{cu}[e_{cm}/e_0] [2/3 – ¼*(e_{cm}/e_0);

M_s = F_s [d – c]

M = M_{cc} + M_s

P = 6*M/l

P = [ ]; δ_1 = [ ]

% cracking

I_g = (b* (d^3))/12;

y_t = d/2;

f_r = 7.55*sqrt(f_{cu});

M_{cr} = f_r*I_g/y_t;

P_{cr} = 6*M_{cr}/l;

δ_{1cr} = 23*P_{cr}*l^3/1296*E_s*I_e

P = [P;P_{cr}]; δ_1 = [δ_1;δ_{1cr}]

% yielding

z = d(0.5 + sqrt(0.25 – (0.14/0.9));

M_y = A_s * f_y*z

P_y = 6*M_y/l

δ_{1y} = 23*P_y*l^3/1296*E_s*I_e

P = [Pcr; Py]; δ1y = [δ1cr; δ1y];

% ultimate

C_t = 0.5*d; c = 0;

While abs (c/c_t – 1) > 0.002;

M_u = rho*b*d^2*f_y(1 – 0.59*rho*f_y/f_{cu});

P_u = 6*M_u/l; δ_{1u} = 23*P_u*l^3/1296*E_s*I_e

P_u = [P_y; P_u]; δ_{1u} = [δ_{1y}; δ_{1u}];

% graph

Plot (P; P_u; δ;δ_u); % make the graph plot

Title (‘plot of load over deflection’) % title of graph

Ylabel (’load (kN)’) % label for y axis

Xlabel (‘Deflection (mm)’) % label for x axis

Legend (‘location’, Northwest’) % move legend to upper left end

APPENDIX I: DATA FOR DUCTILITY INDEX OF TESTED BEAM SPECIMEN

S/NO	Beam ID	fcu (x_1) N/MM^2	steel ratio ρ (x_2)	DI (Y)	$(X_1)^2$	$(X_2)^2$	X_1X_2	Y^2	X_1Y	X_2Y
1	BM 1	21.33	0.012	1.73	454.97	0.000144	0.256	2.993	36.901	0.0208
2	BM 2	21.33	0.012	2.26	454.97	0.000144	0.256	5.108	48.206	1.0271
3	BM 3	21.33	0.012	1.78	454.97	0.000144	0.256	3.168	37.967	0.0214
4	BM4	21.33	0.012	2.28	454.97	0.000144	0.256	5.198	48.632	0.0274
5	BM 5	21.33	0.012	1.87	454.97	0.000144	0.256	3.497	39.887	0.0224
6	BM 6	21.33	0.012	2.72	454.97	0.000144	0.256	7.398	58.018	0.0326
7	BM 7	26.71	0.0092	1.82	713.42	0.0000846	0.2457	3.312	48.612	0.0167
8	BM 8	26.71	0.0092	2.72	713.42	0.0000846	0.2457	7.398	72.651	0.625
9	BM 9	27.81	0.0058	1.98	773.4	0.0000336	0.1613	3.92	55.0638	0.0115
10	BM 10	27.81	0.0058	3.16	773.4	0.0000336	0.1613	9.986	87.8796	0.0185
11	BM 11	27.81	0.0058	1.86	773.4	0.0000336	0.1613	3.46	51.727	0.0108
12	BM 12	27.81	0.0058	3.24	773.4	0.0000336	0.1613	10.498	90.104	0.0188
13	BM 13	26.71	0.0092	1.99	713.42	0.0000846	0.2457	3.96	53.153	0.0183
14	BM 14	26.71	0.0092	2.89	713.42	0.0000846	0.2457	8.352	77.172	0.026
15	BM 15	26.71	0.0092	1.93	713.42	0.0000846	0.2457	3.725	51.55	0.0178
16	BM 16	26.71	0.0092	2.78	713.42	0.0000846	0.2457	7.728	74.254	0.0256
17	BM 17	27.81	0.0058	1.83	773.4	0.0000336	0.1613	3.349	50.892	0.0106
18	BM 18	27.81	0.0058	2.38	773.4	0.0000336	0.1613	5.664	66.158	0.0138
		x_1	x_2	Σy	$Σx_1^2$	$Σx_2^2$	$Σx_1x^2$	$Σy_2$	$Σx_1y$	$Σx_2y$

$Σx_1 = 455.10$

$Ẍ_1 = 25.28$ $Σx_2 = 0.162$ $ΣY = 41.22$ $Σy_2 = 98.714$ $ΣX_1y = 1048.82$

$Ẍ_2 = 0.009$ $Ÿ = 2.29$

$Σx_1^2 = 11650.735$ $Σx_2^2 = 0.0015732$ $ΣX_1X_2 = 3.97794$

MODEL : $y = 1.101 + 0.047x_1 + 0.12x_2$

$Σx_2y = 0.365504$

APPENDIX H: DATA FOR PRE TING DUCTILITY INDEX OF TESTED BEAM SPECIMEN

S/NO	Beam ID	fcu (x_1) N/MM^2	steel ratio ρ (x_2)	DI (Y)	$(X_1)^2$	$(X_2)^2$	X_1X_2	Y^2	X_1Y	X_2Y
1	BM 1	21.33	0.012	1.73	454.97	0.000144	0.256	2.993	36.901	0.0208
2	BM 2	21.33	0.012	2.26	454.97	0.000144	0.256	5.108	48.206	1.0271
3	BM 3	21.33	0.012	1.78	454.97	0.000144	0.256	3.168	37.967	0.0214
4	BM4	21.33	0.012	2.28	454.97	0.000144	0.256	5.198	48.632	0.0274
5	BM 5	21.33	0.012	1.87	454.97	0.000144	0.256	3.497	39.887	0.0224
6	BM 6	21.33	0.012	2.72	454.97	0.000144	0.256	7.398	58.018	0.0326
7	BM 7	26.71	0.0092	1.82	713.42	0.0000846	0.2457	3.312	48.612	0.0167
8	BM 8	26.71	0.0092	2.72	713.42	0.0000846	0.2457	7.398	72.651	0.625
9	BM 9	27.81	0.0058	1.98	773.4	0.0000336	0.1613	3.92	55.0638	0.0115
10	BM 10	27.81	0.0058	3.16	773.4	0.0000336	0.1613	9.986	87.8796	0.0185
11	BM 11	27.81	0.0058	1.86	773.4	0.0000336	0.1613	3.46	51.727	0.0108
12	BM 12	27.81	0.0058	3.24	773.4	0.0000336	0.1613	10.498	90.104	0.0188
13	BM 13	26.71	0.0092	1.99	713.42	0.0000846	0.2457	3.96	53.153	0.0183
14	BM 14	26.71	0.0092	2.89	713.42	0.0000846	0.2457	8.352	77.172	0.026
15	BM 15	26.71	0.0092	1.93	713.42	0.0000846	0.2457	3.725	51.55	0.0178
16	BM 16	26.71	0.0092	2.78	713.42	0.0000846	0.2457	7.728	74.254	0.0256
17	BM 17	27.81	0.0058	1.83	773.4	0.0000336	0.1613	3.349	50.892	0.0106
18	BM 18	27.81	0.0058	2.38	773.4	0.0000336	0.1613	5.664	66.158	0.0138
		x_1	x_2	Σy	$Σx_1^2$	$Σx_2^2$	$Σx_1x^2$	$Σy^2$	$Σx_1y$	$Σx_2y$

$Σx_1$ = 455.10

$Ẍ_1$ = 25.28

$Σx_2$ = 0.162

$Ẍ_2$ = 0.009

ΣY = 41.22

Ÿ = 2.29

Σy2 = 98.714

$ΣX_1y$ = 1048.82

$Σx_1^2$ = 11650.735

$Σx_2^2$ = 0.0015732

$ΣX_1X_2$ = 3.97794

MODEL : $y = 1.101 + 0.047x_1 + 0.12x_2$